

Evaluation of Ash-Free Coal for Chemical Looping Combustion

by

Azar Shabani

A thesis submitted in partial fulfillment of the requirements for the degree of

Doctor of Philosophy

in

Chemical Engineering

Department of Chemical and Materials Engineering
University of Alberta

© Azar Shabani, 2016

ABSTRACT

In this study, performance of ash-free coal (AFC) was evaluated for chemical looping combustion (CLC). Coal is the major source of power generation worldwide and release of ash forming minerals and CO₂ emission are the major issues during its combustion. AFC is used in order to get rid of the problems related to release of ash forming minerals. CLC is considered as a promising technology with inherent CO₂ capture due to its potential to reduce energy penalty and the cost associated with CO₂ separation from combustion off-gas. Several oxygen carrier materials with suitable thermodynamic properties and high oxygen transfer capacity have been identified for the CLC and chemical looping with oxygen uncoupling (CLOU) processes. One of the most promising oxygen carrier materials is CuO/Cu₂O. In this study, introduction of CLC and CLOU systems, status review of CLC of solid fuels, experimental results of CLC of AFC at different ratios, economic considerations and techno-economic evaluations followed by mass and energy balance of the system are presented. As background information, preparation process and properties of AFC were discussed.

CLC combustion experiments of AFC were performed in a thermogravimetric analyzer (TGA) using CuO as an oxygen carrier to evaluate the CLC performance of CuO with AFC during reduction and oxidation processes and to explore the reaction mechanism of the CuO/AFC system. TGA experiments with a CuO/AFC mixture with different ratios (10:1 - 50:1) at various temperatures ranging from 450 to 1000 °C were performed and the results were analyzed in greater details for the close to stoichiometric ratio of CuO/AFC ratio of 30. Advanced analytical techniques such as XRD, SEM, EDX and ultimate analyses were employed to characterize the oxygen carrier and to understand the possible interaction of the oxygen carrier with volatile matter and char. Thermodynamic equilibrium calculations were performed for CuO/AFC system by FactSage.

A combustion mechanism of AFC in CuO has been described in three stages as: Stage 1: most of the volatile matter was released from AFC at around 450 °C and combustion of these gases started at around 400 °C with CuO, which could be due to the induced gas-solid interactions. Stage 2: from 450 to 790 °C, the solid-solid interaction of CuO and AFC-char. Stage 3: auto-decomposition of CuO to Cu₂O took place above 790 °C and oxygen was released, enhancing the solid-solid interaction between CuO and residual char.

Performance of AFC in CLC during multicycle TGA experiments was also investigated. A ratio of CuO/AFC of 30 (close to stoichiometric ratio of 27.1) was selected for the consecutive reduction and re-oxidation cyclic experiments. The reactivity of the first cycle was slightly higher than the consecutive cycles due to the fresh CuO in the first cycle. The thermal behaviors, such as mass change in the consecutive cycles were almost similar and there was no residual ash deposition after each cycle. Furthermore, reduction and oxidation processes were performed with different isothermal times, after one hour the combustion was incomplete but longer combustion period (three hours) led almost the complete combustion. Fresh samples and solid residues were analyzed by several advanced analytical techniques including XRD, SEM and BET. XRD analysis of the residue of CuO/AFC showed the presence of CuO at the end of the cycles; CuO and SiO₂ in residues from CuO/BL raw coal (parent coal of AFC). At higher temperatures (900 °C) increased sintering was observed after each cycle, as a result the surface area, total pore volume and average pore radius of the material decreased; however, the final masses of reduced and oxidized masses at 900 °C were constant for CuO/AFC ratio of 30 due to no ash content in AFC. Based on the data collected in TGA, application of CLC for power generation was assessed; mass and energy balance of the proposed system were also carried out. Overall, AFC as the solid fuel showed a promising oxidation/reduction performance and has great potential to be used in the CLC process.

ACKNOWLEDGMENTS

I am very grateful to my supervisor Dr. Rajender Gupta for his kind supervision, guidance and support during my study and research.

I am also thankful to the members of my supervisory committee Dr. John Nychka and Dr. Steve Kuznicki for their valuable guidance throughout the course of this thesis. I also thank Dr. Zaher Hashisho for giving me the permission to use his lab equipment.

I also appreciate all members of Dr. Gupta's research group for their support and cooperation in laboratory. In particular, I appreciate Dr. Moshfiqur Rahman, Dr. Deepak Pudasainee, Dr. Farshid Vejahati, Dr. Mehdi Mohammad Ali pour, Dr. Arunkumar Samanta, Dr. Partha Sarkar and Shubham Agarwal for their valuable assistance, discussions and technical support during my research. I am also grateful to Gayle Hatchard for SEM and EDX, Shiraz Merali and Diane Caird for XRD.

I also acknowledge Dr. Tony Yeung and Dr. Locksley McGann for their valuable support during my study in University of Alberta.

I also appreciate Canadian Centre for Clean Coal/Carbon and Mineral Processing Technologies (C⁵ MPT) for the financial support during the research. I also thank the professors and support staff at University for all the information and assistance during my study.

I am also thankful to my beloved family for their support during my study in University of Alberta.

TABLE OF CONTENTS

Chapter 1. Introduction.....	1
1.1. Motivation.....	1
1.2. Objectives.....	2
1.3. Presentation of thesis.....	3
Chapter 2. Literature review.....	6
2.1. Chemical looping combustion (CLC).....	6
2.1.1. Process.....	6
2.1.2. CLC: Advantages and Disadvantages	9
2.2. Oxygen carriers	9
2.2.1. Ni-based oxygen carriers.....	12
2.2.2. Fe-based oxygen carriers.....	13
2.2.3. Mn-based oxygen carriers.....	14
2.2.4. Cu-based oxygen carriers.....	15
2.2.5. Mixed-oxide oxygen carriers.....	15
2.2.6. Low cost oxygen carriers.....	17
2.3. Carbon formation.....	17
2.4. Effect of sulfur.....	19
2.5. Synthesis methods of oxygen carriers.....	23
2.5.1. Spray drying.....	23
2.5.2. Mechanical mixing.....	24
2.5.3. Freeze granulation.....	24
2.5.4. Dry impregnation.....	25
2.5.5. Wet impregnation.....	25
2.5.6. Dissolution and co-precipitation.....	26
2.5.7. Sol-gel.....	26
2.6. Development of CLC of solid fuels.....	27
2.7. Chemical looping with oxygen uncoupling (CLOU) for combustion of solid fuels.....	33

2.8. Oxygen carriers for CLC with solid fuels.....	36
2.9. Lab scale and pilot studies.....	41
2.9.1. Thermogravimetric study.....	41
2.9.2. Large CLC units.....	41
2.10. Modeling and optimization of CLC with solid fuels.....	43
2.10.1. Carbon dioxide capture.....	43
2.10.2. Conversion of gases.....	44
2.10.3. Conversion of solids.....	44
2.11. Reactor design: CLC with solid fuels.....	45
2.11.1. Major challenges in designing CLC reactor with solid fuels.....	46
2.11.2. Technical issues and challenges of CLC with solid fuels.....	47
2.11.3. Suggested CLC system configuration for solid fuels.....	47
2.12. Energy requirement and techno-economic evaluations.....	49
2.13. Economic consideration of CLC with solid fuels.....	51
2.14. Mass and energy balance of CLOU process.....	55
2.14.1. Residence time of particles.....	61
2.14.2. Solid inventory.....	62
2.15. Model of fuel reactor	65
2.16. Conclusions.....	68
 Chapter 3. Methods and Methodology.....	 70
3.1. Materials.....	70
3.2. Experimental Procedures.....	72
3.3. Analytical techniques used for characterization of raw materials and residual samples.....	72

3.4. Summary.....	73
Chapter 4. Thermogravimetric study: single cycle and the reaction mechanism.....	74
4.1. Introduction.....	74
4.2. Thermodynamic simulation.....	77
4.3. Results and Discussion.....	77
4.3.1. Properties and thermal behavior of AFC.....	78
4.3.2. CuO/AFC experiments.....	79
4.3.3. Performance of different CuO/AFC ratios at different temperatures.....	80
4.3.4. FactSage predictions.....	90
4.3.5 Morphology changes of solid residues of CuO/AFC after TGA experiments.....	94
4.3.6. Reaction mechanism of CuO as the oxygen carrier and AFC as the solid fuel.....	96
4.4. Reproducibility of data.....	101
4.5. Conclusions.....	102
Chapter 5. Thermogravimetric study: multicycle performance.....	104
5.1. Introduction.....	104
5.2. Results and Discussion.....	104
5.2.1. Performance of CuO/AFC ratio of 30 during multicycle experiments.....	105
5.2.2. Isothermal time effect on performance of CuO/AFC ratio 30 with reduction and oxidation at 820 °C.....	109
5.3. Characterizations of fresh CuO/AFC and solid residues after TGA experiments by analytical techniques.....	110
5.3.1. XRD and SEM characterizations.....	110

5.3.2. BET surface area analysis.....	114
5.4. Conclusions.....	115
 Chapter 6. Application of CLC in power generation.....	 117
6.1. Introduction.....	117
6.2. Suggested CLC of AFC configuration.....	118
6.3. Mass balance.....	119
6.4. Heat energy balance.....	121
6.5. Conclusions.....	123
 Chapter 7. Conclusions and Future work.....	 124
7.1. Conclusions.....	124
7.2. Future work and recommendations.....	126
 References.....	 128
 Appendix.....	 149

LIST OF TABLES

Table 2.1. Different oxygen carriers with their appropriate support.....	11
Table 2.2. Maximum oxygen capacity for different oxygen carriers.....	11
Table 2.3. Synthesized oxygen carriers which have good performance and reactivity.....	23
Table 2.4. CLC of solid fuels in operation units.....	43
Table 2.5. Physical properties of oxygen carriers.....	53
Table 2.6. Enthalpies of reduction reactions reduced by carbon at 1000 °C and 1 atm (Calculations based on data from reference 149).....	53
Table 2.7. Expenses for NiO-based carriers.....	54
Table 2.8. Medium volatile bituminous coal's properties.....	56
Table 2.9. Constant values for calculating enthalpy of gases.....	61
Table 2.10. Kinetic model's parameters for oxygen release.....	65
Table 2.11. Bituminous coal's properties applied in modelings.....	66
Table 2.12. Parameters of operation.....	67
Table 2.13. Obtained results from the simulation of reference.....	67
Table 3.1. The proximate and ultimate analysis of BL raw coal and BL-AFC (mass %).....	71
Table 4.1. The proximate and ultimate analysis of AFC and AFC residual solid char (mass %)	78
Table 4.2. Reaction pathways of CuO and AFC for different ratios (sub-stoichiometric, close to stoichiometric and above stoichiometric) below and above CuO auto-decomposition temperature ranges.....	99

Table 5.1. BET analysis of surface area and porosity for two samples including pure CuO and CuO/AFC ratio of 30 after five cycles of reduction and oxidation at 820 °C.....114

Table 6.1. Coal feed rate and required flow rate of CuO in fuel reactor for a 500 MW_e CLC unit with efficiency of 0.4 and (HHV of AFC = 36.5 MJ/Kg).....120

Table 6.2. CuO material for a 500 MW CLC unit with efficiency of 0.4 and (HHV of AFC = 36.5 MJ/Kg).....120

Table 6.3. Heat releases from the air reactor and the fuel reactor in two interconnected fluidized bed CLC system.....122

Table A.1. Extraction yield of AFC at temperature of 400 °C from BL raw coal.....151

Table A.2. The proximate and ultimate analysis of BL raw coal and BL-AFC (mass %).....151

LIST OF FIGURES

Figure 1.1. Schematic diagram of chapters of thesis.....	5
Figure 2.1. Schematic diagram of CLC process for solid fuel.....	8
Figure 2.2. Preparation procedure of nanocomposite oxygen carrier.....	21
Figure 2.3. Desulfurization and CO ₂ capture in CLC simultaneously.....	22
Figure 2.4. Schematic view of indirect utilization of solid fuel in the CLC system using an air separation unit (ASU) for gasification of solid fuel before entering the fuel reactor.....	30
Figure 2.5. Schematic view of direct utilization of solid fuel in CLC system.....	31
Figure 2.6. Schematic view of CLC of solid fuel (direct utilization) process with a carbon stripper.....	32
Figure 2.7. The three suggested mechanisms for CLC with solid fuels: Indirect utilization (Syngas-CLC), Direct utilization (In-situ gasification (iG-CLC)) and CLOU process.....	35
Figure 2.8. Suggested system for CLC of solid fuels by Cao and Pan.....	48
Figure 2.9. Analyzed CLOU system consisting of two interconnected fluidized bed reactors (Three boundaries are defined in the Figure with dash lines).....	55
Figure 2.10. Oxygen equilibrium pressure of CuO/Cu ₂ O with temperature.....	57
Figure 2.11. Kinetic rate constants for CuO40SiO ₂ as a carrier material.....	58
Figure 2.12. Reactors' solid residence time (variable values for X_{AR} , $\Delta X = 0.3$).....	62
Figure 2.13. Solid inventory as a function of the conversion's change (ΔX) for variable X_{AR} ($T_{AR}=850\text{ }^{\circ}\text{C}$, $T_{FR}=950\text{ }^{\circ}\text{C}$).....	63
Figure 2.14. Obtained minimum solid inventory for various combinations of temperatures for air reactor and fuel reactor.....	64

Figure 4.1. Schematic diagram of CLOU process of CuO with solid fuel (AFC).....	76
Figure 4.2. Thermal behavior of AFC alone, reduction at a) 450 and b) 900 °C.....	79
Figure 4.3. CuO/AFC reduction at different temperatures with ratios of a) 10 and b) 20.....	83
Figure 4.4. CuO/AFC reduction at different temperatures with ratio of 30 a) thermal behavior and b) reactivity	85
Figure 4.5. CuO/AFC reduction at different temperatures with ratios of a) 40 and b) 50.....	89
Figure 4.6. Assessing feasibility of a) CuO and C reaction and b) CuO auto-decomposition by FactSage.....	90
Figure 4.7. Thermal behavior of pure CuO during reduction at 900 °C.....	91
Figure 4.8. FactSage results of the equilibrium composition of solids in residue for CuO/AFC (AFC = C _{7.21} H _{5.73} O _{0.27} N _{0.21} S _{0.014}) ratios of a) 10, b) 20, c) 30, d) 40, and e) 50.....	92
Figure 4.9. XRD patterns of residual solids of CuO/AFC mixtures with ratios of a) 10, b) 20 and c) 30, reduction at 750 °C.....	94
Figure 4.10. SEM images of CuO/AFC ratio of 30, reductions at a) 750, b) 790, c) 820 and d) 900 °C.....	95
Figure 4.11. Thermal behavior of CuO/AFC ratio of 30, reduction at 450, 750 and 800 °C and evaluation of reaction mechanism.....	97
Figure 4.12. Auto-decomposition of CuO at 820 and 900 °C in CuO/AFC ratio of 40.....	97
Figure 4.13. Schematic view of the reaction mechanism of CuO and AFC at different temperatures.....	100
Figure 4.14. CuO/AFC ratio of 20 reduction at 900 °C a) thermal behavior b) reactivity.....	101
Figure 4.15 CuO/AFC ratio of 30 reduction at 820 C a) thermal behavior b) reactivity.....	101

Figure 5.1. Performance of CuO/AFC ratio of 30 after reduction and oxidation for five cycles at 900 °C including a) thermal behavior and b) reactivity.....	106
Figure 5.2. SEM images of a) pure CuO b) CuO/AFC ratio of 30 after first cycle of reduction and oxidation at 900 °C c) CuO/AFC ratio of 30 after five cycles of reduction and oxidation at 900 °C.....	107
Figure 5.3. Mass variation during multicycle experiments for CuO/AFC ratio of 30 at 900 °C.....	108
Figure 5.4. Mass variation during multicycle experiments for CuO/BL raw coal ratio of 30 at 900 °C.....	108
Figure 5.5. Comparison of different isothermal times for CuO/AFC ratio of 30 with reduction and oxidation at 820 °C.....	109
Figure 5.6. XRD patterns of a) CuO/AFC and b) CuO/BL raw coal ratio of 30 after five cycles with reduction and oxidation at 900 °C.....	110
Figure 5.7. SEM images of (a) pure CuO and (b) CuO/AFC ratio of 30 before TGA test.....	110
Figure 5.8. SEM images of residue of CuO/AFC ratio of 30 after first cycle with reduction and oxidation at a) 820, b) 900 and c)1000 °C.....	111
Figure 5.9. SEM images of residue of CuO/AFC ratio of 30 during five cycles after a) first, b) second, c) third, d) forth and e) fifth cycle with reduction and oxidation at 750 °C.....	112
Figure 5.10. SEM images of residue of CuO/AFC ratio of 30 after five cycles with reduction and oxidation at a) 820 °C and b) 900 °C.....	113
Figure 6.1. TGA results of reduction and oxidation of CuO at different temperatures of 800, 850, 900 and 950 °C (dash lines for 900 °C curve show about 15 minutes for reduction time and about 5 minutes for oxidation time).....	118

Figure 6.2. CuO and AFC reactions and overall heat releases in two interconnected fluidized bed reactors.....119

Figure A.1. Experimental procedures of solvent extraction.....153

NOMENCLATURE

AFC: Ash-Free Coal

CLC: Chemical Looping Combustion

CLOU: Chemical Looping with Oxygen Uncoupling

ΔH : Enthalpy of Reaction

P: Pressure

T: Temperature

TGA: Thermogravimetric Analyzer

CHAPTER 1

Introduction

1.1. Motivation

Coal is the major source of power generation worldwide. It is more abundant in nature than gaseous and liquid fuels, cheaper and its consumption worldwide has been increasing. One of the major concerns of the direct coal combustion is release of ash forming minerals that causes problems due to separation of ash from oxygen carriers. Ash-free coal (AFC) is a treated coal in which ash is separated and removed from coal in advance. AFC has an advantage in avoiding interaction of ash and oxygen carrier in chemical looping combustion (CLC) process - one of the CO₂ capture technologies. Use of AFC in CLC is one of the promising ways to address such issues.

Global warming is a big challenge of our modern world. The root cause of it has been sought in the accelerated increase in atmospheric concentration of carbon dioxide over the past decades due to its greenhouse gas (GHG) effect.¹ Carbon dioxide has the largest amount of emissions in comparison with other GHG emission sources from industry. Fossil fuels combustion produces one third of the whole emissions of carbon dioxide.² In this respect, several approaches have been introduced trying to reduce CO₂ emissions. Overall, the CO₂ reduction techniques in industry have been divided into three categories: 1) precombustion in which carbon is separated from fuel before combustion, 2) postcombustion in which carbon dioxide is separated from flue gases and 3) oxyfuel combustion which uses pure oxygen.^{3,4} However, most of these methods are expensive and consume high amounts of energy.³ Structural change in economy, higher prices and stricter CO₂ emission regulations in future have demanded more energy efficient technologies. As a postcombustion approach, CLC has emerged as a promising technology for carbon dioxide capture which has high efficiency and little or no energy penalty. CLC is a good potential candidate as a novel clean coal technology to be applied in plants for generating electricity.⁵

In CLC with solid fuels, ash separation from the oxygen carrier is an important concern. The aforementioned discussion shows that the ideal CLC with solid fuel would be the one in which the fuel contains negligible or no mineral matter. To address this issue in this research work, instead of separating ash from the oxygen carrier after each cycle in the system, AFC was used as

the solid fuel (ash eliminated from coal in advance) to prevent ash separation from oxygen carrier in the system and other relevant problems during operation. However, there is no result reported to date using AFC as solid fuel in CLC. Therefore, single cycle and multi cycle experiments of CLC of AFC were performed by thermogravimetric analyzer (TGA) to investigate the results and performances. The results showed that use of AFC in CLC is one of the promising ways to address the issues stated earlier.

1.2. Objectives

The underlying objective of this study was to investigate an ash free solid fuel performance in CLC application with CuO as an oxygen carrier. The solid fuel was prepared from BL raw coal and overcome the existing shortcomings of ash accumulation and ash separation of solid fuels in CLC.

This study, investigated CLC of AFC with CuO as an oxygen carrier during single cycle and multicycle experiments by TGA, evaluation of the reduction-oxidation (redox) behaviors of the materials and development of reaction mechanisms for CLC of AFC with CuO. Several characterization techniques were used before and after tests. TGA was used to investigate thermal behavior and reactivity of the oxygen carrier with solid fuel during reduction and oxidation processes. Overview of progress in CLC with solid fuel and background information of AFC are also presented. In order to accomplish the stated objectives the following steps were taken into consideration: preparing samples and characterizing raw materials, establishing procedures and preparing the mixture of carrier material with desired ratio to the solid fuel, investigating redox characteristics of the oxygen carrier reaction with solid fuel.

Samples were prepared according to the desired ratio of oxygen carrier to the solid fuel. Initial screening studies using TGA was used to examine cyclic oxidation reduction thermal behaviors. The investigations of oxidation/reduction behavior of samples which were tested by TGA were fulfilled by reacting the carrier with air during the oxidation cycle and the solid fuel during the reduction cycle. When the desired ratio of oxygen carrier to the solid fuel was identified, the final mixture sample was produced by physically mixing and sieving to less than 60 micron particle size. Then the samples were characterized before and after performing tests by several

characterization techniques such as X-ray diffraction (XRD) for crystalline material identification, scanning electron microscope (SEM) for morphology identification, energy-dispersive X-ray spectroscopy (EDX) for elemental investigation, Brunauer-Emmett-Teller (BET) for analyzing surface area, ultimate and proximate analysis for elemental analysis and investigation of properties. Moreover, application of CLC of AFC in power generation was investigated. Mass and energy balance of the proposed system were carried out.

1.3. Presentation of thesis

Chapter 1 presents the brief introduction of the thesis. A literature review on CLC is presented in Chapter 2. This chapter starts with a general review of CLC process, the oxygen carrier materials used in the systems, synthesis methods and effect of operational parameters. Afterwards, in order to focus more in CLC with solid fuels, a status review of chemical looping combustion of solid fuels is presented. In this section the direct and indirect application of solid fuels in CLC systems, chemical looping combustion with oxygen uncoupling (CLOU) concept, lab scales and pilot studies, major challenges, technical issues in the systems and the other concerns relevant to CLC with solid fuels are discussed more in details. The next section of review is the analysis of CLOU for solid fuels which reviews the issues regarding to energy requirement and techno-economic evaluations, energy in CLC with solid fuels, economic consideration of CLC with solid fuels, mass and energy balance of CLOU process, residence time of particles, solid inventory and fuel reactor design. In Chapter 3, Ash-free coal is introduced. Background, preparation process and properties of AFC are presented in this Chapter. In Chapter 4, thermogravimetric single cycle study and evaluation of the reaction mechanism is covered. The experimental set-up and procedure, materials, characterization and Thermodynamic simulation are discussed. The results and discussion, properties and thermal behavior of AFC, performance of different CuO/AFC ratios at different temperatures including sub-stoichiometric ratio, close to stoichiometric ratio and above stoichiometric ratio are discussed. FactSage predictions, characterizations of unreacted CuO/AFC and solid residues after TGA experiments and reaction mechanism of CuO as the oxygen carrier and AFC as the solid fuel are presented in this Chapter. In Chapter 5, thermogravimetric multicycle performance evaluation is covered. The experimental, raw materials, sample preparation and analytical techniques used for characterization of raw

materials and residual samples are provided. The results and discussion, performance of CuO/AFC ratio 30 during multicycle experiments, isothermal time effect on performance of CuO/AFC ratio 30 with reduction and oxidation at 820 °C, characterizations of fresh CuO/AFC and solid residues after TGA experiments by analytical techniques, XRD and SEM characterizations and BET surface area analysis are presented in this Chapter. Results of application of CLC for power generation are discussed in Chapter 6 including mass and heat energy balances of the CLC system. Finally, overall discussions, conclusions and recommendation are presented in Chapter 7. Figure 1.1 shows the schematic diagram of Chapters of thesis through the illustrated box frames.

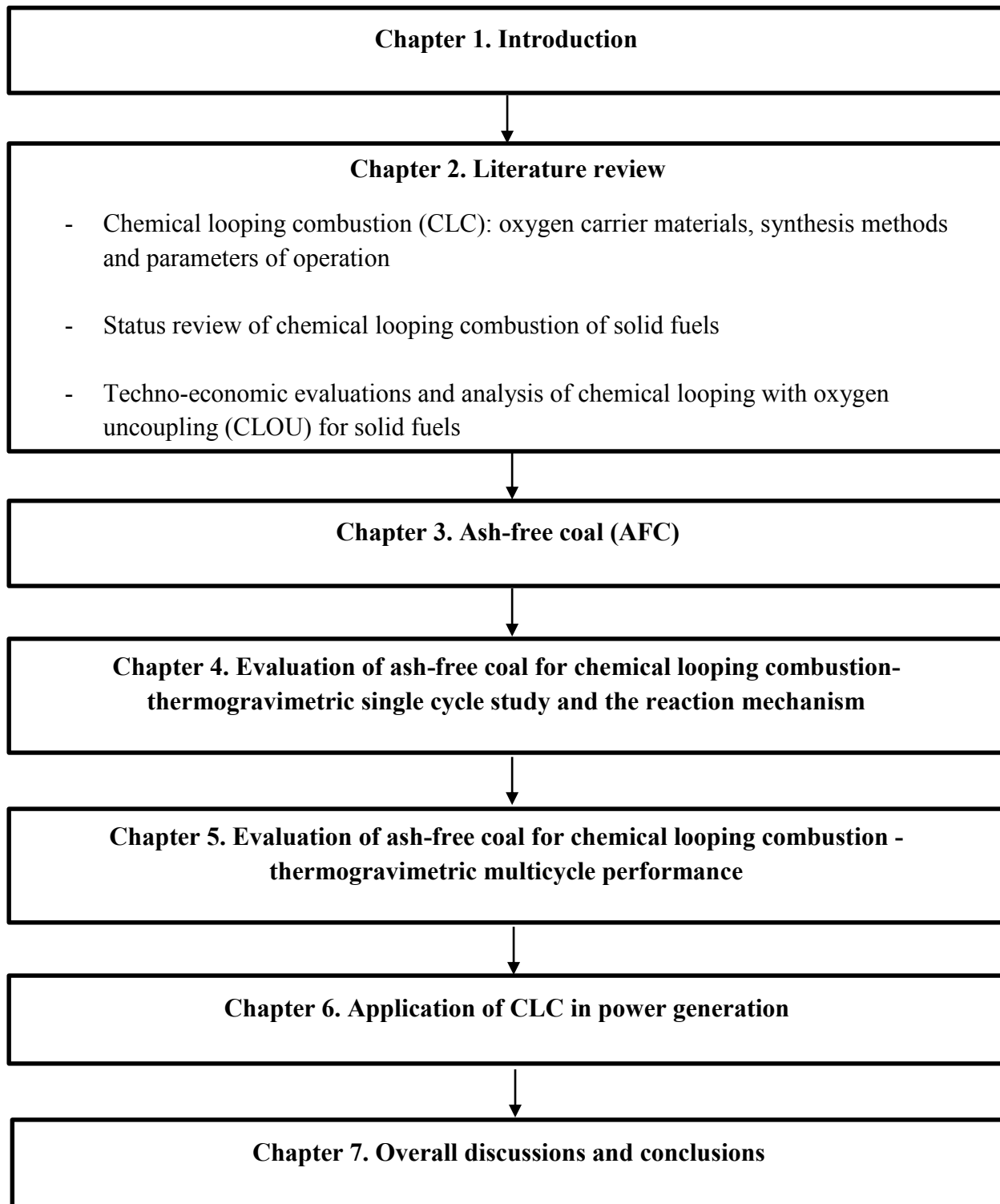


Figure 1.1. Schematic diagram of chapters of thesis

CHAPTER 2

Literature review

2.1. Chemical looping combustion (CLC)

2.1.1. Process

The first concept of chemical looping systems goes back to the mid of 1940s.^{8,10,11} However it was in 1987 in literature by Ishida and co-workers⁶, that the words of chemical looping were initially introduced. The first research group to work on chemical looping was Gilliland and co-workers⁷ at MIT. Then fundamentals of chemical looping combustion for the purpose of enhancing efficiencies were suggested. After that CLC application for CO₂ capture was suggested by Ishida and co-workers⁶. Since 1997 many research groups have become interested to work in this field. Review papers by Hossain and de Lasa⁸, Eyring and Konya⁹, Guang and Tao¹⁰, Fang and co-workers³ are very good sources in this area¹¹. Chalmers University, the Korea institute of energy research, institute de carboquimica in Spain and Vienna University have been actively working in this field during past decade.¹¹

Fossil fuels are one of the main sources of power generation worldwide. Combustion of fossil fuels produces CO₂, a greenhouse gas that causes global warming. Three major CO₂ capture technologies has been suggested to overcome these issues, namely; pre-combustion, oxy-fuel combustion and post-combustion.⁴ These technologies are conventional combustion methods for capturing carbon dioxide.¹²⁻¹⁶ But the problems associated with these techniques are associated with cost and associated with energy penalties mainly because of air separation unit in use. To overcome these problems, a novel technique was developed for CO₂ capture, called as chemical looping combustion (CLC).^{13,17-23}

CLC is a novel technology for CO₂ capture which has been studied widely in last decade. It is more efficient, with no or less energy penalty compared to conventional combustion.²⁴⁻²⁶ CLC technology, for clean energy production from fossil fuels, could avoid the requirement of

pure oxygen by using oxygen carriers which deliver oxygen to the fuel as they circulate between the fuel and the air reactors (Figure 2.1). It thus allows combustion of fuel in oxygen without requiring an expensive air separation unit. Predominantly, CLC produces mainly CO₂ and H₂O as flue gas and, consequently, sequestration-ready CO₂ with little or no energy penalty.

Figure 2.1 shows the schematic diagram of CLC process for solid fuel. Oxygen is transported by an oxygen carrier from the air reactor to the fuel in the fuel reactor. As a result, there would be no dilution of nitrogen with the product gases (CO₂ and H₂O) in the fuel reactor and a high purity carbon dioxide is achieved.¹³ CLC system is composed of two reactors: air reactor and fuel reactor, which are interconnected by a fluidized bed. Mostly a metal oxide has the role to transfer oxygen between these two reactors.

The difference of CLC with conventional combustion is utilization of oxygen carriers in the system, and there is no direct contact between air and fuel. Therefore, nitrogen is inherently separated from oxygen which is transferred to the fuel reactor for combustion of fuel.^{13,27} Oxygen carrier goes to the combustor and transfers oxygen to the fuel. Then the reduced metal oxide will be circulated back to the air reactor. Reduced metal oxide will receive oxygen again from air and then start another cycle. Nitrogen and unused oxygen exit from air reactor. So as a continuous looping system this process is repeated to combust fuel and thus a stream of high purity carbon dioxide will be achieved upon condensation of water.¹³

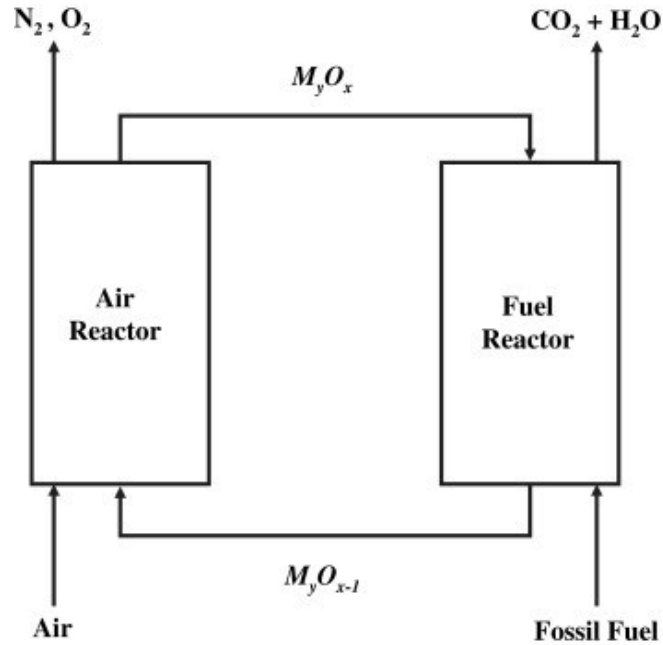


Figure 2.1. Schematic diagram of CLC process for solid fuel²⁸

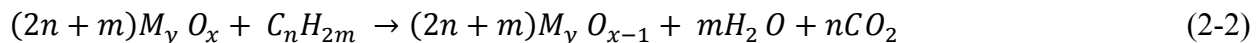
(Reprinted from Saha and Bhattacharya²⁸, 2011, with permission from Publisher (Elsevier))

The CLC would lead to a system where carbon dioxide can be captured from off gas and no separation equipment is required. Nitrogen is inherently separated from carbon dioxide in CLC system.¹³ Therefore, the product will be a high purity stream of CO₂ without nitrogen dilution. Thus, it helps to improve the energy efficiency and lower the cost with no or less energy penalty.¹³ CLC system is very similar to oxy-fuel technology with the difference that oxygen carrier is carrying oxygen with itself to the fuel reactor to combust fuel in CLC process. There are two reactions that occur in the CLC reducer and oxidizer reactors:²⁸

Oxidation in the air reactor:



Reduction in the fuel reactor:



The oxidation reaction in the air reactor is always exothermic, while the reduction reaction in the fuel reactor can be exothermic or endothermic, which depends on the type of oxygen carrier

used in the CLC system. The total heat from the reduction and oxidation reactions is equal to conventional combustion heat with direct contact between air and fuel.^{29,30} If the fuel feed is H₂ or CO, all metal oxides undergo exothermic reactions in both air and fuel reactor. However, for methane feed the majority of metal oxides undergo endothermic reactions with methane except CuO oxygen carrier.³¹

2.1.2. CLC: Advantages and Disadvantages

CLC has several advantages which attract attention to develop this technology. CLC uses low energy for CO₂ capture, its efficiency is high and it has low NO_x and SO_x emission.³² The reaction of oxygen carrier with fuel is without flame and because there is no direct contact between air and fuel and low temperature the system avoids making NO_x.³ In general, the main benefits from the CLC process are as follows: it is a high efficiency system; it generates CO₂ without any nitrogen dilution and reduced NO_x as well^{33,34} and thus no energy consumption for separating CO₂ and N₂.

The fundamental aspects of chemical looping combustion have been tested during many investigations², but there are still problems which need more studies such as: reduction and oxidation kinetics, thermal stability and structural properties of oxygen carriers and separation of ash from oxygen carriers using solid fuels containing ash.

2.2. Oxygen carriers

Oxygen carriers have a key role in CLC performance. The type of oxygen carrier affects CLC operation significantly and is very important to efficiently complete CLC. So, development of a suitable oxygen carrier will lead to a successful CLC system.³ Several metal oxides have been utilized by researches including Ni, Cu, Fe, Mn, Cd and Co.^{21,30,35-41} The most common oxygen carrier particles are Ni, Fe, Mn and Cu.⁴² Beside metal oxides, other type of oxygen carriers were also tested by researchers as the oxygen carriers in CLC process. Expected features of good oxygen carriers are high mechanical properties, high rates of reactions, good conversions, high sulfur tolerance, proper durability in several cycles, high oxygen capacity, lack of sintering, good coke and attrition resistances, ease of preparation, low cost and environmentally friendly.^{3,4}

Lab-scale CLC research have been performed with different oxygen carriers in fluidized bed and fixed bed reactors using gaseous fuels such as methane and syngas (H_2 , CO). In addition, a number of investigations of carrier materials have been carried out in thermogravimetric analyzers (TGA) with gaseous fuels.^{17,21,30,35-41,43-49} Several parameters such as operating temperature, reducing agent, type of oxygen carrier and their particle sizes effect oxygen carrier's reactivity.³⁵ The performance evaluation of different metal oxides such as nickel, copper, cobalt and iron, showed that first three metal oxides have higher mechanical strength in longer operational experiments and higher reactivity than the former ones.^{35,44} Inert materials have also been added in carrier materials to improve their properties, physical characteristics and increase the conversion rate of reaction. Several inert materials as support to modify and enhance the properties of oxygen carriers are suggested including Al_2O_3 , MgO, TiO_2 , SiO_2 and yttria-stabilized zirconium.^{35,44} various temperatures for sintering and crushing strength for making various combined carrier materials and supports.^{30,35,44} One issue that can take place is decrease of reactivity due to carbon deposition. Reduced reactivity due to carbon deposition was observed using methane in CLC. One way to reduce carbon deposition is by getting contribution from the high concentration of water vapor in the combustor.^{35,41,44} The synthesis methods used for oxygen carrier development include impregnation, freeze granulation, mechanical mixing, sol-gel, extrusion, spray-drying, etc.³² Some parameters affect the physical and chemical properties of oxygen carrier particles such as type of inert support employed, synthesis methods and material composition.^{21,32}

In order to modify properties of oxygen carriers, different supports are used. The support selection is also very important. Using support will increase their resistance to attrition and their mechanical properties.²¹ Some materials which are used as supports for metal oxide oxygen carriers are TiO_2 , SiO_2 , Al_2O_3 , ZrO_2 , MgO, YSZ, hexaaluminate, sepiolite.³² Several tests were carried out to measure the crushing strength and reactivity performances of different oxygen carriers. Based on the results, the best inert supports for each metal are given in Table 2.1.

Table 2.1. Different oxygen carriers with their appropriate support²¹

Metal used as oxygen carrier	Support
Cu	SiO ₂ and TiO ₂
Fe	Al ₂ O ₃ and ZrO ₂
Mn	ZrO ₂
Ni	TiO ₂

Another important factor for carrier particles is their oxygen capacity. By using thermogravimetric analysis (TGA) as a characterization technique for determining oxygen capacity of metals, copper and nickel were found to have higher oxygen capacities among iron, manganese, nickel and copper.⁵⁰ The oxygen capacities for various synthesized materials with different weight percentages are available in Table 2.2.

Table 2.2. Maximum oxygen capacity for different oxygen carriers²¹

(Reprinted from Adánez and co-workers²¹, 2004, with permission from Publisher (American Chemical Society))

MeO(wt%)	CuO/Cu	Fe ₂ O ₃ /Fe ₃ O ₄	Fe ₂ O ₃ /FeO	Mn ₃ O ₄ /MnO	NiO/Ni
100	20.10	3.30	10.00	7.00	21.40
80	16.08	2.64	8.00	5.45	17.12
60	12.06	1.98	6.00	3.98	12.84
40	8.04	1.32	4.00	2.58	8.56

There are several approaches for characterizing prepared oxygen carriers: X-ray diffraction (XRD) for identification of crystalline materials, Brunauer-Emmett-Teller (BET) for analyzing surface area with nitrogen adsorption, energy- dispersive X-ray spectroscopy (EDS or EDX) for elemental investigation and material characterization, scanning probe microscope (SEM) for analyzing material composition, Fourier transform infrared spectroscopy (FTIR) for chemical analysis and observing sample capability for absorbing light in various wavelengths, thermogravimetric analyzer (TGA) for testing reactivity of oxygen carriers.

Meanwhile costs of metal oxide have key role in CLC economic issues. To make chemical looping processes economical, it is important that oxygen carriers with high mechanical strength and high oxygen capacity be produced by inexpensive and easy preparation methods.⁵¹

2.2.1. Ni-based oxygen carriers

Nickel based oxygen carriers are the most popular particles that have been investigated so far. It is believed that the most promising materials for oxygen carrier applications in CLC are nickel based particles.³ These materials show excellent reactivity and they have demonstrated their capability as an oxygen carrier at elevated temperatures between 900 and 1100 °C.³ In chemical looping combustion processes, they are able to convert methane almost completely. However a slight amount of carbon monoxide and hydrogen is detected in exit gas stream of reduction reactor because of thermodynamic constraints.⁴ Economically speaking, nickel is an expensive material. This issue can be addressed by using materials which have little amount of nickel, little attrition and high reactivity. It is important to consider that nickel is a toxic material too.⁴

Small reaction rate has been observed for nickel oxides with high purity because of having little porosity.⁴ Therefore, a wide variety of nickel based carriers with various synthesis approaches such as spray drying and freeze granulation with several supports have been investigated in order to make a carrier particle with higher reactivity.⁴

Oxygen carriers based on Ni were tested with and without a support.⁸ Pure NiO exhibits weak redox properties which is because of sintering of nickel and influences its reactivity. So this makes pure NiO inappropriate for CLC applications.⁸

Different supports have been studied in order to improve performance of carriers. Alumina particle is a popular material that has been investigated as a support. The carrier particle which was supported by alumina compound showed very good characteristics such as preventing carbon formation, low attrition rates, no sintering and high reactivity.⁴ Al₂O₃ has attracted many interests because of its high thermal stability and desirable fluidization characteristics. When Ni/Al₂O₃ is used as a carrier material, NiAl₂O₄ may be generated in the system. NiAl₂O₄ is an unwanted compound in a carrier particle. Therefore the reactivity of particle reduces in a time period if generation of NiAl₂O₄ is happening in redox stages.⁸

There were some experiments on nickel based carriers with supports like γ -alumina, α -alumina, calcium aluminate and magnesium aluminate.⁴² TGA results proved that oxygen carriers produced with α -alumina, calcium aluminate and magnesium aluminate by dry impregnation have good reactivity. α -alumina, magnesium aluminate have high mechanical strength but γ -alumina and calcium aluminate have low mechanical strength.⁴²

Furthermore YSZ (Yttria-Stabilized Zirconia) was studied as a support for nickel carrier particles. Ni/YSZ showed high reactivity and good recovery properties and it showed no compound of metal support.⁸ Bentonite was also studied for nickel oxide and it exhibited good stability and performance as a support for carrier particle.⁸ Ni/TiO₂ was studied as a nickel support too; TiO₂ showed lower reactivity than alumina support and also tends to carbon formation and therefore carbon dioxide efficiency will be lowered.⁸

Little work is available in literature related to investigations of SiO₂ and ZrO₂ supports for Ni based carriers. Generally speaking nickel with Al₂O₃ support has been found suitable for large scale chemical looping combustion systems.⁸

Meanwhile the nickel based oxygen carriers synthesized by sol-gel method shows very good reduction and oxidation ability in the cycles. It is proved that these particles are able to be used in chemical looping combustion system which has methane as fuel.³²

2.2.2. Fe-based oxygen carriers

Carrier materials which are based on iron are inexpensive, environmentally friendly and have no toxicity.⁴ However, they have low oxygen capacity and poor CH₄ conversion. Also they do not have good reduction and oxidation properties. These oxygen carriers have several advantages. They have low coke formation and sulphate or sulphide compounds will not be formed in presence of sulfur.⁴

When Fe₂O₃ is reduced various compounds can be observed including Fe₃O₄, FeO or Fe. For CLC interconnected fluidized beds in industry, only conversion of Fe₂O₃ to Fe₃O₄⁴ is feasible.

Fe₂O₃ carrier is prepared with several support materials such as MgAl₂O₄, TiO₂, ZrO₂, SiO₂, YSZ and Al₂O₃. Fe₂O₃/Al₂O₃ and Fe₂O₃/MgAl₂O₄ show very good reactivity.³ Fe with Al₂O₃ support has been widely investigated.⁸ Fe₂O₃ with MgAl₂O₄ as a support has been

synthesized to prevent aluminate generation. When Fe_2O_3 with MgAl_2O_4 support is prepared, it shows good thermal stability and reactivity. Sintering is detected when temperature exceeds limit based on the type of oxygen carrier used and numbers of cycle increases.⁸

TiO_2 is another support used for Fe_2O_3 which shows some interaction with Fe_2O_3 .⁸ SiO_2 for Fe_2O_3 is also used and it has shown good reactivity in cycles initially. But, because of formation of iron silicate, which is not a reactive compound, reactivity of material is reduced. Therefore SiO_2 is not a good support.⁸ YSZ for Fe_2O_3 has been investigated too, but shows lower reactivity than alumina support.⁸

2.2.3. Mn-based oxygen carriers

There is little work available in literature regarding Mn-based oxygen carriers. Mn-based carrier materials are inexpensive and environmentally friendly like iron based particles and their oxygen capacity is slightly more than Fe.⁴

When manganese is reduced various compounds such as MnO_2 , Mn_2O_3 , and Mn_3O_4 can be observed. In chemical looping combustion, generation of Mn_3O_4 and MnO is applicable considering their thermal stability in CLC operating temperatures.⁴

MnO particles with high purity were tested with CH_4 or coal fuels and it was observed that they had a relatively weak reactivity. So, different supports were used to modify these particles.⁴ Manganese based carriers were prepared with several supports by Adánez and co-workers⁴ such as ZrO_2 , TiO_2 , Al_2O_3 , SiO_2 , sepiolite and bentonite. Considering strength and reactivity of supports, ZrO_2 was the best support and the others were not appropriate to be used in CLC applications. It was demonstrated that for manganese based carrier particles the best binder is ZrO_2 which is stabilized by MgO .³ TiO_2 , SiO_2 , MgAl_2O_4 or Al_2O_3 were not acceptable because they were not reversible and they formed materials which were not reactive. Sepiolite was rejected too because of its weak mechanical strength.⁴

ZrO_2 support materials were acceptable. They were stable during different circulations and resulted in high reactivity. After TGA tests this support was also tested in fluidized bed reactors and it was observed that some fractures had been created on the structure and sintering was also detected. In order to improve material performance, Mn based carriers with ZrO_2 were synthesized

by adding MgO, CaO or CeO₂. These new particles resulted in sintering prevention, high reactivity and better stability. Among these additives, MgO indicated best results. Mn based carrier with MgO showed high reactivity for carbon monoxide and hydrogen but lower reactivity for methane.⁴ These prepared materials were tested in a 300W chemical looping combustion unit and the experiments concluded little attrition and no sintering results. For synthesis gas (H₂ and CO) efficiency of the system was more than 99.9 % in 800-900 °C but for natural gas efficiency was about 88-99 %.⁴

2.2.4. Cu-based oxygen carriers

Carrier materials which are based on copper have demonstrated good oxygen capacity and high reaction rate. For converting fuel completely to carbon dioxide and water, these materials do not have any thermodynamic constraints. Cu is inexpensive and it is more environmentally friendly compared to NiO.⁴ The main challenge of copper based materials is sintering which happens because of copper's low melting temperature (1085 °C).⁴

During several experiments carried out by thermogravimetric analyzer using various fuels, copper oxide which had high purity showed good reactivity even in low temperatures. However, oxidization rate of pure copper oxide reduced after several cycles.⁴

In order to make copper oxide particles better materials to be used as oxygen carriers several materials were used as support such as Al₂O₃, MgO, CuAl₂O₄, MgAl₂O₄, SiO₂, ZrO₂, TiO₂, sepiolite, bentonite and BHA. Also various synthesis approaches were tried such as spray drying, mechanical mixing, freeze granulation, impregnation and co-precipitation.⁴ When using alumina support, CuAl₂O₄ was formed which is a reducible material that has high reduction rates. Copper based oxygen carriers showed high reactivity with all the supports and synthesis approaches. Materials with TiO₂, γ -Al₂O₃ or SiO₂ supports produced by impregnation or particles with alumina support prepared by co-precipitation showed high stability and good mechanical strength. Materials with other supports and synthesis approaches showed weak mechanical strength.⁴

2.2.5. Mixed-oxide oxygen carriers

Combining different metal oxides may sometimes show better performance than each of them individually. So for chemical looping combustion some mixed oxides have been synthesized

and investigated in order to study their performance such as Fe-Mn, Fe-Ni, Co-Ni and Cu-Ni materials.⁴

The main goals of making mixed oxides are: (1) stronger reactivity and thermal stability (2) better fuel conversion (3) better mechanical strength / lower attrition rate (4) lower coke formation (5) lower cost (6) more environmentally friendly compounds.⁴

Mixed oxides combining copper and iron with spinel were synthesized by various preparation methods. These materials were tested in thermogravimetric analyzer and also in a reactor of fluidized bed. It was understood that best spinel compound of Cu and Fe showed high oxidation rate but low reduction rate and had high oxygen capacity. Cu-Ni/Al₂O₃ was synthesized too and it was observed that nickel oxide makes copper oxide phase more stable.⁴

In addition, iron and manganese combinations were studied. Carrier particles including Fe₂O₃-MnO₂ with use of ZrO₂ and sepiolite as supports were synthesized. It was proved that the two materials have very good stability in 800 °C and high reactivity in CLC applications.⁴ Iron and nickel mixed oxides have been synthesized by several research groups too. It was proved that activity increase and mechanical strength decrease happens when adding nickel oxide to Fe₂O₃/Al₂O₃ material.⁴

Furthermore CoO-NiO/Al₂O₃ was synthesized and investigated up to 750 °C. They demonstrated significant thermal stability and also strong reactivity.⁴ CoO-NiO particles with YSZ as support were synthesized by Jin and co-workers.^{45,48} It was observed that their redox rates are a little weaker than each of the materials. This is as a result of NiCoO₂ formation. However generally speaking the bimetallic compound has no coke formation and has strong capability of being regenerated.⁴

Beside mixed oxide combinations, perovskite (complex mineral oxide) materials have been suggested for chemical looping combustion application too. Different complex structures of particles were tested such as Ni, Sr, Co, La, Fe, Cr and Cu.⁴ A material structure which was applicable for chemical looping combustion was La_xSr_{1-x}Fe_yCo_{1-y}O_{3-d}. The perovskite mechanical and chemical characteristics are not known completely and more studies are needed in this field.⁴

2.2.6. Low cost oxygen carriers

Low cost materials have attracted many attentions to be used as oxygen carriers in chemical looping combustion for solid fuels. Waste products of industry and natural minerals are good candidates in this area. These kinds of particles are able to be used in gas fuel CLC application too due to the fact that they have high reactivity with carbon monoxide and hydrogen.⁴

Ores such as hematite (Fe_2O_3) and some natural minerals such as ilmenite (FeTiO_3) have also been used as oxygen carrier particles.⁴ Ilmenite application as an oxygen carrier has been investigated widely.⁵²⁻⁵⁴ Its composition is FeTiO_3 ($\text{FeO} \cdot \text{TiO}_2$). In ilmenite structure FeO has the role of active part of compound. It is proved that ilmenite has good capability in CLC applications. Among several natural iron materials, Norwegian ilmenite has shown better reactivity.⁴

Several industrial products and ores of iron and manganese which were studied showed that manganese ores which have high reactivity are the most suitable materials to be used as oxygen carriers in CLC. However ores of manganese exhibited weak fluidizing characteristics and low mechanical stability.⁴

Several iron oxides have been tested as oxygen carriers in chemical looping combustion.^{4,55} The natural and synthetic iron oxides were investigated in both fixed and fluidized bed reactors with CH_4 and air consumption in the system. It was proved that synthetic iron oxides have higher performance than natural ones.²¹

Recently CaSO_4 is attracting attention of several research groups. CaSO_4 is a low cost material which has high oxygen capacity in comparison with other suggested carriers. However using CaSO_4 has disadvantage of forming CaO and SO_2 .^{3,4} For CaSO_4 , elevated temperatures lead to higher methane conversion. There generation of SO_2 has been detected significantly too. Effective parameters on deactivation of CaSO_4 particles are generation of SO_2 and H_2S . Therefore decaying at elevated temperatures is a big issue for CaSO_4 carriers. In this regard using limestone for SO_2 removal and optimizing operating conditions are suggested solutions.³

2.3. Carbon formation

In CLC it is necessary to prevent coke formation because of several reasons. In reduction reactor coke formation can occur on carriers and therefore the particles carry carbon with

themselves to the oxidation reactor where it will burn by air. CO₂ generation in air reactor causes weak efficiency of system for carbon dioxide capture. Also carbon deposition has negative impacts on carrier materials and deactivates them.^{4,41} Carbon formation depends on several factors such as pressure, size of carrier, temperature and gas composition³ and its detection is by TGA when weight of carrier is enhanced.⁴¹

Several experiments on lab scale were carried out on coke formation. It was proved that carbon deposition is related to three parameters: (1) type of metal oxide (2) support material (3). Ratio of water to fuel based on the water gas shift reaction to produce more CO₂.⁴ Carbon formation mechanisms include:

1. Hydrocarbons decomposition (for example methane)⁴¹



2. Conversion of carbon monoxide to carbon dioxide and carbon which is called Boudouard reaction⁴¹



Without catalyst both reactions are slow. Effective catalyst materials can catalyze both reactions.⁴¹ For example coke deposition can be exhibited for nickel based oxygen carriers because these two reactions are catalyzed by Ni.⁴

Coke formation depends on oxygen availability in the system. For nickel-based particles usually when oxygen consumption is 80% in reduction step, carbon formation is detected. For copper based oxygen carriers when conversion is more than 75% carbon deposition will be observed.⁴ In contrast the case is different for Fe-based carriers. No or very little carbon formation is detected even in little conversion of fuels for iron based particles.⁴

An investigation was carried out for studying effect of carbon deposition on nickel and iron oxide produced with freeze granulation. For nickel very small amount of coke formation was detected whereas for iron no carbon deposition was observed.⁴¹ Also carbon deposition was investigated for Ni and Fe with several supports including TiO₂, Al₂O₃ and YSZ in 600 °C. Rate of carbon formation for nickel was more than iron but there was an exception and it was for Fe₂O₃/YSZ material.⁴¹ The Al₂O₃ support for nickel based carriers showed faster rate of coke

formation than YSZ. Also YSZ rate of carbon deposition was more than TiO_2 support. Therefore Al_2O_3 support for nickel showed the highest amount of coke formation.⁴¹ Also it was understood that increase in temperature and $\text{H}_2\text{O}/\text{CO}$ ratio reduce carbon deposition rate.⁴¹

The fact is coke formation is not a big challenge in real cases in industry. The reason is that industrial systems have high amount of fuel conversion but coke formation is related to low conversion of fuel and oxygen availability in system.⁴¹

2.4. Effect of sulfur

Up to now there is very little work about effect of sulfur on oxygen carriers. Most renewable fuels, fossil fuels, natural gas and syngas have high sulfur amount mostly in H_2S form which can interact with metal oxides used as oxygen carriers by forming metal sulfides.^{2,4} Metal sulfides have lower melting temperatures than metal oxides. This can limit operating temperature of CLC system and also causes sintering which affects circulation of solid between two reactors.^{2,4} In addition some of these metal sulfides have poisoning effects on oxygen carriers and result in decreasing their reactivity especially for Ni based materials.⁴

Study about possibility of H_2S removal in CLC relies on several parameters such as type of metal oxides, condition of operation including pressure, temperature, H_2S concentration and fuel gas composition.⁴ CLC systems with nickel based oxygen carriers are capable of working with fuels which have low sulfur amount (the amount of H_2S : below 100 ppmv). Often H_2S amount existing in natural gas is about 20 ppmv¹ and for refinery gas H_2S presence can be up to 800 ppmv. The amount for raw synthesis gas is 8000 ppmv.¹ For fuels which have high sulfur amount there should be a desulfurization unit before combustion of fuel. For example for Cu based oxygen carriers because of large sulfur amount in fuel, it was observed that sulfur is emitted as SO_2 in the fuel reactor and this significantly affects carbon dioxide quality.⁴ Also it was shown that with nickel based oxygen carriers and methane as fuel, H_2S may be converted to SO_2 in fuel reactor. This oxidization can be increased in low pressures and high temperatures. In this case Ni_3S_2 was the most stable sulfide formed. For Cu the most stable sulfide was Cu_2S and for Mn the stable material generated was MnSO_4 .⁴

Furthermore several TGA tests have been carried out for different metal oxides based on nickel, iron, copper and manganese for several redox cycles. It was confirmed that reduction and oxidation rates will be lowered for all the metal oxide species with H₂S presence. The highest amount of decrease was detected for NiO and the lowest amount was observed for Mn₂O₃.⁴ In this regard a study was carried out about effect of H₂S on NiO materials more specifically using several supports such as sepiolite, ZrO₂, TiO₂ and SiO₂. This investigation was performed with TGA analysis which constitutes 5 circulations in 800 °C. Results showed that materials with sepiolite, ZrO₂ and TiO₂ maintain their stability at this temperature⁵⁶ and complete redox reactions were observed. Also H₂S had effects on the reaction but it had no impacts on the carrier capacity. XRD results demonstrated that during the tests stability of carrier was acceptable, no sulfides were formed.⁵⁶

In order to produce a stable sulfur tolerant oxygen carrier, locating metal nanoparticles into a ceramic matrix (barium hexaaluminate (BHA)) will produce a metal with high thermal stability and high reactivity.² The synthesized particles resulted in rapid redox (reduction-oxidation) rates and had sufficient thermal stability during circulations in 700-1000 °C.² Figure 2.2 shows preparation procedure of this nanocomposite oxygen carrier.

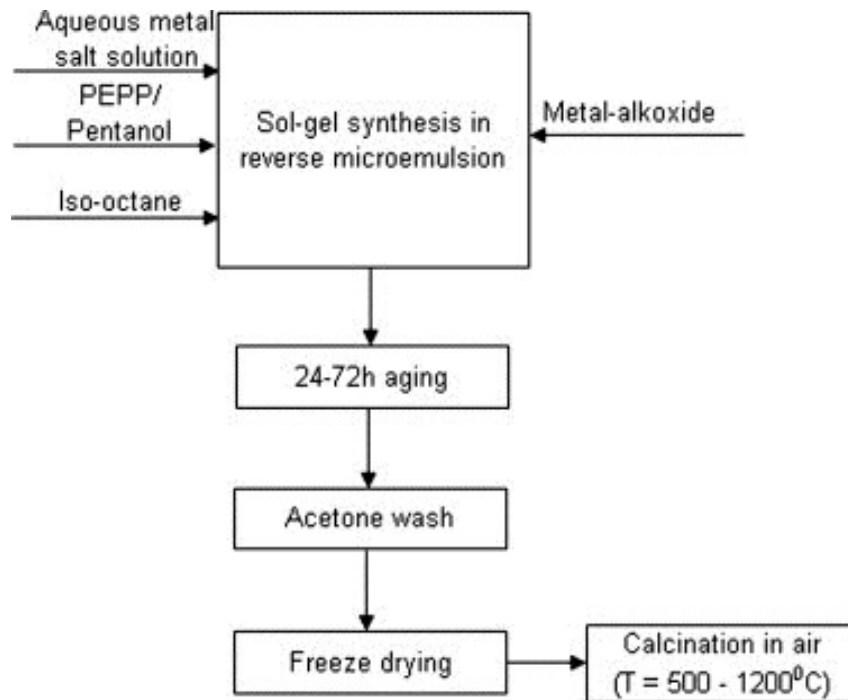


Figure 2.2. Preparation procedure of nanocomposite oxygen carrier⁵⁷

(Reprinted from Solunke and Vesper⁵⁷, 2011, with permission from Publisher (Elsevier))

Synthesized Ni- and Cu-BHA nanocomposite carriers by this method have shown a very good potential to be used in CLC with sulfur contaminated fuels. The presence of H₂S is not affecting the stability of nanocomposite carriers even in high amount of sulfur presence up to 10000 ppmv. But reduction and oxidation kinetics are changed slightly by H₂S presence.² The nanocomposite material has high reactivity of nano size metals and also good resistance at high temperatures because of its ceramic structure.² Furthermore the process has good efficiency and low emission when using a suitable support. A good support will be a material which does not sulfidize and cannot be reduced.⁵⁷

After synthesizing the desired nanocomposite carrier, it can be applied for *in situ* syngas desulfurization besides carbon dioxide capture in CLC.⁵⁷ It was proved that a Cu-BHA nanocomposite material was able to decrease H₂S presence in the fuel reactor. After reduction of oxygen carrier in the fuel reactor if the sulfides have been formed on support when they are

transferred to the air reactor the carriers are oxidized and regenerated and desulfurization of particle happens.⁵⁷ Therefore it was demonstrated that Cu is capable of capturing CO₂ and SO₂ simultaneously. Selection of proper support has a key role in this regard.⁵⁷

Figure 2.3 illustrates this concept more clearly. The syngas fuel includes sulfur contaminants such as H₂S and COS and metal sulfide will be formed on carrier material. In the air reactor the sulfide particle is regenerated while oxidizing and SO₂ will be produced. The advantages of this procedure are: 1) sulfur dioxide and carbon dioxide capture in two different sections 2) There is no need of desulfurizing fuel before using in CLC system 3) preventing generation of corrosive acids 4) preventing separation of sulfur from carbon dioxide.⁵⁷

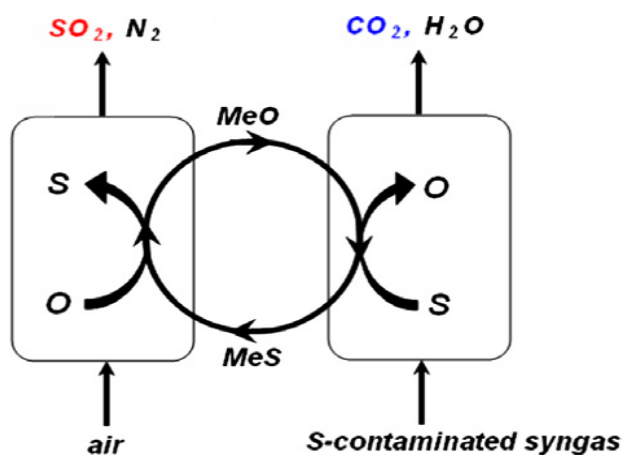


Figure 2.3. Desulfurization and CO₂ capture in CLC simultaneously⁵⁷

(Reprinted from Solunke and Vesper⁵⁷, 2011, with permission from Publisher (Elsevier))

That is a very simple system in chemical looping combustion. Important issues are maintaining reduction and oxidation kinetics rapid and using a stable material in the process.⁵⁷ Some experiments were performed on prepared nanocomposite Cu-BHA carrier in temperatures between 600-900 °C to investigate their sulfur and carbon dioxide capture capabilities. Using synthesis gas with 1% of H₂S, the nanocomposite material could decrease sulfur amount to 90%. The sulfide formation was regenerated in the oxidation reactor by air. Meanwhile limitation of this system is SO₂ generation in the fuel reactor.⁵⁷

Because very few experiments have been done to date on sulfur tolerant capability of oxygen carriers, more research in this area is needed to develop carrier capabilities in presence of sulfur contaminated fuels.⁴

2.5. Synthesis methods of oxygen carriers

Several synthesis methods have been used for production of oxygen carriers including spray drying, freeze granulation, co-precipitation, hot incipient impregnation followed by sintering, mechanical mixing, extrusion, sol-gel, wet and dry impregnation.³² Some successful oxygen carriers which were synthesized by different preparation methods are available in Table 2.3.

Table 2.3. Synthesized oxygen carriers which have good performance and reactivity³²

Oxygen carrier	Preparation method
NiO/NiAl ₂ O ₄	Dissolution or spray drying
NiO/ YSZ	Dissolution or sol gel
Fe ₂ O ₃ /Al ₂ O ₃	Mechanical mixing
Cu-based	Mechanical mixing or impregnation
CoO/YSZ	Dissolution
Mn ₃ O ₄ /ZrO ₂	Mechanical mixing
CoO-NiO/YSZ	Dissolution

There are some constraints for these synthesized oxygen carriers. The limitation of Cu-based particles is its low melting temperature. CoO/YSZ and NiO/YSZ particles have low crushing strength and this leads to fragmentation in different cycles but NiO/NiAl₂O₄, CoO-NiO/YSZ and Fe₂O₃/Al₂O₃ materials have shown better capabilities.³² Some of the preparation methods are described below.

2.5.1. Spray drying

Spray drying is a synthesis method which prepares powders with constant particle size from a liquid by using a hot gas for drying slurries. Application of spray drying in oxygen carrier

synthesis is described with nickel based particles preparation as follows. In order to prepare a nickel based oxygen carrier by spray drying technique, a combination of nickel oxide and α -Al₂O₃ in deionized water which includes proper additives such as Ca(OH)₂ and MgO will be made. Then polyvinylalcohol or polyethyleneglycol or polyethyleneoxide are consumed as binders.⁵⁸ For small scales by a ball mill and for large scales by an attrition mill the combination is homogenized. The mixture is stirred continuously when it is pumping to a two fluid spray dry nozzle. Then in high temperatures between 1400 -1600 °C sintering stage is carried out. Addition of Ca(OH)₂ shows positive effects on synthesized oxygen carrier's strength and MgO additives exhibits increase in methane conversion.⁵⁸

2.5.2. Mechanical mixing

Mechanical mixing is a preparation technique for oxygen carrier particles. In this method metal oxide and support material are dried. Then the process continues until certain amounts of support material and metal oxide are mixed together. In mixture processing, binding additives are added to make composites stronger and more robust. After composite formation, favorable form and size can be achieved by treating particles. For pellet preparation extrusion is appropriate whereas for making powders granulation is desired. Meanwhile graphite can be added to the composite and then calcination takes place when pore formation is needed.⁵¹

Mechanical mixing is a preparation approach which has several benefits. It is cheap and an easy method. In comparison with other approaches, productions of this method have low homogeneity. It was demonstrated that for materials sintered at low temperatures mechanical mixing was not appropriate.⁵¹

2.5.3. Freeze granulation

Freeze granulation technique is typically performed for fine spherical particles preparation.⁵¹ In this method support and metal oxide are mixed together in water. Polyacrylic acid can be added to the mixture to produce homogeneous product. Then by a ball mill this combination is mixed. Meanwhile for enhancing strength of material a bit of binder should be added to the mixture. Then by freeze drying method the mixture is dried and in increased temperatures sintering

step is carried out. Then desired scales will be formed by sieving.⁵¹ Also favorable morphology will be gained by this preparation approach and products will have smooth surface after several treatments. Particle reactivity is relied on strength of interaction between support and metal oxide.⁵¹

Basic principle of both mechanical mixing and freeze granulation is mixing particles directly. Freeze granulation approach has been widely used for Fe and Ni based oxygen carriers for CLC application.⁵¹

Spray drying is a preparation method which is good for large scale and industrial production whereas freeze granulation is only good for lab scale production. Carrier particles synthesized by spray drying were characteristically the same as materials derived by freeze granulation in small scales.⁵⁸

2.5.4. Dry impregnation

Basic principle of this approach is mixing a solution of metal particle and a solid binder. This technique is used to impregnate metals into pores of support for industrial catalysis. Also it can be used for preparation of carrier materials in CLC.⁵¹

Firstly support powders are poured in a salt solution. After metal and support attachment, calcination step takes place. Then metal nitrates decompose to oxides. These steps should be repeated until favorable oxide amount is achieved. In order to reach acceptable stability, material is calcined in high temperatures.⁵¹

For all kinds of carrier particles this preparation approach can be used. In this method choosing proper support is very essential because the synthesized material has the same crushing strength of support.⁵¹

2.5.5. Wet impregnation

Wet impregnation is more practical than previous techniques. It is different because of metal nitrate solution amount. Support is poured in solution of metal nitrate. Then in order to convert nitrates to oxides, the material is calcined in low temperatures. Until reaching favorable

loading, these stages are repeated. For wet impregnation the solution amount consumption is more than the amount needed for dry impregnation. In order to enhance properties of material a high temperature sintering step is carried out.⁵¹

The issue with wet impregnation method is that during repeated cycles attrition happens. That is because of oxide generation outside of particle which is attaching to the inert support with low strength. The characteristics of synthesized particles are the same for both dry and wet impregnation.⁵¹

2.5.6. Dissolution and co-precipitation

The basis of this approach and sol gel method is mixing support and metal oxide solution to achieve materials with more homogeneity. In this method metal salt solution and support are mixed together. For precipitating to powders, agent of precipitation which is often alcohol should be added to the prepared mixture of metal and support solution in co-precipitation approach. For dissolution, metal and support solutions are added to water and alcohol. Procedure is the same as co-precipitation for making powders. Also several drying procedures are carried out. So generally similar production is achieved but the methods have differences in performance.⁵¹ It should be considered that metal and support precipitation at the same time is important. For this purpose pH and reaction rates are important parameters.⁵¹

When the support material has low porosity the impregnation method is not suitable for synthesis, then this approach is used. Precipitating agent, metal salt solution and support solution are fundamental factors in this synthesis method.⁵¹

2.5.7. Sol-gel

Sol-gel is a preparation technique defined as a process which consists of five steps: 1) homogeneous solution creation 2) sol production 3) making gel from sol 4) drying the gel 5) thermal treatment.³²

In sol-gel synthesis method, first of all precursors of a metal oxide and a support solution should be selected and because the purity in production is desired usually precursors of metal alkoxides are used. These materials are mixed together and after that hydrolysis and condensation

steps occur to make a gel. Then the gel is changed to favorable shape and some other treatments including freezing and dehydration are performed. Finally the material is calcined.⁵¹

Sol-gel technique has high control and management on physical factors of material. However this method is expensive and has some complexities. By using this approach, materials with excellent homogeneity are produced and also pore scales of particles can be controlled.⁵¹

2.6. Development of CLC of solid fuels

Carbon dioxide is a major contributor of greenhouse gases (GHGs) emission and has significant effect on the climate change.^{35,36,59} Global warming which is caused by GHGs emissions is an important issue for the whole world. The comparison of industrial with pre-industrial time shows the remarkable increase in the atmospheric carbon dioxide concentration. At present, the carbon dioxide concentration in the atmosphere is around 395 ppm, which was around 280 ppm in pre-industrial time.^{12,26,60,61} Thus, the carbon dioxide concentration in the atmosphere during this time has increased by 40%. Due to the increasing carbon dioxide concentration in the atmosphere, global warming and climate change effects been observed. In order to cope with the increasing climate change effects various efforts on capturing carbon dioxide and storage, such as in a gas field, saline aquifer or depleted oil reservoir have been widely studied.^{13,29}

Fossil fuels combustion is the major source emitting carbon dioxide into the atmosphere. Each year, one-third of the total carbon dioxide emissions is related to fossil fuel combustion.^{35,62} In case of conventional fuel combustion, fuel and air comes in direct contact where huge volume of nitrogen (in air) results low purity for carbon dioxide.³⁵ Sequestration of carbon dioxide from the diluted stream is energy intensive and costly.^{35,63} The expenses for disposal of carbon dioxide per ton of carbon has been estimated to be around 4 - 8 USD.^{35,64} The expenses for sequestration and purifying carbon dioxide from the stream, which consist of a large volume of nitrogen per ton of carbon would cost around 100 - 200 USD.^{35,65} Because of the low concentration of carbon dioxide in the off gas stream, one-fifth of the generated electricity from the power plants, which work based on coal as the solid fuel are to be consumed to sequester and compress the carbon dioxide.^{35,66} In this regard, separation of high concentration carbon dioxide efficiently and economically would be beneficial for industries.

Up to 140 kW units⁶⁷, Chemical looping combustors were demonstrated successfully. Reviews by Adánez and co-workers⁴, Lyngfelt^{67,68} and Hossain and co-workers⁸ are good reviews and provide description about CLC system and its development. CLC achievements up to 2010 are comprehensively discussed and overviewed in Adánez and co-workers⁴ paper. In the review paper by Lyngfelt⁶⁷ more than 4000 hours of operational experience for different oxygen carriers in CLC are presented which mostly are involved with gaseous fuels. Hossain and co-workers⁸ also reviewed recent progresses in CLC. Most of the reviews are about CLC units working with gaseous fuels. Therefore, more detailed studies are needed about CLC of solid fuels and its gaps and challenges in order to be operated successfully.

Since 1983,⁶⁹ once the concept of CLC was introduced, most of the studies were carried out with gaseous fuels such as natural gas and methane.^{19,35,70} The issue with the gaseous fuels is that in the long term the resources are not able to fulfill all the requirements for power generation.³⁵ On the other hand, fossil fuels including coal and petroleum coke are less costly and more abundant in nature compared to gaseous fuels. Therefore, CLC with solid fuels has attracted more attentions, recently. CLC with solid fuels oxygen carriers should have specific characteristics and also the reactor design parameters different than for gaseous fuels. Initially in 1954, Lewis and Gilliland⁷¹ patented the idea of using two interconnected fluidized beds for capturing carbon dioxide using an oxygen carrier with carbonaceous fuels such as natural gas, coal, coke and charcoal. They investigated the CLC with solid fuels with carrier materials including iron oxide and copper.^{13,71} Investigations were again carried out 50 years after the initial studies of CLC with solid fuels continuing the work with the same type of carrier materials. Recently, a design for CLC system with solid fuels was suggested by Pan and co-workers.^{72,73}

Various metal oxides have been tested for oxygen carrier material in CLC system. TGA experiments have proved the utilization of CuO based material as an oxygen carrier with coal as solid fuel.¹³ Using Fe₂O₃ with lignite (Hambach) and its char as fuels in CLC with solid fuel was studied in a fluidized bed reactor by Dennis and co-workers^{74,75} in which the first phase of experiments were performed in an inert bed of silica sand only and the second phase of experiments were performed in bed in presence of Fe₂O₃ particles.^{74,75} In laboratory scale there are works available by Leion and co-workers^{76,77} that tested CLC system with several carrier materials and various type of fuels. As CLC with solid fuel work, they investigated petroleum coke (from the

Cadereyta refinery in Mexico) and various coals (South Africa, China, Indonesia, Taiwan and S. France (raw and sieved)) in laboratory scale. They designed a reactor for CLC with solid fuel which has conical form of quartz above distributor plate for good mixing. Iron based oxygen carrier (60% active material of Fe_2O_3 and 40% MgAl_2O_4) produced by freeze granulation and ilmenite were used as the oxygen carrier in the tests. A 10 kW CLC system at Chalmers university with solid fuels including petroleum coke and South African coal has been studied by Berguerand and Lyngfelt.^{13,78} The fuel conversion for all the experiments of South African coal were between 50 to 79% and also carbon dioxide capture for the coal experiments were reported between 82.5 to 96%.⁷⁸ Currently, some larger units are operating to demonstrate the feasibility of CLC with solid fuels closer to the industrial level in which results look promising. These large units are discussed in section 2.9 “lab scale and pilot studies” more in details.

CLC with solid fuels technology is available with Alstom Power Inc.’s Hybrid Combustion-Gasification Chemical Looping Coal Power Technology.^{35,79-81} This system consist of one bauxite loop with two applications of $\text{CaCO}_3\text{-CaO}$ and $\text{CaSO}_4\text{-CaS}$ loops. In this process initially CaSO_4 reacts with coal (solid fuel) with CO generation. A shift reaction is required to produce CO_2 from CO and then with $\text{CaCO}_3\text{-CaO}$ loop the produced carbon dioxide is purified and concentrated.

Because of wide abundance of solid fuels (e.g. coal), researchers have attempted utilization of solid fuels in CLC system. In order to utilize solid fuels in CLC, the systems should be well adjusted and well adapted for long term efficient use, environmentally friendly and cost-effective. Beside carbon dioxide emissions, other type of gases which are released from combustor including trace metals and oxides of sulfur can be well monitored.³⁵ Utilization of solid fuels including biomass and coal in CLC system has technical issues, such as ash deposition^{35,72,82-84} There are two approaches of utilization of solid fuel in CLC system, first is using solid fuel indirectly in and the second is directly introducing solid fuel in the fuel reactor.

In the first process (indirect utilization), solid fuels are gasified separately in a separate gasifier in presence of pure oxygen to produce syngas (CO , H_2), which is introduced to the CLC system.³⁵ This system will be the same as CLC with gaseous fuel and can be operated with the same type of oxygen carriers.¹³ So the system will be with an additional gasifier to the CLC process and that enhance the expenses of the overall process.³⁵ Figure 2.4 shows a schematic view of CLC

system with indirect utilization of solid fuels including an air separation unit (ASU), separating O_2 for gasifying the solid fuel and producing syngas before introducing to the fuel reactor.

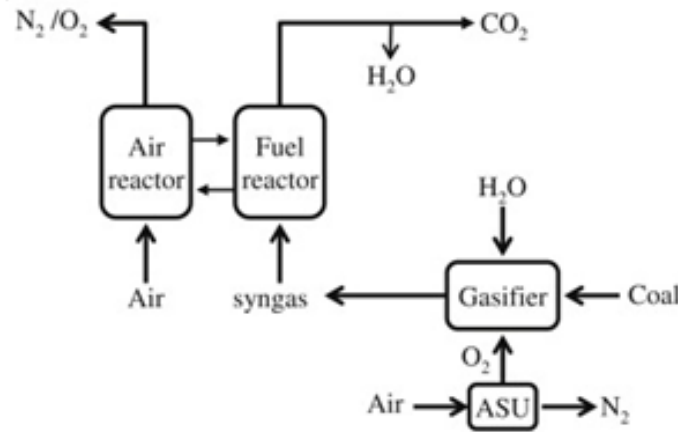


Figure 2.4. Schematic view of indirect utilization of solid fuel in the CLC system using an air separation unit (ASU) for gasification of solid fuel before entering the fuel reactor ⁴

(Reprinted from Adánez and co-workers⁴, 2012, with permission from Publisher (Elsevier))

Another way for using CLC with solid fuels is direct utilization of solid fuels. The advantage of this system is that it is cost-effective since it does not require additional gasifier or air separation unit. The disadvantage is slow rate of reaction. This is mainly because of the solid-solid interactions and insufficient contact between oxygen carrier materials and solid fuels. These technical issues have been raised by different researchers.^{35,72,82-84} In the direct approach, slow rate of gasification of char particles is the main issue. Increasing residence time increases the conversion rate to some extent.

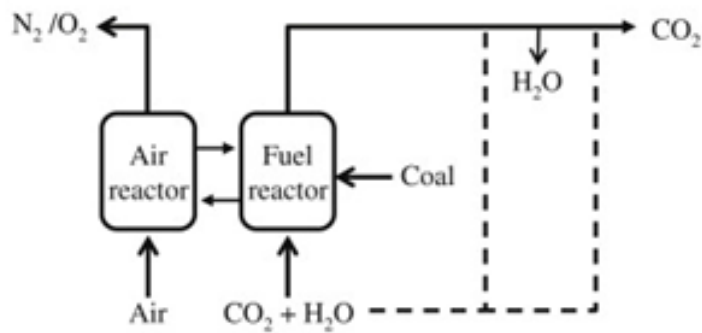


Figure 2.5. Schematic view of direct utilization of solid fuel in CLC system ⁴

(Reprinted from Adánez and co-workers⁴, 2012, with permission from Publisher (Elsevier))

Figure 2.5 shows a schematic diagram of direct utilization of solid fuel in CLC system. In this system the solid fuel can be directly introduced to the fuel reactor and can be gasified to syngas, by gasification agents such as CO₂ or H₂O.^{13,76,85} The produced syngas reacts with the oxygen carrier. This approach (solid fuel gasification) is slow and is the limiting step for rate of reactions.⁸⁶⁻⁸⁹ It is noteworthy that the gasification process in the first approach is even slower than the second approach.⁷⁶ This is because in indirect utilization of fuels concentration of CO and H₂ is more in the environment, but in direct utilization it is mostly CO₂ or H₂O. Slow rate of gasification and direct entry of solid fuel to the fuel reactor is the main problem in this system.¹³ Figure 2.6 shows a schematic view of direct utilization of solid fuel in CLC system using two interconnected fluidized bed reactors. A carbon stripper in the system can separate unreacted char particles from oxygen carriers before entering to the air reactor and their recirculation to the fuel reactor.

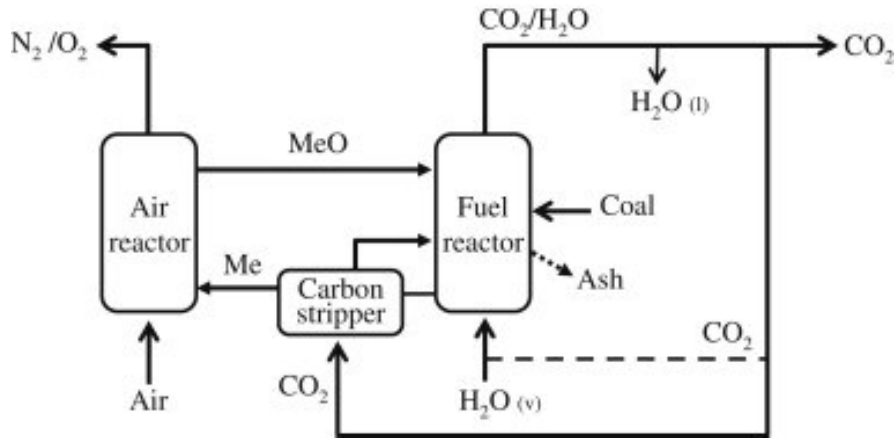
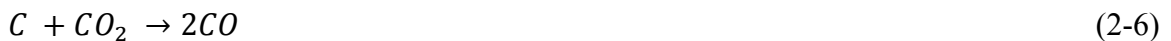


Figure 2.6. Schematic view of CLC of solid fuel (direct utilization) process with a carbon stripper ⁴

(Reprinted from Adánez and co-workers⁴, 2012, with permission from Publisher (Elsevier))

There are two approaches for the evaluation of reaction mechanisms between oxygen carrier and solid fuels, One approach is the direct interaction between solid fuel and oxygen carrier and the other approach is *via* gas intermediates which is an indirect interaction.³⁵ In real cases the mechanism is a mixture of both of these. Several parameters effect the interactions of solid fuel and oxygen carrier including thermodynamics of interactions, kinetics of materials and their characteristics etc. Firstly, the volatile matters from solid fuel are released and which reacts with the carrier material. There should be sufficient contact between the released volatile matters (H₂, CO, C_xH_y) and carrier material because if there is not enough contact they can exit in the fuel reactor unreacted. Afterwards, the reactions of char particles with gasification agents will occur.¹³ The produced carbon monoxide and hydrogen gases react with the oxygen carrier. The overall important char reactions are as follows:¹³



CLC systems with solid fuels have a benefit that most of the carrier materials have high reactivity with the gas products from gasification step from char particles.²⁷ In CLC with solid fuel, the gases are released from char in the combustor but in CLC with gaseous fuel the syngas enters from the bottom of the system. So the main difference is the location of syngas entering in the system. Therefore, gas conversion is not simple since materials in bed and portion of gases which are released in the upper part of the system do not have enough contact with each other. Another issue related to the conversion of gases is methane released within volatile matters which has lower reactivity towards cheap carrier materials.²⁷ Several methods and approaches exist to improve the conversion of gas in combustor and make it fully feasible including regeneration or separation of unreacted gas, utilization of one more reducer, utilization of CLOU materials and oxygen polishing technique.²⁷ Approaches for enhancing the conversion of gases are as follows;

1. Special design of fuel reactors in the system which consist of two reactors. In this case unreacted gases are introduced to the second reactor.
2. Oxygen polishing system which allows pure oxygen to the combustor from the bottom in order to convert unreacted gases from char gasification.
3. Unreacted gases can be separated from carbon dioxide in the exit gas stream and circulated back to the system.
4. Utilizing a special type of carrier material which has the capability of releasing oxygen in CLOU system.

2.7. Chemical looping with oxygen uncoupling (CLOU) for combustion of solid fuels

CLOU is a novel approach for capturing carbon dioxide utilizing solid fuels and oxygen carriers with special capabilities such as being able to release gaseous oxygen through reaction and having suitable thermodynamic properties which was proposed by Mattisson and co-workers in 2005.¹³ In this system oxygen carrier should be able to release oxygen in the fuel reactor and also reduced oxygen carrier be oxidized again by oxygen in air reactor. The following reactions are involved in a CLOU process.¹³



Oxygen carriers in CLOU should have special thermodynamic properties which are not required for oxygen carriers in conventional CLC systems. They should have proper equilibrium oxygen partial pressures in the desired combustion temperature range. Several oxygen carriers have been identified for CLOU process including CuO/Cu₂O, Mn₂O₃/Mn₃O₄ and Co₃O₄/CoO. The reactions for CuO/Cu₂O and Mn₂O₃/Mn₃O₄ are exothermic which is a good advantage for CLOU system because with the increase in temperature equilibrium partial pressure of oxygen gas is increased which lead to higher conversion and rate of reaction. Co₃O₄/CoO reaction is endothermic which causes temperature drop in fuel reactor and a higher circulation rate is needed to prevent this. However, for the other two metal oxide systems low circulation rate is accepted because the reactions are exothermic and temperature increase is for the CLOU process. Experiments for Mn₂O₃/Mn₃O₄ showed no sintering in the system because of the high melting temperatures of both Mn₂O₃ and Mn₃O₄, but in experiments with CuO as the carrier material sintering is detected because of its low melting temperature.¹³

CuO/Cu₂O oxygen carrier has a reversible reaction system and at a certain temperature it has special equilibrium concentration of oxygen.²⁷ This equilibrium concentration shows that while cuprite enter to the oxidizer where the oxygen concentration is higher, it oxidizes with oxygen and converts to CuO.⁶¹ Then in reducer where solid fuel exists, initially the concentration of oxygen is zero and CuO would convert to cuprite. There have been several research work in continuously operating and laboratory scale experiments about utilizing solid fuels with CuO in CLOU process including CuO/ZrO₂ with petroleum coke and CuO/MgAl₂O₄ with bituminous coal.^{13,90,91} Figure 2.7 summarizes three suggested mechanisms for CLC with solid fuels.

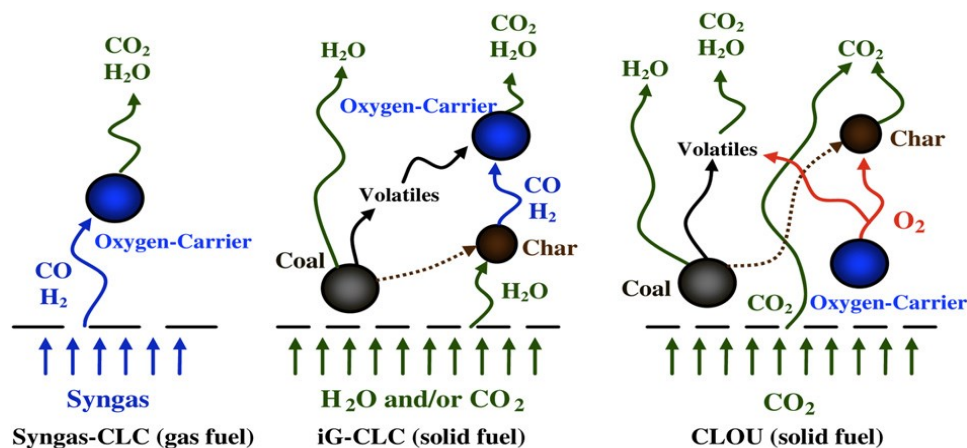


Figure 2.7. The three suggested mechanisms for CLC with solid fuels: Indirect utilization (Syngas-CLC), Direct utilization (In-situ gasification (iG-CLC)) and CLOU process ⁴

(Reprinted from Adánez and co-workers⁴, 2012, with permission from Publisher (Elsevier))

In CLOU process rate of reaction is faster than in normal CLC process because there is no need of contact between carrier material and gases from char gasification in this process. In CLOU oxygen release and rate of combustion control the reaction rates and slow gasification rate is eliminated, but in conventional CLC with solid fuel slow gasification rate is the limiting step. This was proven by experiments of petroleum coke with copper based carrier materials and Fe₂O₃/MgAl₂O₄ by Leion and co-workers.^{13,76} Their results showed the rate of conversion of solid fuel 50 times higher for CLOU process of copper based carrier materials compared to Fe₂O₃/MgAl₂O₄. An essential key point that should be noted in CLC systems is the solid inventory, which is depending on residence time in fuel combustor and circulation. Leion and co-workers⁷⁷ have studied reactivity of various solid fuels including petroleum coke and various coals (South Africa, China, Indonesia, Taiwan and S. France (raw and sieved)) with two different oxygen carries, synthetic Fe₂O₃/MgAl₂O₄ particles and ilmenite, the estimation was requirement of about 400 to 2000 kg materials as oxygen carriers per MW of fuel in fuel reactor. Whereas, CLOU process enhances the rate of reaction and lower solid inventory is required.¹³

2.8. Oxygen carriers for CLC with solid fuels

As discussed above, several parameters affect the successful operation of the CLC system. Development of a good oxygen carrier for CLC with solid fuel is very important. The oxygen carrier should have higher reactivity with CO and H₂ compared to methane as fuels in CLC systems. Furthermore, oxygen carriers used in CLC with solid fuels should be well separable and should not react with deposited ash particles.

The oxygen carriers used in CLC system with solid fuels can be metal oxides or other types. Many metal oxides have been studied in CLC with gaseous fuels; however, limited numbers of metal oxides have been studied for CLC with solid fuels. Most of the investigations on the carrier materials in CLC with solid fuels have been concentrated on few metal oxide materials including Cu, Ni, Fe and Mn.²⁷ NiO is not that much appropriate for the CLC with solid fuel applications because of several reasons including cost and deactivation by sulfur containing gases. Metal oxides including Manganese and iron are cheaper materials. Waste materials and ores of these metal oxides can also be utilized for this purpose. Copper oxide is more expensive but its several special properties make it suitable potential carrier for CLOU process.²⁷

Copper based materials as oxygen carriers in CLC with solid fuels have several advantages. The main benefits that make it more special than other carriers are as follows: high oxygen transport capacity, environmentally friendly, low price, high reactivity, no thermodynamic limitation to combust fully, both reactions in air reactor and fuel reactor are exothermic.⁶¹ Beside these benefits, CuO has a disadvantage of its low melting temperature (~1085 °C), which causes problem in operating CLC process at higher temperatures. High temperature leads to sintering of CuO material so the operating temperature should be narrowed down to 600 to 900 °C.^{24,92} Based on studies on different aspects of CuO including thermodynamic analysis, energy balances and its ability to transport oxygen, CuO material was demonstrated as a suitable oxygen carrier to function well in CLC with solid fuels. To study the possibility of CLC system with solid fuels, various types of solid fuels including biomass, low density polyethylene and PRB coal were utilized by Cao and co-workers,⁹² in the reduction step CuO material converted to Cu completely.⁶¹

In CLOU - an updated method of CLC with solid fuels, oxygen carrier should be able to release oxygen in the fuel reactor and again receive oxygen in the air reactor. CuO possess these

capabilities. CLOU experiments in batch fluidized bed equipment in laboratory scale have been successfully demonstrated with CuO.⁶¹ The rate of reaction with CuO was faster in CLOU process compared to CLC with oxygen carrier that does not release oxygen.^{13,61} Mattisson and co-workers⁹⁰ also utilized petroleum coke as the solid fuel in the CLOU system and a CuO based material as the oxygen carrier (CuO/ZrO₂) to observe how the system works.^{61,90} Petroleum coke showed a conversion rate which depends on the operating temperature within the range of 885-985 °C and the conversion rate changed between 0.5 %/s to 5%/s.^{61,90} While comparing the results from this experiment with the results from CLC with Fe₂O₃/MgAl₂O₃ as an oxygen carrier, the rate of conversion was raised by a factor of 45.⁶¹ For the oxygen carriers which consist of 40 wt% of CuO in their composition, the solid inventory in combustor reactor should be in the range of 120 to 200 kg per MW fuel, however, the estimation is around 2000 kg per MW fuel in the combustor reactor, while utilizing petroleum coke as solid fuel.^{61,76} Based on thermodynamic, energy balance and oxygen carrying capacity Cu has been considered as a better carrier material than others for application in CLC with solid fuels.

For higher operating temperatures, oxygen carriers based on iron (high melting points) can be used.⁶¹ Iron, iron oxide and iron ores are cheap materials with low reactivity, but they can be used in higher pressures and operating temperatures systems in CLC with solid fuels. A thermal analyzer-differential scanning calorimeter-mass spectrometer (TG-DSC-MS) study was carried out by Rubel and co-workers³⁴ to investigate the potential performance of several metal oxides as oxygen carriers in CLC with solid fuels including Fe₂O₃, NiO, CoO and CuO.^{34,61} These results showed that in case of Fe₂O₃ as a carrier material in reaction with a coal char with high carbon content in an inert gas oxidization occurred and this oxygen carrier is able to cause 88% of carbon removal/conversion from the solid char. Fe₂O₃/MgAl₂O₄ as the carrier material with petroleum coke as the solid fuel was studied by Leion and co-workers⁷⁶ in the CLC system. It was found that syngas (CO and H₂) contributes in reactions between the carrier material and solid fuel.^{61,76} A 10 kW CLC prototype system with iron oxide as the carrier material and biomass as the solid fuel was operated by Shen and co-workers⁹³ as the continuous operating system (with the same batch of carrier material, a total 30 hours of experiment was reached). Between 740 to 920 °C, the conversion of the solid fuel biomass was between 53.7 to 65.1%.

One of the cheaper carrier materials researchers have utilized in CLC with solid fuels is ilmenite, which is a combined oxide material (FeTiO_3).²⁷ Furthermore, $\text{Fe}_2\text{O}_3/\text{MgAl}_2\text{O}_4$ and ilmenite were utilized with various solid fuels by Leion and co-workers⁷⁷ to study their performances, both of them showed the better results in the experiments. Oxide scale materials from production of steel and Mt. Wright iron ore were tested in a laboratory scale fluidized bed quartz reactor by Leion and co-workers⁹⁴ to investigate their performance in CLC with solid fuels including two bituminous coals, petroleum coke, lignite and charcoal.⁹⁴ This investigation proved that both of the materials as the oxygen carriers were good and as time passed their reactivity went higher. A 10 kW CLC process was operated by Berguerand and co-workers⁷⁸ utilizing ilmenite as the carrier material and South African coal as the solid fuel.⁶¹ The total duration of test was 22 hours and operating temperatures for the experiments were above 850 °C. The carbon dioxide capture was 82.5 to 96%.⁷⁸ The results showed that ilmenite function as an sintering tolerant material during the experiments.^{61,78} There are several advantages for ilmenite material in CLC including low price, promising characteristics of fluidization and high reactive material with CO and H_2 .²⁷

A CLC system which is pressurized utilizing Companhia Vale do Rio Doce (CVRD) iron ore as the carrier material and coal as the solid fuel was tested and proved by Xiao and co-workers.⁹⁵ The conversion of carbon was increased while raising the pressure of system. After several cycles the presence of porosity was observed in the material; however, was not sintered.^{61,95}

NiO is another metal oxide which can be utilized as the oxygen carrier in CLC with solid fuel. However, it has several limitations such as toxicity, expensive and it start deactivating in presence of sulfur in gas. On the other hand, NiO material has shown a good performance in CLC with gaseous fuels with the highest reactivity. It is noteworthy that in the solid fuel pyrolysis, there would be a little release of CH_4 . In order to raise the rate of conversion in CLC with solid fuel, addition of a little bit of NiO can lead to switch methane to syngas (CO and H_2).⁶¹

In a laboratory scale fluidized bed reactor, several experiments with various solid fuels (Mexican petroleum coke, South African coal and Indonesian coal) with NiO as the carrier material under operating temperature of 970 °C were carried out by Leion and co-workers.^{61,96} NiO demonstrated a high reactivity performance while operating with a low sulfur containing fuel; however, deactivation of the oxygen carrier occurred while a fuel with high sulfur content was

utilized. It has been recommended to remove sulfur prior to perform the CLC tests with NiO. In such case, material showed no sintering and good fluidization properties.⁹⁶ Experiment was carried out in operating temperature range of 800-960 °C by Gao and co-workers,⁹⁷ to investigate the performance of Ni-based oxygen carrier (NiO/NiAl₂O₄) produced by impregnation method with coal (Shen-hua bituminous coal from Inner Mongolia, China) in CLC system. At temperature higher than 900 °C, the material showed high reactivity and produced carbon dioxide concentration was about 95% as dry basis.⁹⁷

Combined metal oxide may possess characteristics that would enhance the performances of releasing oxygen in the CLC process. For example, some of these combinations can lead to create partial CLOU materials in which are capable of releasing some of their oxygen including Mn with Mg, Fe, Cu, Ca, Ni and Si.^{27,98-100} A new compound consisting Mn and Fe with the composition ((Mn_{0.8}, Fe_{0.2})₂O₃) was developed which is able to quickly release large portion of its oxygen at 850 °C and is capable to oxidize methane completely and convert wood char to carbon dioxide fast which was demonstrated by the tests in a batch fluidized bed reactor.^{27,101} It is noteworthy that there is no promising operational experiment with these new combinations except for calcium manganates.^{27,102,103} The perovskite material CaMn_{0.875}Ti_{0.125}O₃ as an oxygen carrier was tested for 70 hours of experiment in a fluidized bed reactor. Overall it functioned well and had the favorable thermodynamic properties.¹⁰² CaMn_{0.9}Mg_{0.1}O_{3-δ} was also tested in a gas-fired 10kW CLC unit. The material showed very good performance to convert fuel and at certain conditions the complete combustion was obtained.¹⁰³

Cheaper materials can also be utilized in CLC with solid fuels such as ore of manganese, industrial wastes, and materials with various resources.^{27,37,104-108} The performance of the oxygen carrier materials in CLC process with solid fuels can be enhanced by mixing such as mixing limestone with ilmenite.^{27,109,110} As for an example, in a 10 kW CLC unit with petcoke as the solid fuel, Cuadrat and co-workers¹⁰⁹ investigated the influence of adding limestone in ilmenite. Two sets of experiments were performed, in one experiment CLC was carried out with ilmenite and the other one with addition of limestone to compare the results. It was observed that adding limestone made a good improvement in conversion of gas at 950 °C and it also enhanced the conversion of char both at 950 and 1000 °C.¹⁰⁹

Some other carriers, not metal oxides, have also been used in this process because of environmental and budget concerns. One of these materials is CaSO_4 which has several benefits. It is a cheap material, it has low environmental concerns, high mechanical strength and high oxygen capacity.⁶¹ Most of the CaSO_4 material as an oxygen carrier is for CLC with gases and there is only a little research available for CLC with solid fuels. A study was performed by Zheng and co-workers¹¹¹ on a CLC system which is pressurized with CaSO_4 as the carrier material and coal as the solid fuel. For this pressurized system the temperature was optimized between 850 to 950 °C. Raising pressure in the combustor led to higher conversion and also reduction in formation of gases including H_2S and SO_2 .^{61,111} Meanwhile, there are some solutions to reduce gases with sulfur content. SO_2 is formed probably because of reactions between CaS and CaSO_4 in reduction step. To have a favorable utilization of CaSO_4 as an oxygen carrier in the CLC system, gases with sulfur content should be reduced. Few solutions that can be considered in this regard are as follows: raising reactor pressure, having reactor temperature in control and adding CaO to capture gases with sulfur content.⁶¹ Thus, by adding CaCO_3 and having the parameters of operation in system in control the extent of gases with sulfur content can be in control as well. It was demonstrated by Hen and co-workers¹¹² that between 730 to 970 °C the reactions between CaS and CaSO_4 can be stopped by raising pressure.⁶¹ It was also figured out by Jerndal and co-workers¹¹³ that working at not very high temperatures can contribute to the prevention of deactivation and decomposition of carrier materials including SrSO_4 and BaSO_4 , while at low temperatures reactivity is reduced.^{61,113} Moreover, CaCO_3 addition to reduce the gases with sulfur content is suggested by Song and co-workers.^{61,114}

2.9. Lab scale and pilot studies

2.9.1. Thermogravimetric study

Several thermogravimetric studies have been performed to evaluate the carrier materials durability and performance during long term CLC operational conditions. Eight TGA redox (reduction and oxidation) cycles for CuO as oxygen carrier with coal were performed in National Energy Technology Laboratory in United States.²⁴ TGA results showed decrease in extent of weight loss after every cycle which was because of ash accumulation. Also extent of weight gain was reduced during oxidation processes reason for which was again ash accumulation. Five TGA redox cycles were performed with CuO and Victorian brown coals including Morewell, acid washed Morwell and Loy Yang coal at Monash University in Australia.¹¹⁵ During experiments, ash was not separated after every cycle. Therefore, ash accumulation occurred in TGA pan during consecutive cycles. Results of TGA weight loss and weight gain showed a little decrease for CuO-Morwell coal. However, there was not that much decrease for CuO-acid washed Morwell and CuO-Loy Yang coal. Materials including CuO, Fe₂O₃, NiO and CoO, NiO/Ca aluminate, Wustite and fused Fe were tested for multi cycle experiments in University of Kentucky, USA.³⁴ Iron oxide and iron based catalysts were shown to be good candidates for CLC of solid fuels. Performance of CLC of AFC with CuO as an oxygen carrier was presented by our group.¹¹⁶ In our study, TGA results showed that using AFC as the solid fuel cause no ash accumulation after each cycle during multi cycle experiments. Therefore, weight loss and weight gain values remained constant after reduction and oxidation processes.

2.9.2. Large CLC units

In 2014, worldwide nine CLC units with solid fuels were operated sizes ranging from 0.5 to 100 kW.²⁷ A 10 kW system was built in Chalmers University in Sweden to test manganese ore and ilmenite as carrier material with various solid fuels including South African coal, petroleum coke, bituminous coal and pet coke.^{27,78,85,106,109,117,118} The results in preliminary studies for conversion of gas were not good but that got better with some improvements in feeding system. Regarding to this, results exhibited improvements for gas conversion to about 80% for petcoke and 77% for coal as solid fuels in CLC.²⁷ Conversion of gas were good for manganese ore with petcoke to about 87%. Steam gasification rate was also enhanced. Adding limestone enhanced gas

conversion.^{109-115,117,118} In Nanjing, China a 10kW system was designed to test carrier materials based on Fe and Ni with solid fuels such as biomass and coal.^{93,119-121} Moreover, a 1kW system was operated in Nanjing for more research on iron ore.^{105,122,123} A 0.5 kW system was built in Instituto de Carboquímica (CSIC) in Spain to test ilmenite and coal.^{27,124-127} This unit was the first system that proved 100% conversion of gas for CLOU process. Results from experiments showed that conversion of gas was about 100% with char as the solid fuel and around 70-95% for coal material with this set-up.^{27,124-127} Also a 1.5 kW CLC unit in CSIC was operated to demonstrate CLOU process with a copper-based oxygen carrier (60 wt.% CuO and MgAl₂O₄ as an inert material) prepared by spray drying method and bituminous coal as the solid fuel.⁹¹ Nearly 100% carbon capture was achieved at 960 °C. In combustor, complete combustion of coal was also reached utilizing approximately 235 kg/MW solids inventory.⁹¹ A 10 kW system was operated in IFP energies nouvelles (IFPEN) in Europe with a special design.^{27,128} This system consisted three reactors out of which two of them were functioning as oxidizer. This system was built to test an ore from nature and coal as the solid fuel. The results from experiments showed 90% conversion of gas.^{27,128}

A 25 kW CLC system in Hamburg University in Germany was designed to test lignite dust with ilmenite from Australia as carrier material.^{27,129} More than 90 % of concentration for carbon dioxide was found out in the exit gas stream from combustor.^{27,129} At Ohio University in Unites States, a 25 kW and 2.5 kW systems were designed to test various type of solid fuels and coals with iron oxide materials.^{27,130,131} The results from experiments showed more than 99% of concentration for carbon dioxide.^{27,130,131} At Chalmers University in Sweden a 100 kW system was designed to test ilmenite as the carrier material with bituminous coal from Colombia as the solid fuel and an analytical model of conversion of gas in a 100kW CLC unit with solid fuels was carried out to compare the results with experimental achievements.^{27,132-134} The experimental results showed 98% capture of carbon dioxide and maximum conversion of gas about 84% and the model described the experimental data well.^{27,132-134} Table 2.4 shows the list of operational tests carried out related to CLC of solid fuels.

Table 2.4. CLC of solid fuels in operation units ²⁷(Reprinted from Lyngfelt ²⁷, 2014, with permission from Publisher (Elsevier))

Location	Size (kW)	Oxides tested, References	Time	Fuel	Year
Chalmers	10	Ilmenite, Mn ore,[58,60,88,91,99,100]	90	Coal,petcoke	2008
Nanjing	10	NiO, Fe ₂ O ₃ , [75,101-103]	230	Coal,biom	2009
Nanjing	1	Fe ₂ O ₃ (ore),[87,104,105]	>20	Coal,biom	2010
CSIC	0.5	Ilmenite, CuO, Fe ₂ O ₃ ,[106-109]	164	Coal	2011
IFP	10	Natural ore[110]	52	Coal	2012
Hamburg	25	Ilmenite[111]	21	Coal	2012
Ohio	2.5	Fe ₂ O ₃ [112,113]	300	Solid fuels	2012
Ohio	25	Fe ₂ O ₃ [112,113]	230	Coal	2012
Chalmers	100	Ilmenite,[114-116]	23	Coal	2012

The feasibility of CLC with solid fuel has been carried assessed in the facilities close to the industrial scale.^{135,136} Preliminary results from these large units showed promising performances. One of the large systems is at Darmstadt University in Germany which is a 1 MW system. In Alstom power plant a 3 MW CLC system been operated. Experimental operations were carried out in these units and the obtained results were promising.

2.10. Modeling and optimization of CLC with solid fuel

In order to optimize CLC reactors and the whole process, several parameters need to be considered including capturing carbon dioxide, conversion of gas and conversion of solid fuel.²⁷

2.10.1. Carbon dioxide capture

In CLC process, char may enter into the air reactor during recirculation and thus, carbon dioxide sequestration and capture might not be complete. On the basis of oxygen and heat content requirement for the combustor the minimum recirculation flow can be adjusted. In fact, prediction of carbon dioxide capture and amount of char particles passing to the oxidizer is possible based on the rate of conversion of char particles and required residence time in the reducer.^{27,137-140} It is also

feasible to place a carbon stripper between oxidizer and reducer to increase conversion time and separate carrier materials and char particles in order to achieve higher carbon dioxide capture.²⁷

2.10.2. Conversion of gases

Converting the product gases from gasification step to steam and carbon dioxide with high conversion rate is an important issue. Based on the type of carrier materials and characteristics of solid fuels, 75 to 95% conversion of gas in CLC system have been reported. Higher conversion of gas was reported for the solid fuels with little or no volatile matters.²⁷ With the assumption of the feeding system that feeds the fuel in the bottom and volatile matters are released from solid fuel from bottom of the combustor, the modeling for volatile materials will be the same as for CLC with gaseous fuels in which fuels is introduced at the bottom of fuel reactor.²⁷ It is assumed that the char is physically mixed well with the carrier material and in char gasification step inside the mixture the produced syngas are released in an even manner. But beside this there are other modeling such as computational fluid dynamic (CFD) modeling and two phase modeling.^{27,134-136,139-143} The results obtained from real operational procedures exhibited lower conversion of gas produced from char gasification compared to the values obtained from modeling.^{27,141} Results from large continuous operation units, pilot plants and modeling¹³⁹ have shown that conversion of gas is incomplete.²⁷ Complete conversion of gas might be possible by utilizing CLOU process and carrier materials with special properties (e.g. being able to release gaseous oxygen through reaction and having suitable thermodynamic properties).²⁷

2.10.3. Conversion of solids

Since some unreacted char particles from the combustor entering into the gas stream the conversion of solid fuel in CLC system is not complete. The reason for this is the slow gasification step in CLC with solid fuel compared to the combustion systems; as a result more unreacted char particles leaves the reactor.²⁷ This problem can be addressed by enhancing efficiency of cyclone, raising height of reactor or utilization of an extra cyclone to collect char particles. This is an area of research where more studies are required.

2.11. Reactor design: CLC with solid fuels

Designing and optimization of a good reactor plays a key role in operating CLC system properly. Interconnected fluidized bed reactors has been utilized mostly for CLC systems because of their suitable properties in mass and heat transfer.⁶¹ Interconnected fluidized bed reactors are the main focus in designing reactors for CLC with solid fuel systems. Initially, the idea of utilizing a fluidized bed for CLC with solid fuel was proposed by Cao and co-workers.³⁵ The first system for CLC with solid fuel was a 10 kW CLC system which was operated by Berguerand and Lyngfelt.⁷⁸ The air reactor, fuel reactor, a cyclone and a riser were the main components of the system. In order to increase solid fuel residence time, the fuel reactor was built with three chambers. South African coal was utilized in the combustor for 22 hours of operation and the system had nearly stable CLC conditions for about 12 hours. In their experiments with South African coal the rate of conversions were 50 to 79% only, because of the poor separation in the cyclone.^{61,78} Based on the results of this work another experiment was carried out in this system to investigate limestone's impact on ilmenite as the carrier material in CLC with Mexican petcoke as a fuel for the process by Cuadrat and co-workers.¹⁰⁹ The conversion of gas and efficiency of the system for CO₂ sequestration (up to 86% at 1000 °C) were both increased considerably after adding limestone.^{61,109} A 10 kW system of interconnected fluidized beds was built by Shen and co-workers.⁹³ The main body of this system consists of a bed of spout shape, a fast fluidized bed as the oxidizer and a cyclone. This system was operated with iron oxide as the carrier material and biomass as the fuel for 30 hours of operation. In operating temperature 740 to 920 °C, the biomass conversion to the carbon dioxide was between 53.7-65.1%. In addition, the fuel feeding type can affect the rate of conversion. Improvement in feeding style of fuel into the system was carried out by Linderholm and co-workers¹⁰⁶ in which the volatile matter and carrier material contact was higher in the combustion reactor which caused considerable improvements in conversion of gas. Moreover, losing char to the oxidizer decreased from 28% to 2-6%. In this feeding method, using pet-coke as the solid fuel and manganese ore as the carrier material, CO₂ sequestration efficiency was about 98%.

Based on these forgoing discussion, it is evident that operating conditions plays a significant role in operating a successful CLC process and are summarized as follows; (i) allow enough contact time between air and oxygen carrier and fuel and oxygen carrier; (ii) leakage of

carbon dioxide between the two reactors should be inhibited, (iii) system may be operated under high pressure and high temperature to have full combustion; (iv) enough circulation of materials between the oxidizer and reducer.

2.11.1. Major challenges in designing CLC reactor with solid fuels

One of the challenges in reactor design and optimization is regarded as the separation of oxygen carriers from the unreacted fuel and ash particles remained after the reaction. It is essential to have well separation of oxygen carrier from unreacted fuel and ash in order to not lose the oxygen carrier. A suitable cyclone can help to increase the separation efficiency since ash particles and solid fuel have lower density compared to the carrier particles. In addition, as time passes because of reactions and attrition the particle size reduces.⁶¹ The leakage of gases between two reactors: air reactor and fuel reactor is another main issue in operation of CLC system with solid fuels, which must be minimized. This issue was addressed by Kronberger and co-workers¹⁴⁴ in which they designed a dual-fluidized bed reactor which was representative of a 10 kW CLC unit and also a flow model was designed and studied.^{61,144} They found that raising inert gas flow can monitor this issue or injecting inert gas to make an obstacle with gas in front of leaking gases can reduce gas leakage between the reactors remarkably.

For CLC with solid fuels a circulating fluidized bed system is suggested to be more appropriate. In direct solid fuel CLC system, solid fuel reactions are as follows: firstly, volatile matters are released from solid fuel and the released volatile matters react with oxygen. Then the leftover char from solid fuel are gasified to produce syngas (CO, H₂), followed by reaction of syngas from char gasification with the oxygen carrier. After solid fuel releases the volatile matters, intermediate gases contribute for the interactions between leftover char and oxygen carrier.²⁷ There are some design parameters that should be considered while designing reactor system, as follows: (i) system should avoid entering char to the oxidizer to achieve high carbon dioxide capture; (ii) system should avoid unreacted char leave the fuel reactor with exit gas stream for achieving high conversion of solid fuel; (iii) system should avoid having unreacted gases including methane and syngas (CO and H₂) for having high gas conversion in the system.²⁷

2.11.2. Technical issues and challenges of CLC with solid fuel

Direct introduction of solid fuels in the CLC process has the advantage, since there is no need of air separation unit; therefore it is cost effective. However, choosing proper oxygen carrier is an important aspect. Another important aspect is designing appropriate reactors for this system. Several technical challenges^{35,72,82-84} related to application of CLC with solid fuels include balancing pressure in the system, avoiding the entrance of unreacted char particles into the air reactor, regeneration and recycling of materials, avoiding leakages of gas between air reactor and fuel reactor, separation of carrier material from ash particles and unreacted char, energy balance and its distribution in the system when dealing with endothermic reactions in fuel reactor.

Feeding type is important in order to achieve high gas and volatile matter conversion since feeding should be in a proper way to promote sufficient contact between volatile matters and particles.²⁷ Another important point to consider is that the selected carrier materials should be inexpensive. Since most solid fuels have ash amount in common, oxygen carriers may be contaminated by the ash particles shortening the lifetime of the carrier material. Portion of carrier material might be lost while removing ash particles. The design of system should be a suitable to prevent the entry of char particles into the air reactor to maintain the total efficiency of the system. In order to complete the gasification reaction in the fuel reactor and to prevent the char entry into the oxidizer enough residence time need to be provided in the fuel reactor.

2.11.3. Suggested CLC system for solid fuels

In order to overcome the technical issues and problems related to the CLC of solid fuels, Cao and Pan,³⁵ has suggested a system consisting of a circulating fluidized bed reactors with a number of loop seals in the process (CFB with three loop seals) (Figure 2.8). In their system air reactor is an oxidizing riser, the combustor (moving bed or fluidizing bed) and separator (turbulent fluidized bed) is the larger loop seal. For balancing pressure of the system other two loop seals are applied. Separator is used for separating carrier material, ash particles and unreacted char from each other.

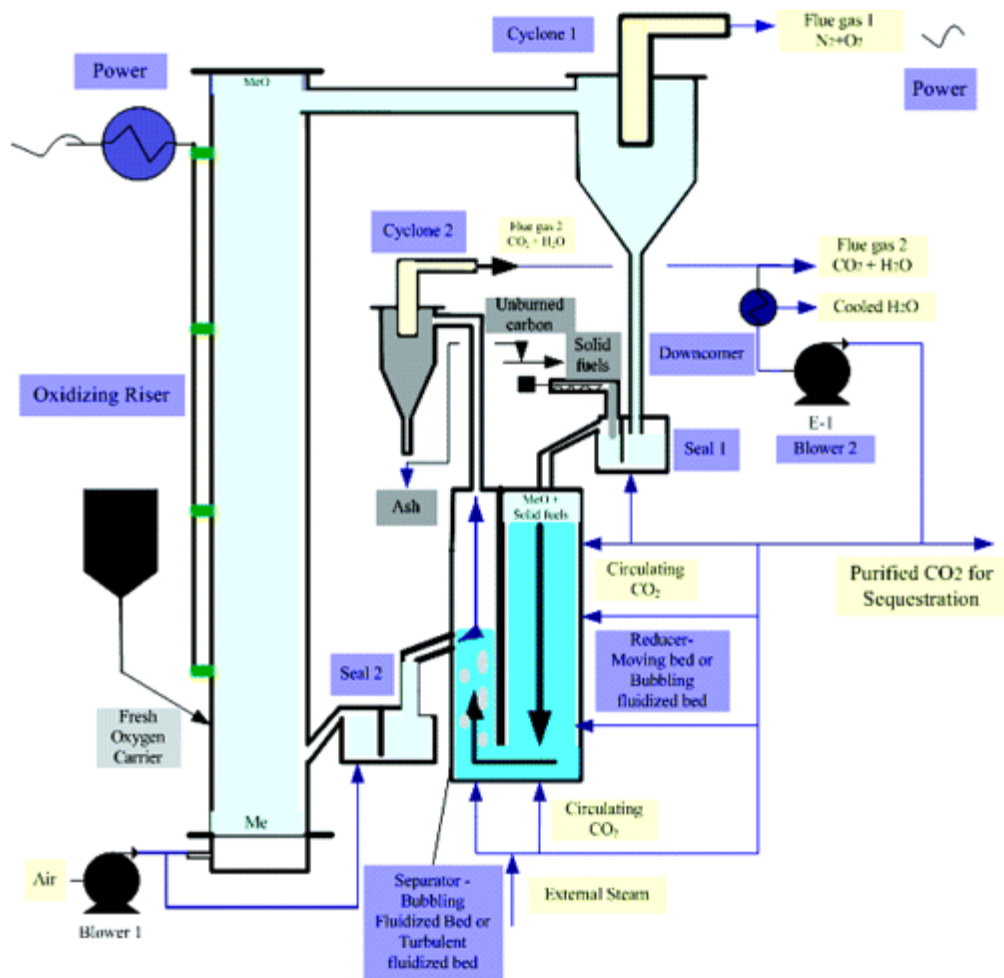


Figure 2.8. Suggested system for CLC of solid fuels by Cao and Pan³⁵

(Reprinted from Cao and Pan³⁵, 2006, with permission from Publisher (American Chemical Society))

Further, the reduced metal oxide will be oxidized by air in oxidizer. Afterwards, it passes from a separating cyclone and goes to the combustor. Recycled stream of carbon dioxide from fuel reactor or steam are the gasification agents in the system. Combustion of solid fuels occurs as the metal oxides releases oxygen. The reduced metal oxide is circulated back to the air reactor following the path of the loop seal. Then recycling of unreacted char particles to combustor will take place since they are less reactive and will be combusted in another apparatus. In order to keep the reactivity of the material in a desirable level, new carrier material can enter into the system. Because of the presence of a large volume of nitrogen in air introduced into the air reactor, the volume of gas in air reactor is significantly higher than in fuel reactor. Also in air reactor, the rate

of oxidization of the carrier material is higher than their reduction rate in the fuel reactor. The reason for choosing a bubbling fluidized bed or flow moving bed is due to the requirement of lesser volume of gas for gasification step. In addition, the residence time is long enough in the reactor for maximum conversion of solid fuel and the carrier material. The density of carrier material which is based on its porosity and is almost higher than 5000 kg/m^3 , is much heavier than density of unreacted char particle and ash particles which are between $800\text{-}1200 \text{ kg/m}^3$. Therefore, due to different densities of carrier material, unreacted char particles and ash particles they can be separated by a cyclone by adjusting a suitable velocity.³⁵

As mentioned earlier, a proper design of CLC system with solid fuels could be with two interconnected reactors in which one of them is a fast fluidized bed reactor acting as the air reactor and the other one can be moving bed or fluidized bed reactor acting as the fuel reactor.³⁵ Preventing sintering is feasible for the fluidizing or moving bed reactors in which materials are flowing. To evaluate the possibility of sintering and reduction in reactivity of the carrier materials in the system it is necessary to know the melting point of the metal oxides, the reduced forms and the metal elements. Mostly metal oxides have high melting point (more than $1200 \text{ }^\circ\text{C}$)³⁵ which are in favorable melting point ranges for CLC application. Since CLC operating temperature is between $600\text{-}1200 \text{ }^\circ\text{C}$ metal oxides that have lower melting point than $1200 \text{ }^\circ\text{C}$ will have tendency to sinter and melt in CLC application. But for the carrier materials which have high reactivity the operating temperature can be adapted with their application and can be narrowed down to a reasonable range.³⁵ For example CuO which has high reactivity but its melting point is $1083 \text{ }^\circ\text{C}$, the operating temperature can be narrowed down to $600\text{-}900 \text{ }^\circ\text{C}$ and copper based carrier material showed complete combustion and reduction in this temperature range.^{19,35,38,70} Moreover, when supports are utilized for CuO, the results showed that the maximum rate of reduction and oxidation as $100\%/min$ and $25\%/min$, respectively.^{21,30,35,43}

2.12. Energy requirement and techno-economic evaluations

The mechanism of reduction of carrier material by fuel in CLC with gaseous fuels is simpler than that of in CLC with solid fuels. Kinetics and thermodynamics are the parameters governing the mechanisms of reduction. For solid fuels, gasification and pyrolysis characteristics

of materials should be considered if the reduction mechanism is controlled by gasification of solid fuels in the system. For CLC with solid fuels there are oxidization reaction in air reactor and reduction reaction in fuel reactor. Total enthalpies summation of these parts is the same as combustion of solid fuel enthalpy.³⁵

Different carrier materials have different enthalpies and consequently reactions may be exothermic or endothermic. It is to be noted that all the reactions related to fossil fuels gasification and pyrolysis processes are endothermic. In conventional methods the needed heat amount used to be supplied by the auto thermal reaction, which is combustion of solid fuels for heat generation. But in the reducing atmosphere reduction of carrier material occurs with gasification of solid fuel simultaneously, which is the available condition for the suggested CLC, either by utilization of a material with high heat transfer to carry heat from air reactor to the fuel reactor in the system the needed heat for gasifying solid fuel is fulfilled or by reducing carrier material by solid fuel in an indirect manner or the produced gases.³⁵ The second option looks better than the first approach of providing heat supply for the system. In this way, system will save energy that can be utilized for material regeneration and so on. For CLC with solid fuels based on the thermodynamics and characteristics study of carrier materials, it was found that CuO, NiO and CoO are expected to be more suitable carrier materials since all these materials have higher oxygen transfer properties than others.

The only option for auto thermal system is utilization of exothermic carrier materials based on copper.³⁵ The special characteristics of copper based carrier materials make the system more simplified. Copper based materials have high reactivity at 600-900 °C.^{19,38,70} By reducing the operating temperature of CLC system and narrowing it down to 600-900 °C, the drawback of copper based carrier materials (low melting temperature and their sintering tendencies) will be overcome.³⁵ Iron based carrier materials have several drawbacks including low reactivity and endothermic reduction reactions. Also carrier materials based on manganese have several drawbacks including thermodynamic constraints for carbon dioxide purification, low melting temperature, endothermic reduction reactions and low oxygen transfer capacity.³⁵

2.13. Economic consideration of CLC with solid fuels

Since, there is no need of air separation unit in CLC with solid fuels; this system is considered as an economic with less or no energy penalty. The energy penalty for CLC systems is similar with the energy consumption for compressing carbon dioxide, which is 2.5% units in ideal case.²⁷ The techniques used to compensate the incomplete conversion in reducer, for example oxygen polishing unit, will consume additional energy and add cost for operating the system.²⁷ As for example an energy penalty of 0.6%-units will be for an air separation of 0.25 kW h/kg¹⁴⁵ oxygen and 90% conversion of gas.²⁷ More studies were carried out by Kempkes and Kather¹⁴⁶ on carbon dioxide capture and sequestration and efficiency of consumed energy caused by unreacted gases.²⁷ Also additional energy consumption is for the steam utilization for the combustor and loop seals.^{27,147}

A circulating fluidized bed unit in industry would have several numbers of common features with a power plant utilizing CLC with solid fuel.²⁷ The oxidizer would be almost similar. The oxidizer is much larger than the adiabatic reducer. It is noteworthy that a CLC unit will have additional expenses compared to a circulating fluidized bed unit. Overall, CLC has a good potential for decreasing the expenses and energy penalties for carbon dioxide capture.

An initial design of 455 MW CLC system with solid fuel unit was carried out in the European project ENCAP (ENhanced CAPture of CO₂).¹⁴⁸ Significantly low expenses for carbon dioxide capture and efficiency penalty was shown (10 €/tone of carbon dioxide)¹⁴⁸ compared to a combustion unit which has fluidized bed mode.²⁷ Compression of carbon dioxide showed high expenses. Apparently, utilization of techniques to compensate incomplete conversion of gas contributes to more energy penalties. CLC with pet coke, coal and natural gas looks good potential candidate and promising in economic evaluations due to the lower expenses and enhanced electric efficiencies, however, more investigation and studies are required.¹⁴² The expenses in order to have a reasonable carbon dioxide capture and sequestration unit, conversion of gas and fuels are not yet been available in the literature.²⁷

Another benefit of CLC system is that flue gases in the exit gas stream of oxidizer is free of SO_x and NO_x, therefore cost associated with SO_x, and NO_x control is not involved. Generally, the main criteria for cost estimation of optimized reducer in CLC system with solid fuel are as

follows: cost of combustion unit, expenses for additional energy consumption for completing gas conversions and cost for carrier materials.²⁷ More investigation and research is required to understand the optimized system for CLC with solid fuel specially the fuel reactor, where complex mechanisms and processes are involved. Overall, CLC with solid fuel is a promising technology and has a large capability to decrease the costs, expenses and additional energy consumptions for carbon dioxide sequestration.

In order to monitor purification of carbon dioxide, thermodynamics should be highly considered. For different CLC temperatures for the gasifying solid fuels and reducing carrier materials, calculations can be carried from equilibrium parameters. Solid fuel gasification products include carbon monoxide, hydrogen and methane gases. Carrier material reduction is more exothermic for CO compared to hydrogen gas as the produced gases from solid fuel gasification. But at high operating temperatures CO is not reducing carrier material as well as hydrogen gas and hydrogen functions better in this regard. Also methane is more reactive for carrier material reduction compared to the produced syngas at high operating temperatures which has been proven by thermodynamic calculations.³⁵ To have better understanding of thermodynamics of CLC and oxygen carriers used in the process, it is noteworthy to consider physical properties of oxygen carriers including their melting temperatures. Moreover, enthalpies of reduction reactions of various oxygen carriers in fuel reactors are important to consider precisely.

Table 2.5 presents the physical properties of different oxygen carriers. Also Table 2.6 presents enthalpies of reduction reaction of different oxygen carriers by carbon at 1000 °C and P equals to 1 atm.

Table 2.5. Physical properties of oxygen carriers^{35,149}(Reprinted from Cao and Pan³⁵, 2006, with permission from Publisher (American Chemical Society))

Reduction reaction	Melting point of the reduced metal		Melting point of the oxidized metal	
	form °C		form °C	
$2\text{CuO} + \text{C} = 2\text{Cu} + \text{CO}_2$	1083		1026	
$2\text{Cu}_2\text{O} + \text{C} = 4\text{Cu} + \text{CO}_2$	1083		1235	
$2\text{NiO} + \text{C} = 2\text{Ni} + \text{CO}_2$	1452		1452	
$2\text{Co}_3\text{O}_4 + \text{C} = 6\text{CoO} + \text{CO}_2$	1480		895	
$1/2\text{Co}_3\text{O}_4 + \text{C} = 3/2\text{Co} + \text{CO}_2$	1480		895	
$2\text{CoO} + \text{C} = 2\text{Co} + \text{CO}_2$	1480		1800	
$6\text{Mn}_2\text{O}_3 + \text{C} = 4\text{Mn}_3\text{O}_4 + \text{CO}_2$	1564		1080	
$2\text{Mn}_2\text{O}_3 + \text{C} = 4\text{MnO} + \text{CO}_2$	1650		1080	
$2/3\text{Mn}_2\text{O}_3 + \text{C} = 4/3\text{Mn} + \text{CO}_2$	1260		1080	
$2\text{Mn}_3\text{O}_4 + \text{C} = 6\text{MnO} + \text{CO}_2$	1650		1564	
$1/2\text{Mn}_3\text{O}_4 + \text{C} = 3/2\text{Mn} + \text{CO}_2$	1260		1564	
$2\text{MnO} + \text{C} = 2\text{Mn} + \text{CO}_2$	1260		1650	
$6\text{Fe}_2\text{O}_3 + \text{C} = 4\text{Fe}_3\text{O}_4 + \text{CO}_2$	1538		1560	
$2\text{Fe}_2\text{O}_3 + \text{C} = 4\text{FeO} + \text{CO}_2$	1420		1560	
$2/3\text{Fe}_2\text{O}_3 + \text{C} = 4/3\text{Fe} + \text{CO}_2$	1275		1560	
$2\text{Fe}_3\text{O}_4 + \text{C} = 6\text{FeO} + \text{CO}_2$	1420		1538	
$1/2\text{Fe}_3\text{O}_4 + \text{C} = 3/2\text{Fe} + \text{CO}_2$	1275		1538	
$2\text{FeO} + \text{C} = 2\text{Fe} + \text{CO}_2$	1275		1420	
$2\text{PbO} + \text{C} = 2\text{Pb} + \text{CO}_2$	327.5		886	
$2\text{CdO} + \text{C} = 2\text{Cd} + \text{CO}_2$	320.9		900	

Table 2.6. Enthalpies of reduction reactions reduced by carbon at 1000 °C and 1 atm (Calculations based on data from reference 149)^{35,149}(Reprinted from Cao and Pan³⁵, 2006, with permission from Publisher (American Chemical Society))

$\text{C} + \text{O}_2 \longrightarrow \text{CO}_2, -392.75 \text{ kJ/mol}$			
endothermic		exothermic	
$2\text{NiO} + \text{C} \longrightarrow 2\text{Ni} + \text{CO}_2,$	75.21 kJ/mol	$2\text{CuO} + \text{C} \longrightarrow 2\text{Cu} + \text{CO}_2,$	-96.51 kJ/mol
$2\text{CoO} + \text{C} \longrightarrow 2\text{Co} + \text{CO}_2,$	73.92 kJ/mol	$2\text{Cu}_2\text{O} + \text{C} \longrightarrow 4\text{Cu} + \text{CO}_2,$	-61.04 kJ/mol
$1/2\text{Co}_3\text{O}_4 + \text{C} \longrightarrow 3/2\text{Co} + \text{CO}_2,$	53.9 kJ/mol	$6\text{Co}_3\text{O}_4 + \text{C} = 6\text{CoO} + \text{CO}_2,$	-8.63 kJ/mol
$2/3 \text{Mn}_2\text{O}_3 + \text{C} = 4/3\text{Mn} + \text{CO}_2,$	239.61 kJ/mol	$6\text{Mn}_2\text{O}_3 + \text{C} = 4\text{Mn}_3\text{O}_4 + \text{CO}_2,$	-216.63
		kJ/mol	
$6\text{Mn}_3\text{O}_4 + \text{C} = 4 \text{MnO} + \text{CO}_2,$	54.21 kJ/mol	$2\text{Mn}_2\text{O}_3 + \text{C} = 4 \text{MnO} + \text{CO}_2,$	-36.07 kJ/mol
$1/2\text{Mn}_3\text{O}_4 + \text{C} \longrightarrow 3/2\text{Mn} + \text{CO}_2,$	296.65 kJ/mol		
$2\text{MnO} + \text{C} \longrightarrow 2\text{Mn} + \text{CO}_2,$	378.98 kJ/mol		
$6\text{Fe}_2\text{O}_3 + \text{C} \longrightarrow 4\text{Fe}_3\text{O}_4 + \text{CO}_2,$	83.56 kJ/mol		
$2\text{Fe}_2\text{O}_3 + \text{C} \longrightarrow 4\text{FeO} + \text{CO}_2,$	158.40 kJ/mol		
$2/3\text{Fe}_2\text{O}_3 + \text{C} \longrightarrow 4/3 \text{Fe} + \text{CO}_2,$	146.37 kJ/mol		
$2\text{Fe}_3\text{O}_4 + \text{C} = 6\text{FeO} + \text{CO}_2,$	195.78 kJ/mol		
$1/2\text{Fe}_3\text{O}_4 + \text{C} = 3/2 \text{Fe} + \text{CO}_2,$	151.27 kJ/mol		
$2\text{FeO} + \text{C} = 2\text{Fe} + \text{CO}_2,$	136.44 kJ/mol		

In the GRACE project, based on the obtained data a lifetime of up to 40000 hours was proposed for the particles and the required mass was determined using the rate of reaction parameters.¹⁵⁰ The cost of oxygen carrier was proposed 1 €/tonne CO₂ capture based on the presumptions and 4000 hours of lifetime.¹⁵⁰ Table 2.7 presents expenses for NiO-based carriers.

Cormos and Cormos¹⁵¹ investigated CLC plant with direct utilization of coal. Results showed that the system can have more than 99% of CO₂ capture and about 42% of electrical efficiency.¹⁵¹

Table 2.7. Expenses for NiO-based carriers¹⁵⁰
(Reprinted from Lyngfelt and co-workers¹⁵⁰, 2005, with permission from Publisher (Elsevier))

particle inventory ¹	0.1 – 0.2	ton/MW	¹ Somewhat uncertain value, but without doubt in the correct order of magnitude
lifetime ²	4000	h	² Loss of fine material in prototype tests suggests a lifetime that is 10 times longer, i.e. 40 000 h.
specific particle cost ³	4	€/kg	³ If fine material lost in the process can be used as raw material in the production, the costs can be decreased significantly, but not below the production cost of approximately 1 €/ton.
specific emission	0.2	Ton CO ₂ /MWh	
resulting particle cost	0.5 - 1	€/ton CO ₂ captured	

2.14. Mass and energy balance of CLOU process

In this section CLOU system is analyzed and techno-economic evaluations and scale up considerations are discussed more in detail. Peltola and co-workers¹⁵² analyzed a hypothetical CLOU system as shown in Figure 2.9. This scheme of CLOU consists of an air reactor and a fuel reactor which are both circulating fluidized bed ones. Oxygen carrier material is transferring oxygen between two reactors as indicated in figure with flux 7 and 8. Atmospheric air is the input for the air reactor (flux 2) and bituminous coal is the feed for fuel reactor (flux 1). The exit gas from air reactor mostly consist of nitrogen and the remaining oxygen (flux 3). The feed in fuel reactor is fluidized with the recycled flue gas (flux 5). Ash is eliminated from fuel reactor (flux 6). Cooling systems is considered for air reactor, fuel reactor and recirculation of gas section (flux 11, 12, 13). Each flux description is also given in the figure. Three different boundaries for the system are defined as shown in Figure 2.9.¹⁵²

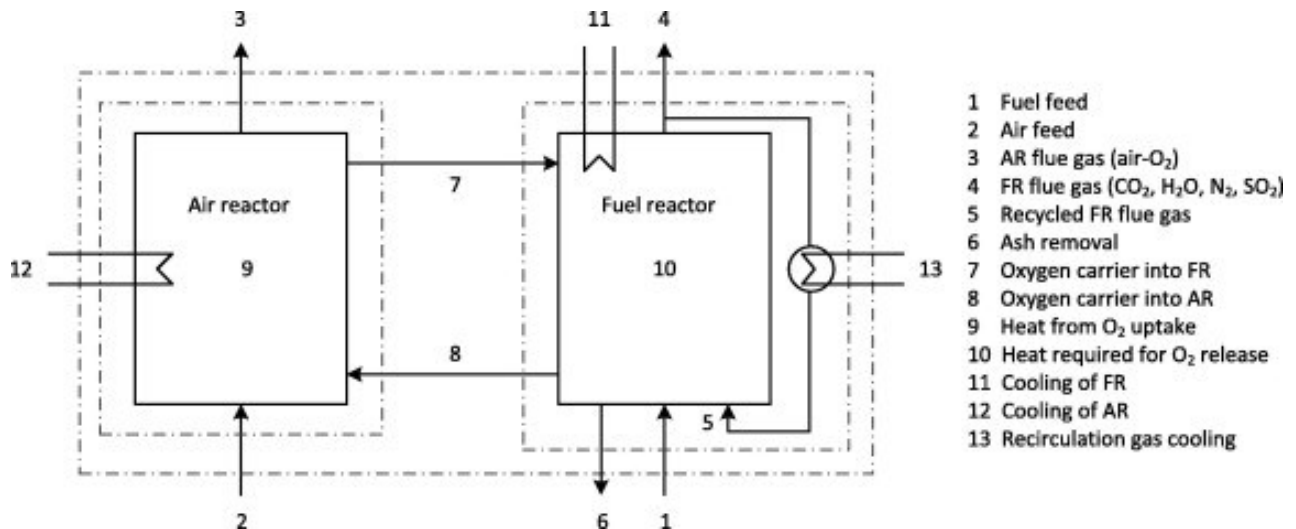


Figure 2.9. Analyzed CLOU system consisting of two interconnected fluidized bed reactors (Three boundaries are defined in the Figure with dash lines)¹⁵²

(Reprinted from Peltola and co-workers¹⁵², 2014, with permission from Publisher (Elsevier))

The properties of bituminous coal used for the analysis is shown in Table 2.8. CuO as the oxygen carrier is used because of its special properties and releasing oxygen capabilities. The reaction of CuO to uptake or release oxygen in a CLOU system is as follows;¹⁵²



Table 2.8. Medium volatile bituminous coal's properties¹⁵²
 (Reprinted from Peltola and co-workers¹⁵², 2014, with permission from Publisher (Elsevier))

Fuel properties	
Proximate analysis wt(%)	
Moisture	4.2
Volatiles	25.5
Ash	14.4
Fixed carbon	55.9
Ultimate analysis wt(%)	
C	69.3
H	3.9
N	1.9
S	0.9
O	5.4
LHV(MJ/Kg)	25.5

On the basis of studies and experiments with CuO-based oxygen carriers, proper temperatures for air reactor are in the range of 850 to 900 °C and for fuel reactor are in the range of 900 to 950 °C.¹⁵²⁻¹⁵⁵

In order to analyze, several assumptions were considered for the system such as complete fuel conversion, negligible ash accumulation in oxygen carrier material, not considering the compensating oxygen carrier stream.¹⁵²

For investigation of CLOU oxygen carrier's kinetic a few studies experimentally were carried out in literature.¹⁵⁶

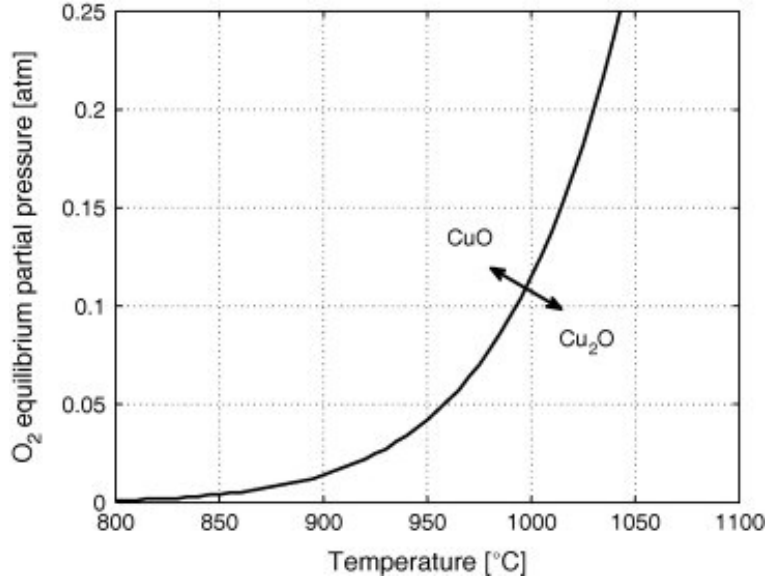


Figure 2.10. Oxygen equilibrium pressure of CuO/Cu₂O with temperature¹⁵²
 (Reprinted from Peltola and co-workers¹⁵², 2014, with permission from Publisher (Elsevier))

Oxygen equilibrium partial pressures at different temperatures for CuO/Cu₂O are shown in Figure 2.10. As seen in this Figure with increase in temperature, oxygen equilibrium partial pressure increases. Thermodynamic driving force which is on the basis of difference between oxygen equilibrium partial pressure and real partial pressure effects the rate of reduction or oxidation of oxygen carrier in both reactors in a CLOU process.^{152,157-159} The overall rate equation is as follows:¹⁵⁷

$$r = kf(X)f(p_{O_2,eq}) \quad (2-13)$$

In this equation, the effective parameter for equilibrium partial pressure of oxygen is defined as $f(p_{O_2,eq})$. Another important parameter which relies on the effects of changes in solid and mechanism of reaction is function of conversion defined as $f(X)$. The Arrhenius equation determines the kinetic rate constant known as k .¹⁵²

$$k = A \exp(-E/R_u T) \quad (2-14)$$

In this equation, kinetic parameters are known as A and E , temperature is expressed with T and universal gas constant is indicated with R_u .¹⁵²

Driving force of oxygen for oxidation and reduction processes (reaction order not considered) are shown as follows.¹⁵²

$$f(p_{O_2,eq})|_{\text{oxd}} = (p_{O_2} - p_{O_2,eq}) \quad (2-15)$$

$$f(p_{O_2,eq})|_{\text{red}} = (p_{O_2,eq} - p_{O_2}) \quad (2-16)$$

The oxygen carrier's oxygen equilibrium partial pressure is determined by calculations on the basis of thermodynamic data (relied on values of Gibbs free energy of O₂, Cu₂O and CuO) at different temperatures. Based on these calculations, [Eq. 2-17] is acquired.¹⁵⁷

$$p_{O_2,eq} = \exp [-9.383 (1000/T)^4 + 47.54 (1000/T)^3 - 86.30(1000/T)^2 + 48.45 (1000/T) - 2.473] \quad (2-17)$$

In this analysis to make the work easier, conversion is considered as a first order expression. Peterson and co-workers¹⁵⁵ determined the rate constants [K_{CuO} (decomposition) and K_{Cu_2O} (oxidation)] in the operating temperature range of 850 °C to 950 °C for CuO (40 wt% CuO) supported with SiO₂ (60 wt% SiO₂) known as CuO40SiO₂ which are shown in Figure 2.11.¹⁵²

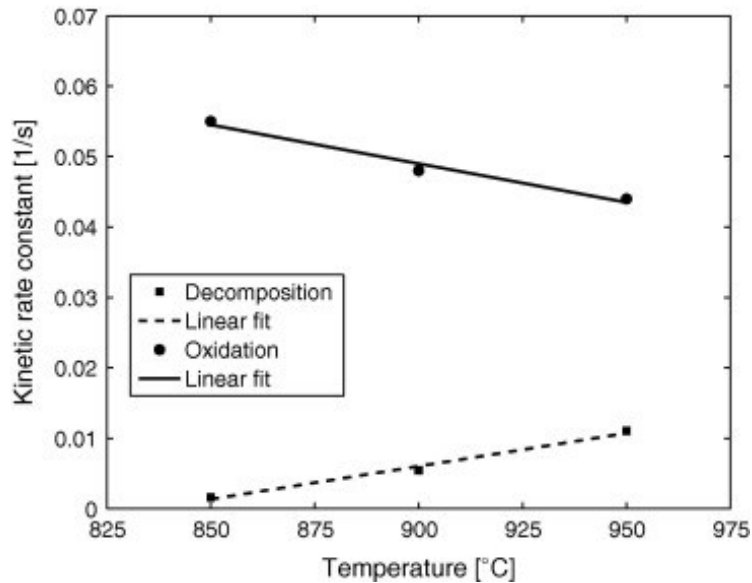


Figure 2.11. Kinetic rate constants for CuO40SiO₂ as a carrier material ^{152,155}
 (Reprinted from Peltola and co-workers¹⁵², 2014, with permission from Publisher (Elsevier))

Regarding to Figure 2.9, the mass balance in a steady state for the system is as follows. “ \dot{m}_i ” is representative of mass flow rate of stream “i” in the system. As a \dot{m}_i value, input is positive and output is negative.¹⁵²

$$\sum_i \dot{m}_i = 0 \quad (2-18)$$

The consumed fuel (with the assumption of complete conversion of fuel) is as follows.¹⁵²

$$\dot{m}_{\text{fuel}} = P_{\text{fuel}} / \text{LHV} \quad (2-19)$$

In this expression, power of fuel is defined as P_{fuel} and lower heating value of fuel is shown by LHV. For the stoichiometric combustion of fuel, the amount of needed oxygen is expressed as follows.¹⁵²

$$\Omega = w_c/M_c + 1/4(w_H/M_H) + w_s/M_s - 1/2(w_o/M_o) \quad (2-20)$$

In this expression the weight fraction is defined as w_c and component c’s molar mass in fuel is shown as M_c . On the basis of ultimate and proximate analysis of fuel the amount of required oxygen (Ω , mol O_2 /kg fuel) can be obtained. The mass flow rates of oxygen and air are also given as follows.¹⁵²

$$\dot{m}_{O_2} = M_{O_2} \Omega \dot{m}_{\text{fuel}} \quad (2-21)$$

$$\dot{m}_{\text{air}} = \dot{m}_{O_2} \lambda / 0.233 \quad (2-22)$$

In the expression for the feed rate of air, the value of 0.233 is related to oxygen mass fraction in air global air/fuel ratio is defined as λ .¹⁵² The oxygen carrier’s circulation rate is defined as follows.¹³

$$\dot{m}_{OC} = [1 + R_o w_{CuO}(X_{AR} - 1)] \dot{m}_{\text{oxd}} \quad (2-23)$$

In this expression the circulation rate of the oxygen carrier completely oxidized is shown as \dot{m}_{oxd} which is expressed as [Eq. 2-24]. In this relation, w_{CuO} is CuO mass fraction in materials and oxygen ratio is defined as R_o . Oxygen ratio is showing the mass fraction of oxygen in the oxygen carrier [Eq. 2-25].¹⁵²

$$\dot{m}_{\text{oxd}} = \dot{m}_{O_2} / (w_{CuO} R_o \Delta X) \quad (2-24)$$

$$R_O = 1 - (m_{\text{red}}/m_{\text{oxd}}) \quad (2-25)$$

In this relation, completely reduced and oxidized materials' masses are indicated as m_{red} and m_{oxd} . Also between air reactor and fuel reactor, the difference conversion is defined as $\Delta X = X_{\text{AR}} - X_{\text{FR}}$. X_{AR} expresses conversion in air reactor and X_{FR} stands for conversion in fuel reactor. The conversion is shown as follows.¹⁵²

$$X = m_{\text{oxd}} / (m_{\text{oxd}} + m_{\text{red}}) \quad (2-26)$$

For reduction of CuO, the needed residence time of particles with the assumption of a plug-flow reactor is as follows.¹⁵³

$$\tau_{\text{FR}} = 1/K_{\text{CuO}} \ln(1 / (1 - (\Delta X / X_{\text{AR}}))) \quad (2-27)$$

Also the needed residence time of particles for oxidation of Cu₂O is expressed as follows.¹⁵²

$$\tau_{\text{AR}} = 1/K_{\text{Cu}_2\text{O}} \ln(1 / (1 - (\Delta X / (1 - X_{\text{FR}})))) \quad (2-28)$$

Finally, the needed mass of oxygen carrier in the process is obtained as follows.¹⁵²

$$m_{\text{OC}} = \dot{m}_{\text{OC}} (\tau_{\text{FR}} + \tau_{\text{AR}}) \quad (2-29)$$

First law of thermodynamics for the analysis and few assumptions such as neglecting the energy changes are considered for the energy balance of the system. Regarding this, the system energy balance is expressed as follows.¹⁵²

$$\sum_i \dot{m}_i h_i + \sum_j Q_j + \sum_k r_k \Delta H_{c,k} = 0 \quad (2-30)$$

In this equation, stream i enthalpy is defined as h_i , the heat flow j which is transferred between environment and system is defined as Q_j , rate of reaction is indicated as r_k and combustion heat is shown as $\Delta H_{c,k}$. In the energy balance, input has a positive value and output has a negative value. A stream of gas total enthalpy is defined as follows.¹⁵²

$$h_{\text{gas}} = \sum_c w_c h_c \quad (2-31)$$

In this relation w_c stands for weight fraction of c constituent in the stream and h_c is defined as specific enthalpy of c constituent.¹⁵² Based on work of Gyftopoulos and Beretta¹⁶⁰, h_c can be obtained as follows. In this calculation a, b, c and d are constants as shown in Table 2.9.

$$h_c = aT + 1/2bT^2 + 1/3cT^3 + 1/4dT^4 \quad (2-32)$$

Table 2.9. Constant values for calculating enthalpy of gases^{152, 160}
(Reprinted from Peltola and co-workers¹⁵², 2014, with permission from Publisher (Elsevier))

Gas	a	b	c	d
CO ₂	19.8	73.4	-56.0	17.2
H ₂ O (g)	32.3	1.9	10.6	-3.6
N ₂	31.2	-13.6	26.8	-11.7
O ₂	28.1	0.0	17.5	-10.7

The enthalpy of oxygen carrier is defined as follows. Based on work of Chase¹⁶¹ the enthalpies of CuO, Cu₂O and SiO₂ are acquired. If not having good understanding of composition of ash, it will be assumed as SiO₂ and on this basis the enthalpy is obtained.¹⁵²

$$h_{OC} = w_{CuO} [Xh_{CuO} + (1-X)h_{Cu_2O}] + (1-w_{CuO})h_{SiO_2} \quad (2-33)$$

The properties of selected oxygen carrier is effecting the operating conditions for the CLOU process, but for any selected oxygen carrier in the system the procedure of calculations would be the same as mentioned in this section.¹⁵²

2.14.1. Residence time of particles

Based on the relations [2-27, 2-28] and using the kinetics of CuO/40SiO₂, the needed solids residence time for the determined conversion can be obtained. For low inventories of particles, ΔX with the range of 0.2 to 0.4 was proposed in literature.¹⁶² Therefore, with ΔX=0.3 and variable values for X_{AR}, residence time of particles are acquired as shown in Figure 2.12.¹⁵² Based on this Figure, with increase in temperature the required residence time for CuO reduction is decreased (e.g. from 249s at 850 °C to 37s at 950 °C). But for oxidation of Cu₂O with increase in temperature the required residence time is increased too (e.g. from 12s at 850 °C to 16s at 950 °C).¹⁵²

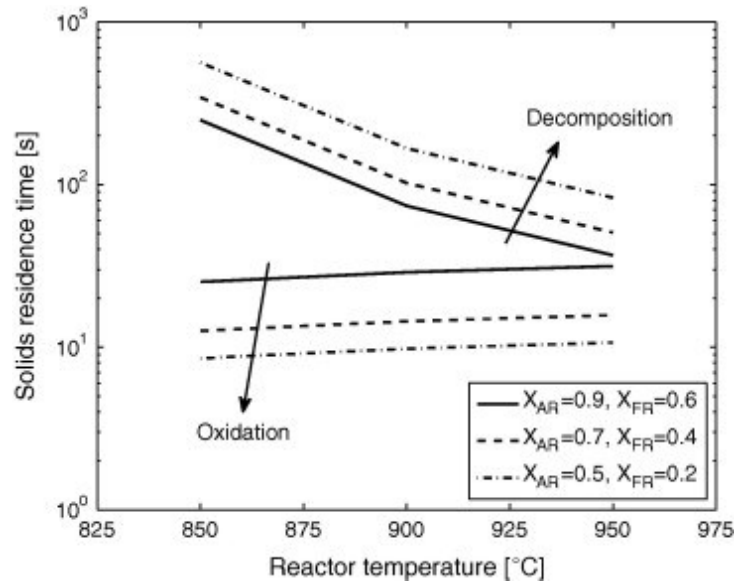


Figure 2.12. Reactors' solid residence time (variable values for X_{AR} , $\Delta X = 0.3$)¹⁵²
 (Reprinted from Peltola and co-workers¹⁵², 2014, with permission from Publisher (Elsevier))

2.14.2. Solid inventory

The inventory of particles in the process depends on reactivity, type of oxygen carrier used in the system, conversion at air reactor and fuel reactor inlets and circulation of particles.¹⁵² The solid inventory is obtained based on the assumptions for the analysis of the system mentioned earlier. However, the solid inventory and time for reactions in actual cases can be estimated higher. Figure 2.13 shows minimum solid inventory of the system for different values of ΔX at a certain value of X_{AR} .¹⁵²

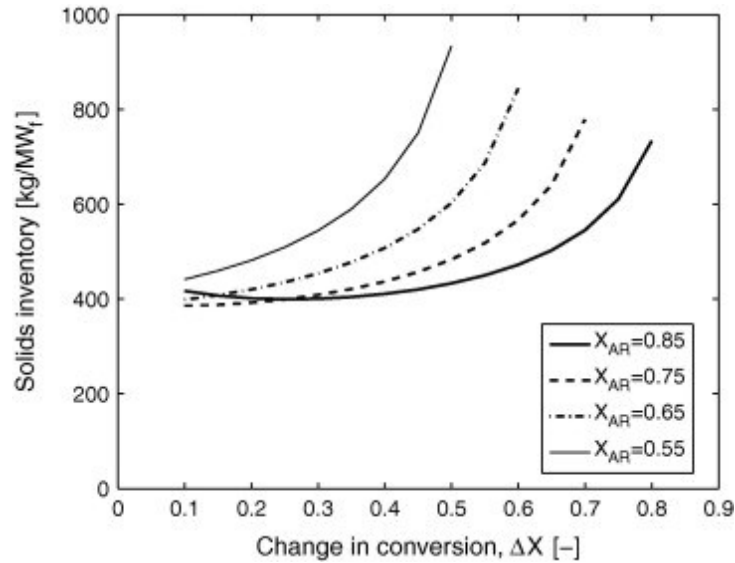


Figure 2.13. Solid inventory as a function of the conversion's change (ΔX) for variable X_{AR} ($T_{AR}=850$ °C, $T_{FR}=950$ °C)¹⁵²

(Reprinted from Peltola and co-workers¹⁵², 2014, with permission from Publisher (Elsevier))

For stoichiometric combustion, about 400 kg/MW_f is the minimum value for solid inventory of system.¹⁵² Arjmand and co-workers¹⁶³ investigated the kinetics of reaction for 40 wt % CuO/MgAl₂O₄ as the carrier material in the system. Relying on these studies considering use of char as the solid fuel, the estimation for solid inventory was around 73 to 147 kg/MW_f.¹⁵² A set of experiments were performed in a CLOU process using 60 wt % CuO/MgAl₂O₄ by Abad and co-workers⁹¹. In these experimental procedures bituminous coal was converted completely to carbon dioxide with application of 240 kg/MW_f solids inventory.¹⁵² Adanez-Rubio and co-workers¹⁶⁴ continued the works with this CLOU system and the similar carrier material to perform experiments with various coals as the solid fuel. It was understood that for 95% efficiency of carbon dioxide capture, a solid inventory up to 490 kg/MW_f is required in the combustor.¹⁵² Figure 2.14 shows the minimum solid inventory for various temperatures used for air reactor and fuel reactor in the system.¹⁵²

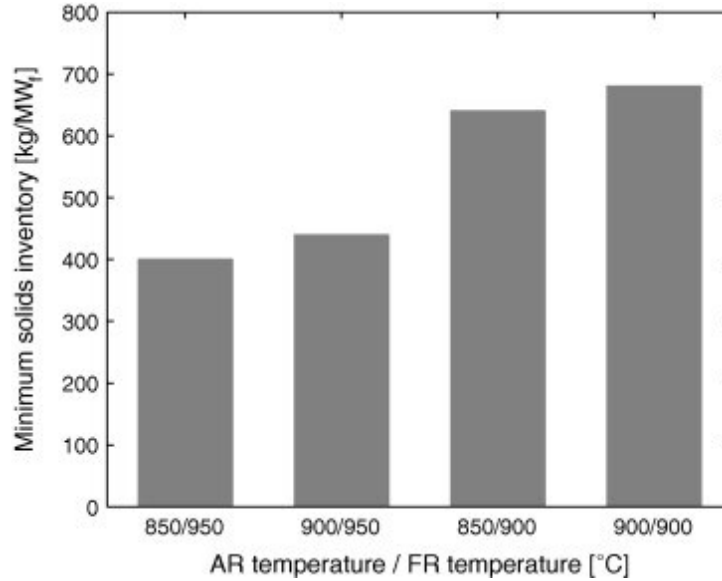


Figure 2.14. Obtained minimum solid inventory for various combinations of temperatures for air reactor and fuel reactor¹⁵²

(Reprinted from Peltola and co-workers¹⁵², 2014, with permission from Publisher (Elsevier))

Considering total heat balance of the process, the circulation rate of solid can distinguish the maximum difference of temperatures between air reactor and fuel reactor.¹⁵² The oxygen carrier which is exiting the air reactor with low temperature should be heated to reach the fuel temperature. In this case, negative heat balance would be obtained if oxygen carrier needs very high energy. Based on this, difference of temperatures between air reactor and fuel reactor up to 50 °C can be possible for CuO-based oxygen carriers considering ΔX value in the range of 0.2 to 0.4.¹⁵² For stoichiometric combustion in the system, minimum solid inventory of 400 to 680 kg/MW_f is required based on the obtained kinetics for CuO/40 SiO₂.¹⁵²

2.15. Model of fuel reactor

The fuel reactor behavior has a key role in a successful CLOU process. Therefore, a one-dimensional (1D) fluidized bed model for a CLOU fuel reactor is considered with fast fluidization regime.¹⁶⁵⁻¹⁶⁷ In this model a CuO-based oxygen carrier supported with TiO₂ is used with a bituminous coal as the solid fuel.¹⁶⁵

In order to increase the capture of carbon in the system a carbon stripper which is used as a separation unit can be utilized between air reactor and fuel reactor.¹⁶⁸ A very high char conversions of 95% and higher values have been reported for CLOU system.^{91,164} While having high conversion, it is not necessary to add another unit in the process, but if solid fuels with lower reactivity are used in the system then carbon stripper can be a proper choice.¹⁶⁵

On the basis of work of Clayton and co-workers¹⁶⁹, a model for release of oxygen is used. They developed a kinetic expression for CuO-based oxygen carrier. In Table 2.10 the details of the model and parameters for a CuO-based oxygen carrier consisting 50 wt% of CuO/Cu₂O and 50 wt% of TiO₂ are presented.¹⁶⁵

Table 2.10. Kinetic model's parameters for oxygen release^{165, 169}
(Reprinted from Peltola and co-workers¹⁶⁵, 2015, with permission from Publisher (Elsevier))

Item	Value	Unit
f(X)	X _{OC}	-
f(p _{O2,eq})	(p _{O2,eq} - p _{O2}) ^β	Pa
f(T)	Aexp(-E/(R _u T))	1/(Pa s)
A	4.15*10 ⁻⁸	1/(Pa s)
E	67*10 ³	J/mol
β	1.0	-
R _u	8.314	J/(mol K)

The conversion of oxygen carrier is defined according to [Eq. 2-26]. Table 2.11 shows the properties of bituminous coal used in the analysis.¹⁶⁵

Table 2.11. Bituminous coal's properties applied in modelings ¹⁶⁵
 (Reprinted from Peltola and co-workers¹⁶⁵, 2015, with permission from Publisher (Elsevier))

Fuel property	
Proximate analysis (wt%)	
Char	56
Volatiles	27
Moisture	7
Ash	10
Ultimate analysis (wt%)	
C	79.4
H	4.1
S	1.6
N	0.9
O	14
LHV, wet (MJ/kg)	25.16
Char particle diameter (mm)	0.5
Char particle density (kg/m ³)	1000

On the basis of operating parameters and design factors listed in Table 2.12, the main results from the simulation is presented in Table 2.13 for the 500 MW_{th} CLOU fuel reactor using CuO-based oxygen carrier and bituminous coal as the solid fuel. No carbon stripper was considered in the simulation in the process.¹⁶⁵

Table 2.12. Parameters of operation ¹⁶⁵(Reprinted from Peltola and co-workers¹⁶⁵, 2015, with permission from Publisher (Elsevier))

Parameter	Value	Unit
Fuel reactor		
Fuel input	19.8	kg/s
Total height	35	m
Sloped section height	14	m
Elevation to outflow channel	33.3	m
Freeboard cross-sectional area	121	m ²
Grid cross-sectional area	84	m ²
Oxygen carrier inventory	400	kg/MW _f
Gas velocity	5.0	m/s
Temperature	960	°C
Flue gas recirculation		
Mass flow	168	kg/s
Input temperature	450	°C
Oxygen carrier		
Active phase	CuO/Cu ₂ O	—
Inert phase	TiO ₂	—
CuO/Cu ₂ O content	50	wt%
Apparent density	4650	kg/m ³
Particle size	0.1	mm
Solids entering fuel reactor		
Degree of oxidation	1	—
Temperature	945	°C

Table 2.13. Obtained results from the simulation of reference ¹⁶⁵(Reprinted from Peltola and co-workers¹⁶⁵, 2015, with permission from Publisher (Elsevier))

Parameter	Value	Unit
Char conversion	84.7	%
CO ₂ capture efficiency	89.2	%
OC decomposition rate	10.2	% _{OC} /min
Total O ₂ released	34.0	kg/s
Total O ₂ consumed	31.7	kg/s
Change in OC conversion	0.223	—
Average reactor temperature	960	°C
Reactor cooling duty	23.9	MW
Gas flow at outlet	217.2	kg/s
Solids entrainment flux	12.2	kg/(m ² s)
Solids residence time	136	s
Pressure drop	16.1	kPa

For the solid inventory in the fuel reactor, the simulation showed that with increase in the solid inventory from 50 kg/MW_f to 750 kg/MW_f, the rate of circulation for the materials was enhanced from 2.3 kg/m²s to 20.4 kg/m²s.¹⁶⁵ Moreover the residence time of solids was increased from 92 s to 153 s and because of more conversion of char in the system, the efficiency of carbon capture was enhanced from 79.3 % to 90.5 %.¹⁶⁵

2.16. Conclusions

In this Chapter, initially, the general concept of CLC was reviewed followed by oxygen carrier materials, the synthesis methods and parameters of operation. Afterwards, backgrounds of CLC of solid fuels with oxygen carriers that have been widely used were reviewed. The designing parameters for reactors, selection of proper oxygen carriers including the technical issues and challenges followed by energy requirement and techno-economic evaluations were discussed. The technology of CLC with solid fuels is the same as CLC with other fuels consist of interconnected circulating fluidized bed reactors. Using CLC with solid fuels for combustion of coal and fossil fuels which are more abundant in nature contribute to decrease the expenses and additional energy consumptions and penalties.

Among potential candidates as oxygen carriers, Cu based materials are most promising ones because of their special suitable properties for application in CLOU processes. Utilization of inexpensive oxygen carriers can help in reducing the total operational costs. A low cost material ilmenite, has been reported to be a promising candidate; however, it still needs more improvements. Moreover, there should be more modifications on iron ore and CaSO₄ as the inexpensive materials to be used in CLC with solid fuels. Other carrier materials with better performances are available; however, reasonable price of them has not yet been demonstrated.

More detailed studies and investigations are required to understand the mechanisms of reactions and processes design in order to build the larger CLC units with solid fuels. Energy balance and thermodynamics should be considered especially, for designing CLC with solid fuel. There should be more developments on oxygen carrier and design of cost effective suitable reactors for CLC with solid fuels. Moreover, economic consideration of CLC with solid fuels should be studied precisely for operating a successful CLC systems using solid fuels.

Furthermore, another main part of study should be concentrated on mass and energy balance of CLOU process. With review of literature, based on the modeling, an efficiency of carbon dioxide capture about 90 % was estimated without using a carbon stripper, solid inventory of 400 kg/MW_f and temperature of 960 °C in combustor.¹⁶⁵ It is noteworthy to mention that coal reactivity has an important role in the performance of the system. Results also showed a huge decrease for capture of carbon dioxide and conversion of char, when inventory of particles is below 100 kg/MW_f which is because of lack of oxygen in the process.¹⁶⁵ The efficiency of carbon dioxide capture was enhanced from 81.9 % at 935 °C to 93.7 % at 985 °C which proves the fact that temperature of the fuel reactor is important for coal conversion.¹⁶⁵ The carbon dioxide capture efficiency is decreased with increase in rate of circulation with a certain inventory of solids because of lowering the residence time of particles in the system.¹⁶⁵ Furthermore, for an efficiency of carbon dioxide capture more than 95%, a carbon stripper with efficiency higher than 90% is required in the systems working with low rank coals having low reactivity.¹⁶⁵

CHAPTER 3

Methods and methodology

To investigate CuO and AFC performance in CLC process, single cycle and multicycle TGA experiments were performed. The reduction and oxidation processes and thermal behavior of the CuO/AFC mixtures with different ratios (sub-stoichiometric, close to stoichiometric and above stoichiometric) and at temperatures above and below the decomposition temperature of CuO were studied during single cycle experiments. Close to stoichiometric ratio (R30) of CuO/AFC was also tested for multicycle experiments. Moreover, the characterizations of the samples were investigated by advanced analytical techniques.

In this chapter, the methods and methodology of performing the experiments of CuO/AFC mixtures during single cycle and multicycle experiments conducted in a TGA are discussed. The raw materials, sample preparation, experimental procedures and analytical techniques used for characterization of raw materials and residual samples are presented.

3.1. Materials

AFC produced from low-rank Canadian lignite coal (BL)¹⁷⁰ as heavy residue of solvent extraction process with a particle size of 7 μm (D-50) was used in the experiments. Furthermore, HHV (High Heating Value) of AFC is equal to 36.5 MJ/kg.¹⁷⁰

The sum of volatile matter and moisture in AFC was 64.33% (about 35% of char). The properties, proximate and ultimate analysis of BL raw coal (parent coal of AFC) and BL-AFC coal are presented in Table 3.1. More background information and producing process of AFC are provided in detail in Appendix section.

Table 3.1. The proximate and ultimate analysis of BL raw coal and BL-AFC (mass %) ¹⁷⁰

Coal	M/%	V/%	A/%	FC/%	C/%	H/%	N/%	S/%	O ^a /%
BL raw	6.9	31.7	19.2	42.2	54.3	3.91	1.22	1.15	20.26
BL-AFC	1.40	62.93	0.07	35.60	86.50	5.73	3.00	0.45	4.31

^a Oxygen by difference

M-Moisture; V-Volatile Matter; A-Ash; FC-Fixed Carbon

Copper (II) oxide, Puratronic 99.995% (metals basis) from Alfa Aesar was used as the oxygen carrier in experiments. The particle size of the CuO used in the experiments was 63 μm . CuO has special thermodynamic properties which makes it proper candidate to be used in CLOU process. CuO as the oxygen carrier has the capability to release its oxygen and converts to Cu₂O. The auto-decomposition temperature of CuO to Cu₂O is about 790 °C based on TGA results and thermodynamic calculations which are discussed in Chapter 4. Molecular weights of CuO and Cu₂O are equal to 79.545 g/mol and 143.09 g/mol respectively.

Copper oxide (CuO) showed very high reactivity in CLC of solid fuels¹¹⁵ and has been used for both gaseous and solid fuels. However, there are more reports based on oxygen carriers using gaseous fuels than solid fuels.³³ CuO has several advantages as an oxygen carrier in CLC performance; low price, high reactivity, high oxygen transfer capability, and no restriction thermodynamically for complete combustion. Also, it is exothermic both in reduction and oxidation environments. CuO/Cu₂O, Co₃O₄/CoO and Mn₂O₃/Mn₃O₄ are the candidates for the CLOU process, but among these oxygen carriers CuO is better suited based on its special capabilities.¹⁷¹ CuO is also able to release oxygen in the reducer and react with oxygen in the oxidizer, which makes CuO one of the best and most promising oxygen carriers for CLC process. However, Cu and CuO have drawbacks of having low melting temperature and sintering tendency, which causes them to deactivate.^{172,173} The low melting temperature of copper narrows the CLC operating temperature for a CuO oxygen carrier between 600 and 900 °C.^{35,154}

3.2. Experimental Procedures

Thermogravimetric analyses were carried out using a thermogravimetric analyzer (SDT Q600, TA instruments, USA) to assess reduction and oxidation performances of the oxygen carrier in all experiments using an alumina crucible pan under N₂ and air with a flow rate of 100 mLmin⁻¹ and a ramping rate of 20 °Cmin⁻¹. A clean alumina pan was used as the reference pan in TGA. Cleaning of TGA pan was carried out by using a propane ignition fire extinguisher (USA).

CuO and AFC were mixed well with mortar and pestle to prepare the CuO/AFC mixture with desired ratio before performing TGA experiments. For example for CuO/AFC ratio of 10, 100 mg of CuO and 10mg of AFC were mixed well to prepare the mixture with ratio 10.

The sample of CuO/AFC which was used in the experiments was about 50 mg for single cycle experiments and about 100 mg for multi cycle ones. For multicycle experiments after each cycle (reduction and oxidation), the same amount of AFC as the one used in the initial sample was added and mixed in the TGA pan.

3.3. Analytical techniques used for characterization of raw materials and residual samples

The CuO/AFC sample and residue were characterized to understand the thermo-chemical changes occurring before and after the experiments. Solid residues, after the completion of TGA experiments, were collected carefully for several characterizations.

Scanning electron microscopy (SEM), energy-dispersive X-ray spectroscopy (EDX), X-ray diffraction (XRD), Brunauer-Emmett-Teller (BET), proximate and ultimate (CHNS) analyses were analytical techniques used for characterization of raw materials and residual samples. Microstructure, morphology of particles and elemental distributions in materials were observed by SEM (Hitachi S-2700 SEM equipped with a PGT (Princeton Gamma-Tech) IMIX digital imaging system) and a PGT PRISMIG (Intrinsic Germanium) detector for Energy Dispersive X-Ray analysis (EDX). The back-scattered electron (BSE) detector was a GW Electronics system.

Crystalline structures of oxygen carriers were observed by XRD equipment (Ultima IV, ADS) operated at 38 kV and 38 mA. The diffraction patterns were collected between 10 and 112°

two theta (2θ) with a continuous scan rate of 2° per minute using an X-ray source of a Co rotating anode.

The BET instrument used for the surface area analysis experiments was a Quantachrome ASiQwin, version 2.02 automated gas sorption. Nitrogen was used as an adsorbate for the BET procedure with 28.013 molecular mass at -195.8°C temperature. The liquid density was 0.808 gcm^{-3} and the cross section was 16.20 \AA^2 . Out gas time was 12 hours, out gas temperature was 150°C and analysis time was 3hr 28min with standard analysis mode. Furthermore, cell type was a 6mm without rod, Bath temperature was -195.8°C , Cold zone V was 1.56577 cm^3 and warm zone V was 7.74458 cm^3 . As an example, the sample weight of 0.1628 g was used for performing BET experiment for pure CuO.

The moisture and ash contents of coal samples were determined according to ASTM D3173 and ASTM D3174, respectively. The ultimate analyses were performed on the coal samples using an elemental analyzer (Model: Vario Micro, USA).

3.4. Summary

In this chapter, the methods and methodology of performing CuO/AFC experiments during single cycle and multicycle experiments were discussed. The raw materials, sample preparation, experimental procedures and analytical techniques used for characterization of raw materials and residual samples were presented.

Different ratios of CuO/AFC (sub-stoichiometric, close to stoichiometric and above stoichiometric) were prepared before performing TGA experiments to assess their thermal behavior during reduction and oxidation processes. Moreover, the characterizations of the samples were investigated by advanced analytical techniques including SEM, EDX, XRD, BET and CHNS analysis.

CHAPTER 4

Thermogravimetric study: single cycle and the reaction mechanism

4.1. Introduction

Most of the former studies on CLC have been investigated with gaseous fuels; however, the use of solid fuel such as coal and pet-coke in CLC has attracted considerable attention in recent years²⁷, because of their availability and the relatively low cost. There are two routes to feed solid fuels to the gasifier: direct and indirect. In an indirect route, solid fuel enters into a separate gasifier and is gasified using pure O₂. Afterwards, produced syngas is introduced to the fuel reactor of CLC, whereas in the direct route (“in-situ gasification CLC”, or iG-CLC), solid fuel is directly introduced into the fuel gasifier in the presence of a gasification agent. The drawback of both of the aforementioned routes is a slow rate of gasification of the solid fuel. In order to overcome this problem, Mattisson and co-workers^{13,61} developed an approach of chemical looping with oxygen uncoupling (CLOU). In the CLOU process, metal oxide as the oxygen carrier releases part of its oxygen, which reacts with the solid fuel.⁶¹

The CLC approach has several advantages. However, there are several issues, such as; (i) separation of unburned carbon, (ii) separation of ash formation during combustion, and (iii) prevention of unburned carbon entering into the air reactor. Apart from these, there are also some technical issues including gas leakage between fuel and air reactors, distributing energy properly among the reactors, and ensuring proper material circulation and pressure balance in the process.³⁵ Using solid fuel with a negligible or a lower amount of mineral matter for the CLC process helps to overcome the problem related to ash deposition or contamination.

Selecting proper oxygen carriers for CLC of solid fuels is essential for a successful CLC system. The most preferable characteristics of a good oxygen carrier include high oxygen transport capacity, high mechanical strength, high reactivity, and low sintering due to reaction with coal particles and fly ash. Several oxides of different metals such as Ni, Cu, Fe, Mn, Co, Zn and Cd have been studied in the CLC process.²⁸ Oxygen carriers based on Cu, Fe and Ni are the most studied candidates for CLC of solid fuels.⁶¹ Although Ni has a high reactivity, its toxicity, high price and reacting properties with the sulfur content of solid fuels (which cause it to deactivate) are the main drawbacks of using NiO as an oxygen carrier in CLC of solid fuel.⁶¹ On the other hand, CuO showed very high reactivity in CLC of solid fuels.¹¹⁵ CuO as an oxygen carrier has been used for both gaseous and solid fuels. However, there are more results based on oxygen carriers using gaseous fuels than solid fuels.³³

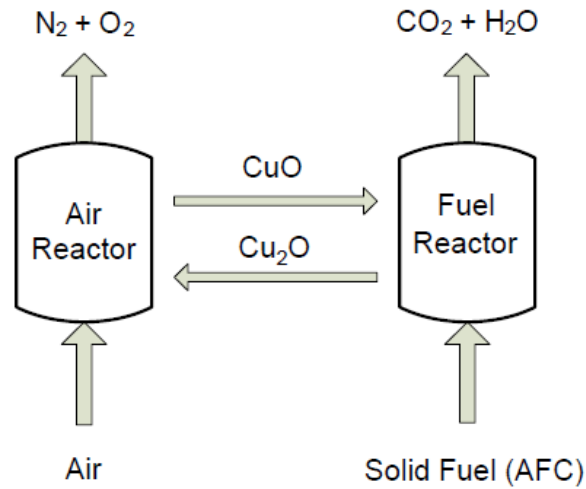


Figure 4.1. Schematic diagram of CLOU process of CuO with solid fuel (AFC)

Figure 4.1 shows the schematic diagram of CLC process with solid fuel. In the CLC experiments of AFC with CuO as an oxygen carrier the reactions which take place in the fuel reactor and in the air reactor are as follows; In the fuel reactor, two reactions take place. The first reaction is auto-decomposition of CuO which produces Cu₂O and oxygen as shown in Eq. (4-1). The second reaction is combustion of carbon with the released oxygen from CuO as shown in Eq. (4-2). The overall reaction in fuel reactor which (CuO) reacts with carbon (C) to produce cuprite (Cu₂O) and CO₂ is also shown in Eq. (4-3). In the air reactor, oxidation of Cu₂O to CuO occurs as shown in Eq. (4-4) and CuO would be regenerated for starting a new CLC cycle.⁹²

In fuel reactor:



In air reactor:



In this chapter, the experimental results of CuO/AFC mixtures during reduction of CuO and oxidation of AFC processes (fuel reactor only) conducted in a TGA with nitrogen are presented. The reduction and oxidation processes or thermal behaviour of the AFC and CuO mixtures with different ratios (sub-stoichiometric, close to stoichiometric and above stoichiometric) and at temperatures above and below the decomposition temperature of CuO are investigated. Thermodynamic simulation calculations were carried out using FactSage to compare predicted and experimental observations. The characterizations of the samples were investigated by advanced analytical techniques such as SEM, EDX, XRD and CHNS analyzer. Finally, based on the experimental results, the reaction mechanism involved to understand the fundamentals during the CLC process in different temperature ranges is proposed.

4.2. Thermodynamic simulation

FactSage software version 6.1 (Thermfact and GTT-Technologies, 1976-2009) was used to predict, equilibrium products and their thermodynamic properties for a certain range of temperatures at 1 atm under the equilibrium conditions. Predictions were made by equilibrium mode in FactSage, which is based on Gibb's free energy minimization. The simulations were made for reduction over a certain range of temperatures using CuO, AFC and nitrogen gas as inputs. Finally, simulation results were compared with the experimental results (discussed in section 4.3.2 and 4.3.3).

4.3. Results and Discussion

In this study, experimental investigations were carried out to assess the feasibility of using CuO as an oxygen carrier with AFC in the CLC process. A series of TGA experiments under nitrogen environment were performed to analyze the effect of CuO/AFC mixing ratio and

temperature, followed by detailed reactivity characteristics and a behavior study of CuO during TGA experiments. Finally, the reaction mechanism of CuO/AFC at different temperature ranges was proposed and evaluated.

4.3.1. Properties and thermal behavior of AFC

Table 4.1 shows the ultimate and proximate analysis of AFC. Initially, the proper ratios of CuO/AFC 10, 20 (sub-stoichiometric), 30 (close to stoichiometric), 40 and 50 (above stoichiometric) were prepared by physical mixing with a mortar and pestle. Then, the CuO and coal mixture was heated from the ambient temperature to a desired temperature (600-900 °C) with a heating rate of 20 °Cmin⁻¹ under nitrogen environment, maintaining a flow rate of 100mLmin⁻¹.

Table 4.1. The proximate and ultimate analysis of AFC and AFC residual solid char (mass%)

Coal	M/%	V/%	A/%	FC/%	C/%	H/%	N/%	S/%	O ^a /%
AFC ¹⁷⁰	1.40	62.93	0.07	35.60	86.50	5.73	3.00	0.45	4.31
AFC Char ^b	-	-	-	-	96.04	0.94	2.05	0.94	0.03

^a Oxygen by difference, ^bAfter TGA reduction at 900 °C under N₂

M-Moisture; V-Volatile Matter; A-Ash; FC-Fixed Carbon

The thermal behavior of AFC under N₂ environment was investigated by TGA at 450 and 900 °C (Figure 4.2). It was seen that devolatilization of volatile matters of AFC started at about 250 °C and continued to about 900 °C. It was observed that at around 450 °C, most of the volatiles (about 55%) evaporated. The sum of volatile matter and moisture in AFC was 64.33% (about 35% of char). The residual solid char from the TGA experiment at 900 °C was also analyzed for ultimate analysis which the results showed that all the volatiles released from coal. The results obtained are presented in Table 4.1.

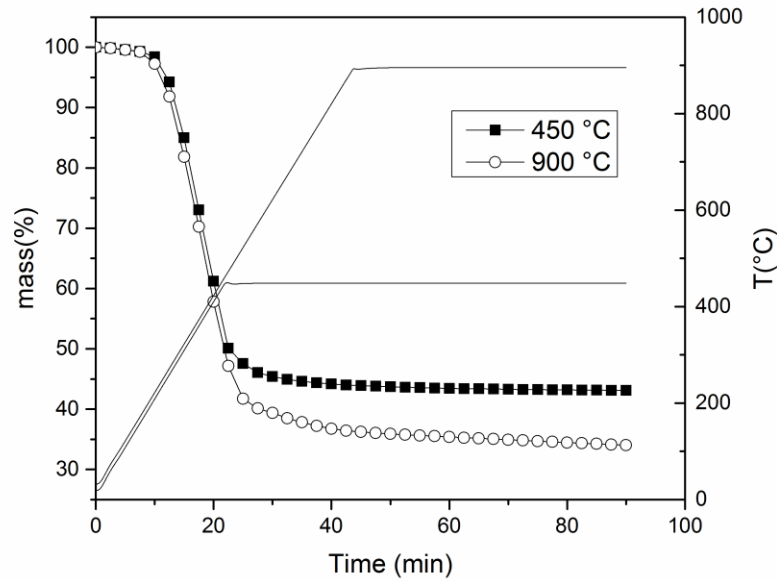
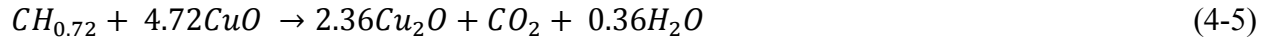


Figure 4.2. Thermal behavior of AFC alone, reduction at 450 and 900 °C

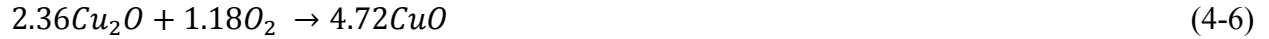
4.3.2. CuO/AFC experiments

In the CLC process, solid fuel devolatilizes and oxidation of volatile matter occur simultaneously by the oxygen carrier. Detailed steps of the reactions are as follows: we assumed in our current study that initial pyrolysis of AFC occurs, followed by the oxidation of the pyrolysis gases. Finally, the residual solid char will react with the metal oxide to generate CO_2 and H_2O . For the sake of convenience in mass balance calculations, the whole AFC is considered as a compound of C and H, after neglecting S and N and removing oxygen in AFC and corresponding part of hydrogen in AFC that would form water which similar approach is carried out by Cao and co-workers.⁹² Thus, the remaining H and C (dry basis) for 100 grams of AFC for reducing CuO based on the ultimate analysis of AFC are: H = 5.2 %, C = 86.5 % ($\text{CH}_{0.72}$). Therefore, out of 100 grams of AFC after water formation from oxygen in AFC and part of hydrogen in AFC, 91.69 grams of carbon and remaining hydrogen are available as $\text{CH}_{0.72}$ compound. The stoichiometric reactions, thus, have been proposed for the CuO/AFC CLC process as follows [Eq. (4-5) and (4-6)];

In the fuel reactor:



In the air reactor:



4.3.3 Performance of different CuO/AFC ratios at different temperatures

In order to investigate the effect of the reduction stage, TGA experiments were performed with CuO/AFC for different ratios (sub-stoichiometric, close to stoichiometric and above stoichiometric) and at above and below the decomposition temperature of CuO (with 20 °Cmin⁻¹ ramping rate, under nitrogen environment) to assess mass loss and reactivity characteristics of CuO/AFC mixtures. The stoichiometric ratio for CuO/AFC was determined to be 27.07 and the decomposition temperature for CuO was 790 °C. CuO/AFC ratios of 10 and 20 as sub-stoichiometric ratios, ratio of 30 as close to stoichiometric ratio and ratios of 40 and 50 as above stoichiometric ratios were tested by TGA.

4.3.3.1 Sub-stoichiometric ratio

Figure 4.3 (a) and (b) show TGA results for CuO/AFC ratios of 10 and 20 (containing not enough oxygen supply for complete combustion of AFC) for above and below the decomposition temperature of CuO (450 and 790 °C are the intersections of dash lines and the temperature line). Based on these experiments for CuO/AFC ratio of 10, the final residual mass was higher for 750 °C than that for 900 °C which is due to the incomplete combustion at 750 °C. For CuO/AFC ratio of 20 at 750 °C, the final mass was around 92%, whereas at 900 °C, the final mass was about 85%. These results indicate that more mass loss occurred at higher temperatures which is due to an incomplete reaction at lower temperatures. Each of the ratios and temperatures are discussed as follows;

CuO/AFC ratio of 10 at 750 °C: for the sub-stoichiometric ratio of 10 of CuO/AFC at 750 °C, ratio of 10 is below the stoichiometric ratio of 27 for complete combustion of AFC with CuO. Therefore, CuO amount is not sufficient and enough oxygen supply for complete combustion of AFC does not exist in the sample. Moreover, 750 °C is below decomposition temperature of CuO which is 790 °C. Thus, the auto-decomposition of CuO at 750 °C does not take place to release oxygen. Initially, at about 250 °C devolatilization of volatile matters starts. At 450 °C about 55 % of volatile matters are released (Figure 4.2). Devolatilization of volatile matters continues and at 750 °C most of the volatile matters are released from AFC (between 55% and 65%). Most of the volatile matters react with CuO which are induced gas-solid interactions. In this case, complete combustion can not be achieved and carbon is leftover. At ratio 10, Cu₂O converts to Cu to produce more oxygen. In agreement with this statement, Cu was detected by XRD (Figure 4.9) and also was found out by thermodynamic calculations (FactSage) (Figure 4.8) for CuO/AFC ratio of 10. For CuO/AFC ratio of 10 for 100 mg basis of CuO/AFC mixture, 90.9 mg of CuO and 9.09 mg of AFC exist in the sample. Figure 4.3 (a) shows that for CuO/AFC ratio of 10 at 750 °C, after 10 minutes devolatilization of AFC starts at about 250 °C. After 40 minutes 20 % of mass loss is observed from TGA result which is because of release of volatile matters from AFC, combustion of volatile matters with CuO and conversion of Cu₂O to Cu. Cu and unburned carbon remain after reduction which are shown in results of thermodynamic calculations (FactSage) for CuO/AFC ratio of 10 (Figure 4.8(a)).

CuO/AFC ratio of 10 at 900 °C: for the sub-stoichiometric ratio of 10 of CuO/AFC at 900 °C, ratio of 10 is below the stoichiometric ratio of 27 for complete combustion of AFC with CuO. Therefore, CuO amount is not sufficient and enough oxygen supply for complete combustion of AFC does not exist in the sample. Moreover, 900 °C is above decomposition temperature of CuO which is 790 °C. Thus, the auto-decomposition of CuO at 900 °C takes place and oxygen is released from CuO. Initially, at about 250 °C devolatilization of volatile matters starts. At 450 °C about 55 % of volatile matters are released (Figure 4.2). Devolatilization of volatile matters continues and at 900 °C all the volatile matters are released from AFC (65% of AFC based on Figure (4.2)). Most of the volatile matters react with CuO which are induced gas-solid interactions. All CuO decomposes to Cu₂O and the released oxygen burns most of the volatile matters. In this case, complete combustion can not be achieved and some AFC char is leftover. At ratio 10, Cu₂O converts to Cu to produce more oxygen. In agreement with this statement, Cu was found out by

thermodynamic calculations (FactSage) (Figure 4.8) for CuO/AFC ratio of 10. For CuO/AFC ratio of 10 for 100 mg basis of CuO/AFC mixture, 90.9 mg of CuO and 9.09 mg of AFC exist in the sample. Figure 4.3 (a) shows that for CuO/AFC ratio of 10 at 900 °C, after 10 minutes devolatilization of AFC starts at about 250 °C. After 40 minutes 24 % of mass loss is observed from TGA result which is because of release of all the volatile matters from AFC, auto decomposition of CuO, combustion of volatile matters with the released oxygen from CuO and conversion of Cu₂O to Cu. Cu and unburned carbon remain after reduction which are shown in results of thermodynamic calculations (FactSage) for CuO/AFC ratio of 10 (Figure 4.8(a)).

CuO/AFC ratio of 20 at 750 °C: for the sub-stoichiometric ratio of 20 of CuO/AFC at 750 °C, ratio of 20 is below the stoichiometric ratio of 27 for complete combustion of AFC with CuO. Therefore, CuO amount is not sufficient and enough oxygen supply for complete combustion of AFC does not exist in the sample. Moreover, 750 °C is below decomposition temperature of CuO which is 790 °C. Thus, the auto-decomposition of CuO at 750 °C does not take place to release oxygen. Initially, at about 250 °C devolatilization of volatile matters starts. At 450 °C about 55 % of volatile matters are released (Figure 4.2). Devolatilization of volatile matters continues and at 750 °C most of the volatile matters are released from AFC (between 55% and 65%). Most of the volatile matters react with CuO which are induced gas-solid interactions. In this case, complete combustion can not be achieved and carbon is leftover. At ratio 20, solid char reacts with CuO (solid-solid interactions). For CuO/AFC ratio of 20 for 100 mg basis of CuO/AFC mixture, 85.66 mg of CuO and 4.76 mg of AFC exist in the sample. Figure 4.3 (b) shows that for CuO/AFC ratio of 20 at 750 °C, after 15 minutes devolatilization of AFC starts at about 250 °C. After 30 minutes 8 % of mass loss is observed from TGA result.

CuO/AFC ratio of 20 at 900 °C: for the sub-stoichiometric ratio of 20 of CuO/AFC at 900 °C, ratio of 20 is below the stoichiometric ratio of 27 for complete combustion of AFC with CuO. Therefore, CuO amount is not sufficient and enough oxygen supply for complete combustion of AFC does not exist in the sample. Moreover, 900 °C is above decomposition temperature of CuO which is 790 °C. Thus, the auto-decomposition of CuO at 900 °C takes place and oxygen is released from CuO. Initially, at about 250 °C devolatilization of volatile matters starts. At 450 °C about 55 % of volatile matters are released (Figure 4.2). Devolatilization of volatile matters continues and at 900 °C all the volatile matters are released from AFC (65% of AFC based on

Figure 4.2). Most of the volatile matters react with CuO which are induced gas-solid interactions. All CuO decomposes to Cu₂O and the released oxygen burns most of the volatile matters. In this case, complete combustion can not be achieved and carbon is leftover. At ratio 20, solid char reacts with CuO (solid-solid interactions). For CuO/AFC ratio of 20 for 100 mg basis of CuO/AFC mixture, 85.66 mg of CuO and 4.76 mg of AFC exist in the sample. Figure 4.3 (b) shows that for CuO/AFC ratio of 20 at 900 °C, after 15 minutes devolatilization of AFC starts at about 250 °C. After 45 minutes 15 % of mass loss is observed from TGA result.

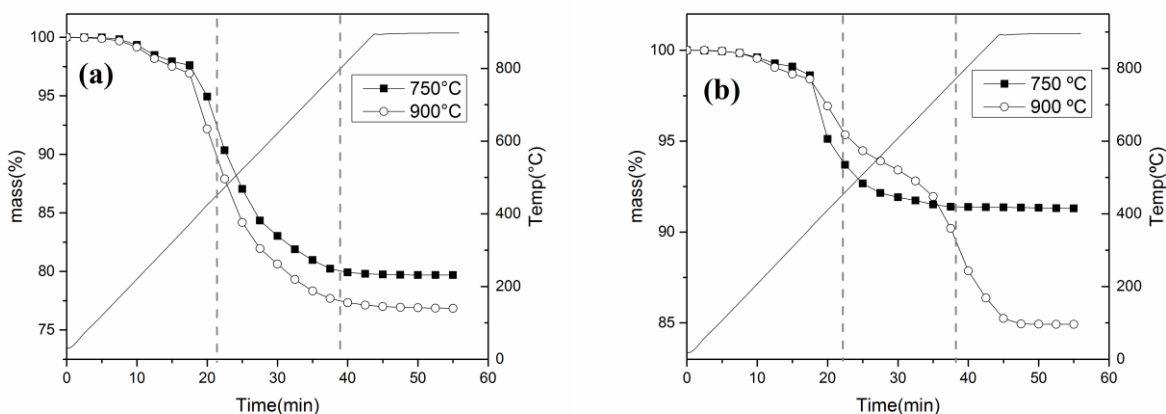


Figure 4.3. CuO/AFC reduction at different temperatures with ratios of a) 10 and b) 20

4.3.3.2 Close to stoichiometric ratio

Figure 4.4 (a) shows the thermal behavior of CuO/AFC ratio of 30 at various temperatures. At higher temperatures (790 and 900 °C), the mass loss was more than that of at 750 °C. These results indicate that there is a complete combustion at temperatures greater than or equal to 790 °C with lower reactivity at 790 °C compared to 900 °C. However, complete combustion is not achieved at 750 °C. Figure 4.4 (b) shows reactivity of CuO/AFC ratio of 30 at different temperatures. Reactivity curves around 450 °C show sharp reactivity peak due to release of volatile matters. The reactivity at 750 and 790 °C do not show peak because these are lower than the auto-decomposition temperature of CuO; whereas, wider peak arises at 900 °C due to auto-decomposition of CuO and combustion of char. Each of the temperatures are discussed as follows;

CuO/AFC ratio of 30 at 750 °C: for the ratio of 30 of CuO/AFC at 750 °C, ratio of 30 is close to stoichiometric ratio of 27 for complete combustion of AFC with CuO. Therefore, CuO amount is sufficient and enough oxygen supply for complete combustion of AFC exists in the sample. Moreover, 750 °C is below decomposition temperature of CuO which is 790 °C. Thus, the auto-decomposition of CuO at 750 °C does not take place to release oxygen. Initially, at about 250 °C devolatilization of volatile matters starts. At 450 °C about 55 % of volatile matters are released (Figure 4.2). Devolatilization of volatile matters continues and at 750 °C most of the volatile matters are released from AFC (between 55% and 65%). Most of the volatile matters react with CuO which are induced gas-solid interactions. In this case, complete combustion can not be achieved and carbon is leftover. At ratio 30, a small amount of CuO is also leftover. At ratio 30, solid char reacts with CuO (solid-solid interactions). For CuO/AFC ratio of 30 for 100 mg basis of CuO/AFC mixture, 96.77 mg of CuO and 3.23 mg of AFC exist in the sample. Figure 4.4 shows that for CuO/AFC ratio of 30 at 750 °C, after 15 minutes devolatilization of AFC starts at about 250 °C. After 25 minutes 7 % of mass loss is observed from TGA result.

CuO/AFC ratio of 30 at 790 °C: for the ratio of 30 of CuO/AFC at 790 °C, ratio of 30 is close to stoichiometric ratio of 27 for complete combustion of AFC with CuO. Therefore, CuO amount is sufficient and enough oxygen supply for complete combustion of AFC exists in the sample. Moreover, 790 °C is equal to decomposition temperature of CuO. Thus, the auto-decomposition of CuO at 790 °C takes place and oxygen is released from CuO. Initially, at about 250 °C devolatilization of volatile matters starts. At 450 °C about 55 % of volatile matters are released (Figure 4.2). Devolatilization of volatile matters continues and at 790 °C most of the volatile matters are released from AFC (between 55% and 65%). Most of the volatile matters react with CuO which are induced gas-solid interactions. In this case, complete combustion can be achieved if enough time is given to the experiment which is because of not high reactivity of 790 °C. For ratio of 30 at 790 °C, all CuO decomposes to Cu₂O. At ratio 30, solid char reacts with CuO (solid-solid interactions). For CuO/AFC ratio of 30 for 100 mg basis of CuO/AFC mixture, 96.77 mg of CuO and 3.23 mg of AFC exist in the sample. Figure 4.4 shows that for CuO/AFC ratio of 30 at 790 °C, after 15 minutes devolatilization of AFC starts at about 250 °C. This experiment requires more time for complete combustion of AFC compared to 900 °C.

CuO/AFC ratio of 30 at 900 °C: for the ratio of 30 of CuO/AFC at 900 °C, ratio of 30 is close to stoichiometric ratio of 27 for complete combustion of AFC with CuO. Therefore, CuO amount is sufficient and enough oxygen supply for complete combustion of AFC exist in the sample. Moreover, 900 °C is above decomposition temperature of CuO which is 790 °C. Thus, the auto-decomposition of CuO at 900 °C takes place and oxygen is released from CuO and Cu₂O is produced. Initially, at about 250 °C devolatilization of volatile matters starts. At 450 C about 55 % of volatile matters are released (Figure 4.2). Devolatilization of volatile matters continues and at 900 °C all of the volatile matters are released from AFC (65% of AFC based on Figure (4.2)). Most of the volatile matters react with CuO which are induced gas-solid interactions. In this case, complete combustion can be achieved. At ratio 30, oxygen released from CuO is a little more than oxygen needed for combusting all volatile matters and all the char. For ratio of 30 at 900 °C, all CuO decomposes to Cu₂O. At ratio 30, solid char reacts with CuO (solid-solid interactions). For CuO/AFC ratio of 30 for 100 mg basis of CuO/AFC mixture, 96.77 mg of CuO and 3.23 mg of AFC exist in the sample. Figure 4.4 shows that for CuO/AFC ratio of 30 at 900 °C, after 15 minutes devolatilization of AFC starts at about 250 °C. After 55 minutes 13 % of mass loss is observed from TGA result. Because of the high reactivity of 900 °C complete combustion occurs faster than 790 °C.

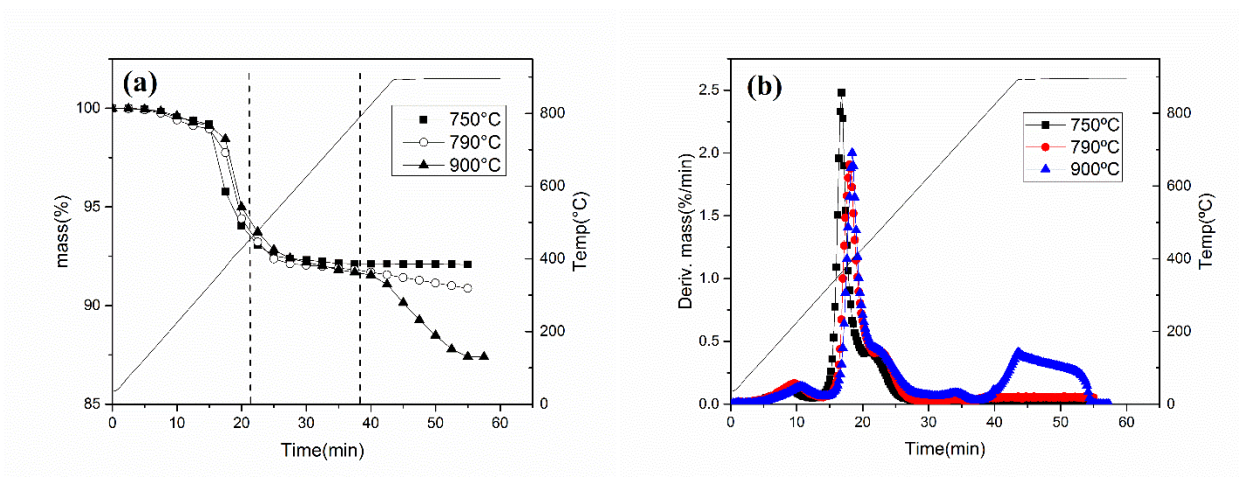


Figure 4.4. CuO/AFC reduction at different temperatures with ratio of 30 a) thermal behavior and b) reactivity

4.3.3.3 Above stoichiometric ratio

Figure 4.5 (a) and (b) show TGA results for CuO/AFC ratios of 40 and 50 (containing more than required oxygen supply for complete combustion of AFC) at different temperatures. It is evident from Figure 4.5 (a) and (b) that for CuO/AFC ratios of 40 and 50, combustion at 750 °C was not complete (because this is below the decomposition temperature of CuO). However, it was complete at higher temperatures with lower reactivity at 790 °C compared to 900 °C which is due to a very slow rate of reaction at 750 °C and auto-decomposition of CuO to Cu₂O (release of O₂) at equal or above the decomposition temperature of CuO. Each of the ratios and temperatures are discussed as follows;

CuO/AFC ratio of 40 at 750 °C: for the ratio of 40 of CuO/AFC at 750 °C, ratio of 40 is above the stoichiometric ratio of 27 for complete combustion of AFC with CuO. Therefore, CuO amount is more than sufficient and more than enough oxygen supply for complete combustion of AFC exists in the sample. Moreover, 750 °C is below decomposition temperature of CuO which is 790 °C. Thus, the auto-decomposition of CuO at 750 °C does not take place to release oxygen. Initially, at about 250 °C devolatilization of volatile matters starts. At 450 °C about 55 % of volatile matters are released (Figure 4.2). Devolatilization of volatile matters continues and at 750 °C most of the volatile matters are released from AFC (between 55% and 65%). Most of the volatile matters react with CuO which are induced gas-solid interactions. In this case, complete combustion can not be achieved and carbon is leftover. At ratio 40, excess amount of CuO is also leftover. At ratio 40, solid char reacts with CuO (solid-solid interactions). For CuO/AFC ratio of 40 for 100 mg basis of CuO/AFC mixture, 97.56 mg of CuO and 2.44 mg of AFC exist in the sample. Figure 4.5 (a) shows that for CuO/AFC ratio of 40 at 750 °C, after 15 minutes devolatilization of AFC starts at about 250 °C. After 25 minutes 7 % of mass loss is observed from TGA result.

CuO/AFC ratio of 40 at 790 °C: for the ratio of 40 of CuO/AFC at 790 °C, ratio of 40 is above the stoichiometric ratio of 27 for complete combustion of AFC with CuO. Therefore, CuO amount is more than sufficient and more than enough oxygen supply for complete combustion of AFC exists in the sample. Moreover, 790 °C is equal to decomposition temperature of CuO. Thus, the auto-decomposition of CuO at 790 °C takes place and oxygen is released from CuO. Initially, at about 250 °C devolatilization of volatile matters starts. At 450 °C about 55 % of volatile matters are released (Figure 4.2). Devolatilization of volatile matters continues and at 790 °C most of the

volatile matters are released from AFC (between 55% and 65%). Most of the volatile matters react with CuO which are induced gas-solid interactions. In this case, complete combustion can be achieved if enough time is given to the experiment which is because of not high reactivity of 790 °C. For ratio of 40 at 790 °C, all CuO decomposes to Cu₂O. At ratio 40, solid char reacts with CuO (solid-solid interactions). For CuO/AFC ratio of 40 for 100 mg basis of CuO/AFC mixture, 97.56 mg of CuO and 2.44 mg of AFC exist in the sample. Figure 4.5 (a) shows that for CuO/AFC ratio of 40 at 790 °C, after 15 minutes devolatilization of AFC starts at about 250 °C. This experiment requires more time for complete combustion of AFC compared to 900 °C.

CuO/AFC ratio of 40 at 900 °C: for the ratio of 40 of CuO/AFC at 900 °C, ratio of 40 is above the stoichiometric ratio of 27 for complete combustion of AFC with CuO. Therefore, CuO amount is more than sufficient and more than enough oxygen supply for complete combustion of AFC exists in the sample. Moreover, 900 °C is above decomposition temperature of CuO which is 790 °C. Thus, the auto-decomposition of CuO at 900 °C takes place and oxygen is released from CuO and Cu₂O is produced. Initially, at about 250 °C devolatilization of volatile matters starts. At 450 °C about 55 % of volatile matters are released (Figure 4.2). Devolatilization of volatile matters continues and at 900 °C all of the volatile matters are released from AFC (65% of AFC based on Figure (4.2)). Most of the volatile matters react with CuO which are induced gas-solid interactions. In this case, complete combustion can be achieved. At ratio 40, oxygen released from CuO is more than oxygen needed for combusting all volatile matters and all the char. For ratio of 40 at 900 °C, all CuO decomposes to Cu₂O. At ratio 40, solid char reacts with CuO (solid-solid interactions). For CuO/AFC ratio of 40 for 100 mg basis of CuO/AFC mixture, 97.56 mg of CuO and 2.44 mg of AFC exist in the sample. Figure 4.5 (a) shows that for CuO/AFC ratio of 40 at 900 °C, after 15 minutes devolatilization of AFC starts at about 250 °C. After 55 minutes 13 % of mass loss is observed from TGA result. Because of the high reactivity of 900 °C complete combustion occurs faster than 790 °C.

CuO/AFC ratio of 50 at 750 °C: for the ratio of 50 of CuO/AFC at 750 °C, ratio of 50 is above the stoichiometric ratio of 27 for complete combustion of AFC with CuO. Therefore, CuO amount is more than sufficient and more than enough oxygen supply for complete combustion of AFC exists in the sample. Moreover, 750 °C is below decomposition temperature of CuO which is 790 °C. Thus, the auto-decomposition of CuO at 750 °C does not take place to release oxygen.

Initially, at about 250 °C devolatilization of volatile matters starts. At 450 °C about 55 % of volatile matters are released (Figure 4.2). Devolatilization of volatile matters continues and at 750 °C most of the volatile matters are released from AFC (between 55% and 65%). Most of the volatile matters react with CuO which are induced gas-solid interactions. In this case, complete combustion can not be achieved and carbon is leftover. At ratio 50, excess amount of CuO is also leftover. At ratio 50, solid char reacts with CuO (solid-solid interactions). For CuO/AFC ratio of 50 for 100 mg basis of CuO/AFC mixture, 98.04 mg of CuO and 1.96 mg of AFC exist in the sample. Figure 4.5 (b) shows that for CuO/AFC ratio of 50 at 750 °C, after 15 minutes devolatilization of AFC starts at about 250 °C. After 25 minutes 6 % of mass loss is observed from TGA result.

CuO/AFC ratio of 50 at 790 °C: for the ratio of 50 of CuO/AFC at 790 °C, ratio of 50 is above the stoichiometric ratio of 27 for complete combustion of AFC with CuO. Therefore, CuO amount is more than sufficient and more than enough oxygen supply for complete combustion of AFC exists in the sample. Moreover, 790 °C is equal to decomposition temperature of CuO. Thus, the auto-decomposition of CuO at 790 °C takes place and oxygen is released from CuO. Initially, at about 250 °C devolatilization of volatile matters starts. At 450 °C about 55 % of volatile matters are released (Figure 4.2). Devolatilization of volatile matters continues and at 790 °C most of the volatile matters are released from AFC (between 55% and 65%). Most of the volatile matters react with CuO which are induced gas-solid interactions. In this case, complete combustion can be achieved if enough time is given to the experiment which is because of not high reactivity of 790 °C. For ratio of 50 at 790 °C, all CuO decomposes to Cu₂O. At ratio 50, solid char reacts with CuO (solid-solid interactions). For CuO/AFC ratio of 50 for 100 mg basis of CuO/AFC mixture, 98.04 mg of CuO and 1.96 mg of AFC exist in the sample. Figure 4.5 (b) shows that for CuO/AFC ratio of 50 at 790 °C, after 15 minutes devolatilization of AFC starts at about 250 °C. This experiment requires more time for complete combustion of AFC compared to 900 °C.

CuO/AFC ratio of 50 at 900 °C: for the ratio of 50 of CuO/AFC at 900 °C, ratio of 50 is above the stoichiometric ratio of 27 for complete combustion of AFC with CuO. Therefore, CuO amount is more than sufficient and more than enough oxygen supply for complete combustion of AFC exists in the sample. Moreover, 900 °C is above decomposition temperature of CuO which is 790 °C. Thus, the auto-decomposition of CuO at 900 °C takes place and oxygen is released from CuO and Cu₂O is produced. Initially, at about 250 °C devolatilization of volatile matters starts. At

450 °C about 55 % of volatile matters are released (Figure 4.2). Devolatilization of volatile matters continues and at 900 °C all of the volatile matters are released from AFC (65% of AFC based on Figure (4.2)). Most of the volatile matters react with CuO which are induced gas-solid interactions. In this case, complete combustion can be achieved. At ratio 50, oxygen released from CuO is more than oxygen needed for combusting all volatile matters and all the char. For ratio of 50 at 900 °C, all CuO decomposes to Cu₂O. At ratio 50, solid char reacts with CuO (solid-solid interactions). For CuO/AFC ratio of 50 for 100 mg basis of CuO/AFC mixture, 98.04 mg of CuO and 1.96 mg of AFC exist in the sample. Figure 4.5 (b) shows that for CuO/AFC ratio of 50 at 900 °C, after 15 minutes devolatilization of AFC starts at about 250 °C. After 65 minutes 13 % of mass loss is observed from TGA result. Because of the high reactivity of 900 °C complete combustion occurs faster than 790 °C.

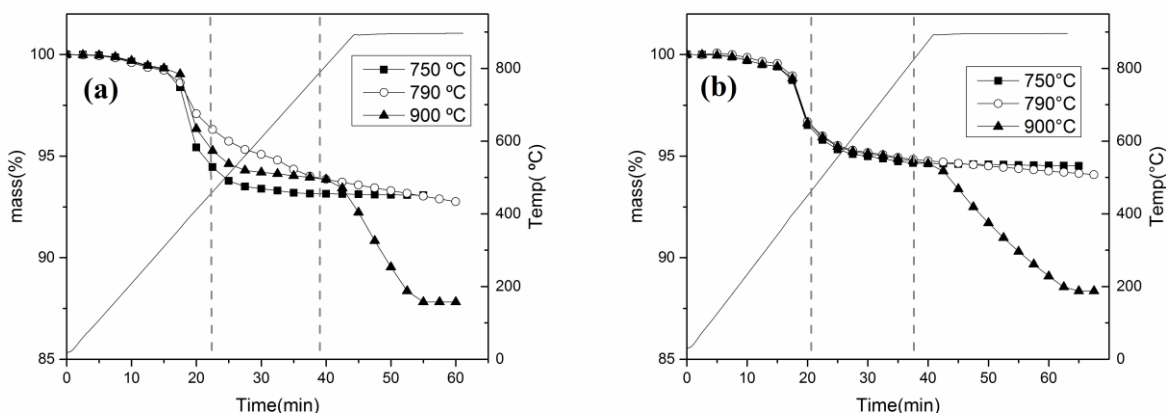


Figure 4.5. CuO/AFC reduction at different temperatures with ratios of a) 40 and b) 50

To further explain these observations, CuO/AFC mixtures were analyzed in detail by several characterization techniques including XRD and SEM. Also, quantitative analysis such as CHNS was performed for solid residues. Based on the elemental analysis of solid residue obtained from reducing CuO/AFC at different temperatures such as 700, 750, 790, 820 and 900 °C, it was found that very small amount of unburned carbon (0.02 - 0.57%) was left in the solid residue irrespective of the ratios and operating temperatures. These results indicate that a reasonably complete combustion occurred at ≥ 790 °C and a partial combustion occurred at temperatures below 790 °C. The detail reaction steps, the mechanism and the discussion related to these are presented in section 4.3.5.

4.3.4 FactSage predictions

Thermodynamic calculations were also performed using FactSage to predict the thermodynamic feasibility of reactions and to confirm if any side reactions were feasible. Predictions were performed by equilibrium mode in FactSage, which is based on Gibb's energy minimization. TGA experiments were carried out under the N₂ environment. As a result, the amount of O₂ in TGA chamber and CO₂ released from combustion was negligible. Therefore, the O₂ partial pressure of 0.0001 atm was assumed for the FactSage calculations. The FactSage prediction results are shown in Figure 4.6.

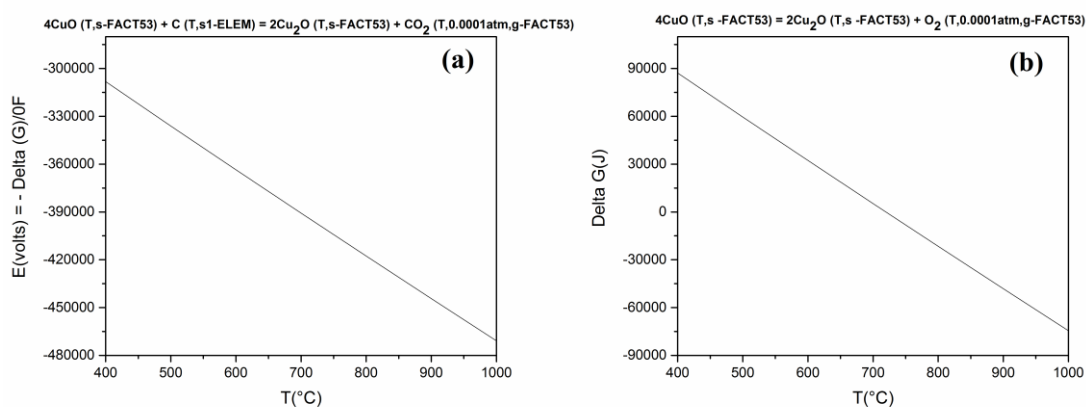


Figure 4.6. Assessing feasibility of a) CuO and C reaction and b) CuO auto-decomposition by FactSage

Figure 4.6(a) shows that the reaction of CuO with C is thermodynamically feasible at temperatures above 400 °C since a change in the total Gibb's free energy (ΔG) was negative. The auto-decomposition of CuO to Cu₂O and release of O₂ at a relatively higher temperature is shown in Figure 4.6(b). It was observed that this reaction is thermodynamically feasible at temperatures above 719 °C. A TGA experiment was performed with CuO under nitrogen atmosphere to verify the auto-decomposition temperature of CuO which was found out to be 790 °C as shown in Figure 4.7.

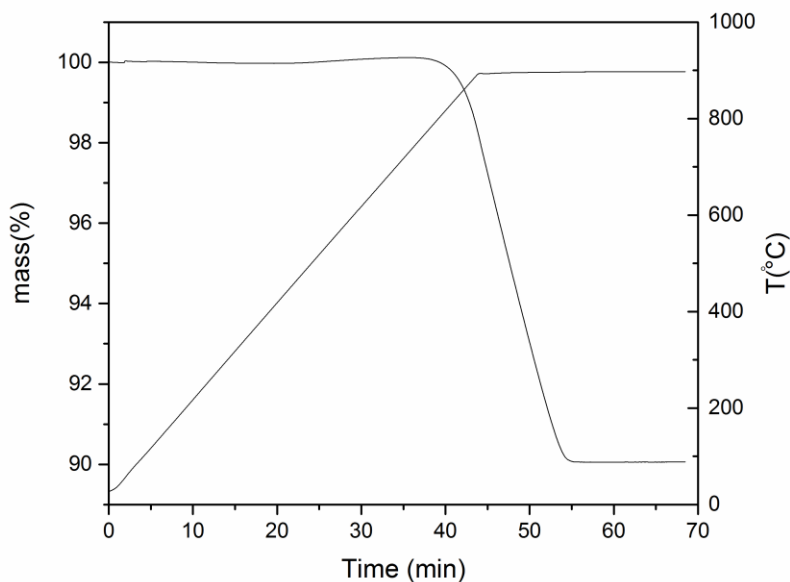


Figure 4.7. Thermal behavior of pure CuO during reduction at 900 °C

From the TGA experiment curve (Figure 4.7), it was observed that the auto-decomposition of CuO to Cu₂O starts at temperatures above 790 °C, which is also supported by the FactSage calculation (above 719 °C) in equilibrium condition. Simulations were carried out for CuO and AFC (AFC = C_{7.21} H_{5.73} O_{0.27} N_{0.21} S_{0.014} based on the ultimate analysis of AFC) as inputs during reductions in different temperatures.

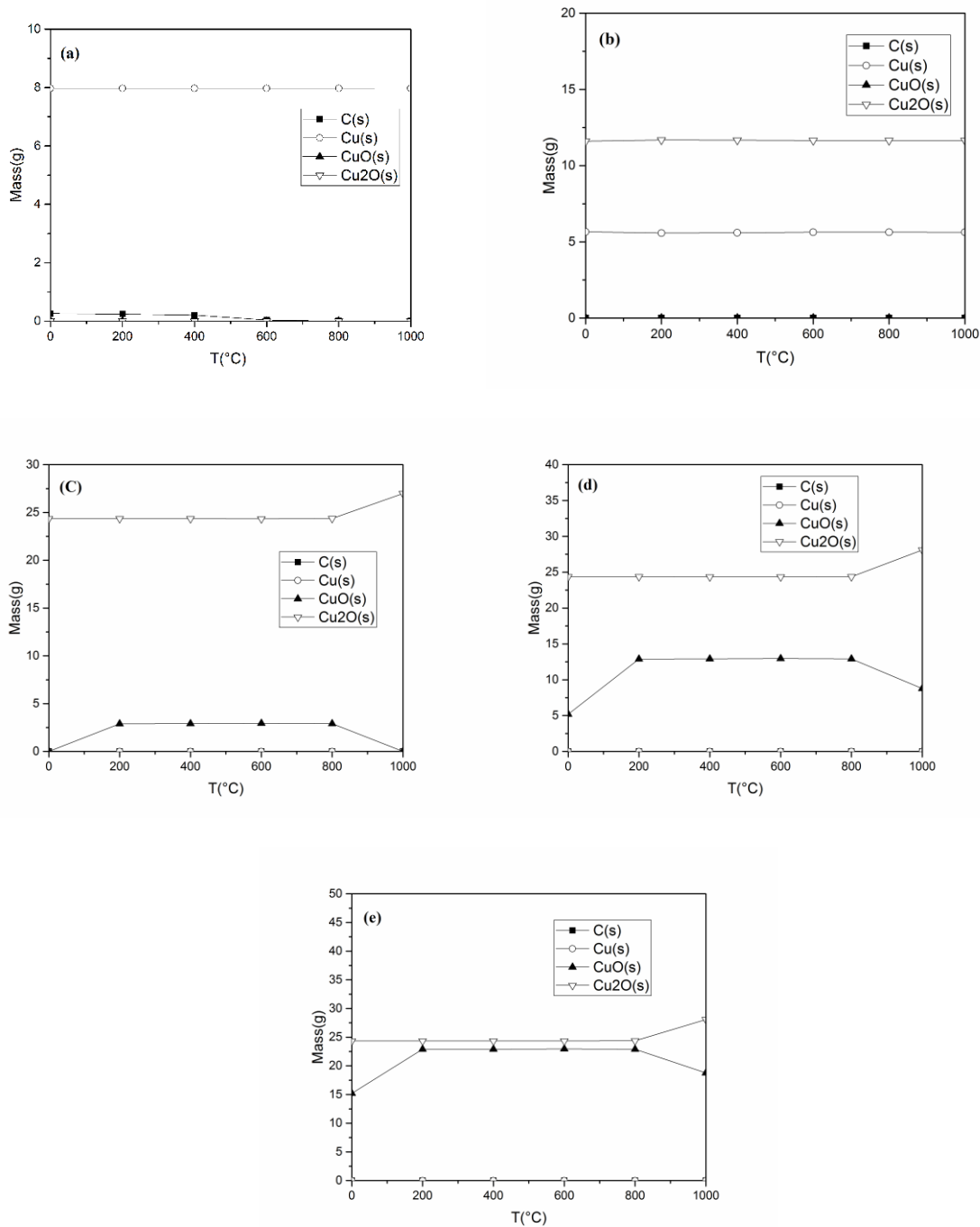


Figure 4.8. FactSage results of the equilibrium composition of solids in residue for CuO/AFC (AFC = $C_{7.21}H_{5.73}O_{0.27}N_{0.21}S_{0.014}$) ratios of a) 10, b) 20, c) 30, d) 40, and e) 50

Figure 4.8 (a) shows that for CuO/AFC ratio of 10, there is a formation of Cu and some amount of unburned residual carbon. XRD also detected Cu as shown in Figure (4. (a)). Figure 4.8 (b) for CuO/AFC ratio of 20 shows the presence of both Cu and Cu₂O, but XRD results of the

reduced sample (Figure 4. (b)) did not show any Cu in the solid residue which is because the FactSage results were obtained for the equilibrium composition of the mixture, which assumes that all CO formed reacts with Cu_2O to form CO_2 and Cu. However, no Cu formation was detected by XRD analysis for CuO/AFC ratio of 20 in the reduced mass (Figure 4. (b)) which is probably due to the slower rate of reaction within these ranges of temperatures; thus this reaction is not dominant. On the other hand, based on Figure 4.8 (c), (d) and (e) for ratios of 30, 40 and 50, only Cu_2O is formed and the residual CuO underwent auto-decomposition to form Cu_2O at higher temperatures (around 800 °C), which was also shown by TGA result (Figure 4.7).

In order to investigate in greater detail the crystal structures of CuO/AFC mixtures, solid residues were collected from the TGA pan and analyzed by XRD. Figure 4.9 shows XRD patterns of residual solids of CuO/AFC mixtures with ratios of 10, 20 and 30 after reduction at 750 °C. Cu_2O and Cu were observed in a solid residue of CuO/AFC ratio of 10, whereas only CuO and Cu_2O were observed in all other ratios. The XRD patterns of residual solids of CuO/AFC mixtures after reduction at 900 °C also showed presence of Cu and Cu_2O in ratio of 10 and CuO and Cu_2O for ratios of 20 and 30.

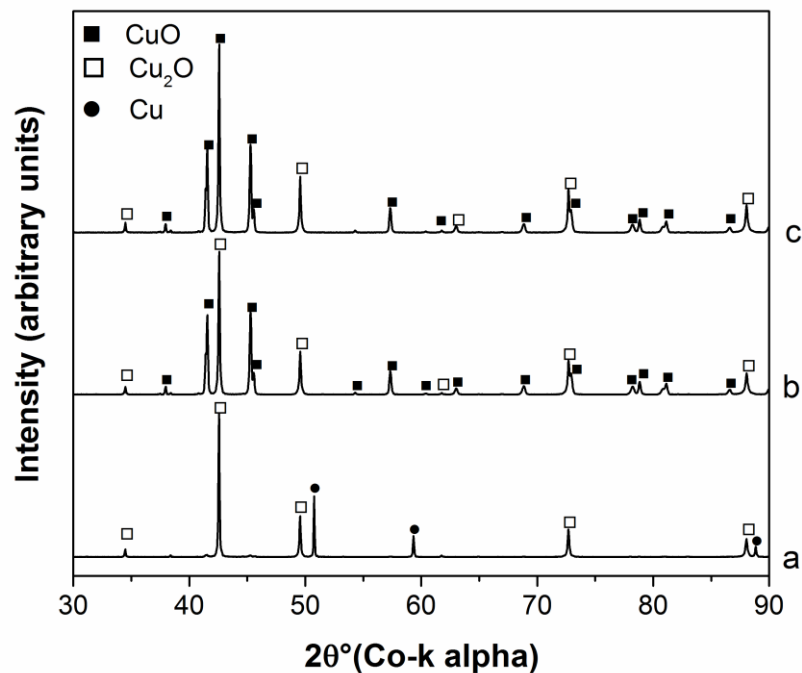


Figure 4.9. XRD patterns of residual solids of CuO/AFC mixtures with ratios of a) 10, b) 20 and c) 30, reduction at 750 °C

Based on the EDX result of AFC, it was evident that this type of coal contains mainly carbon and traces of other materials including oxygen, and it contains no ash forming minerals.

4.3.5 Morphology changes of solid residues of CuO/AFC after TGA experiments

Several SEM images were taken to investigate morphological changes in CuO/AFC mixtures with different ratios. For example, based on SEM images for CuO/AFC ratio of 20 after a reduction at 900 °C, sintering of the reduced CuO was observed. To study in greater detail the sintering effect of higher temperatures for the proper ratio of the CuO/AFC mixture (ratio of 30), several SEM images at different temperatures were also investigated.

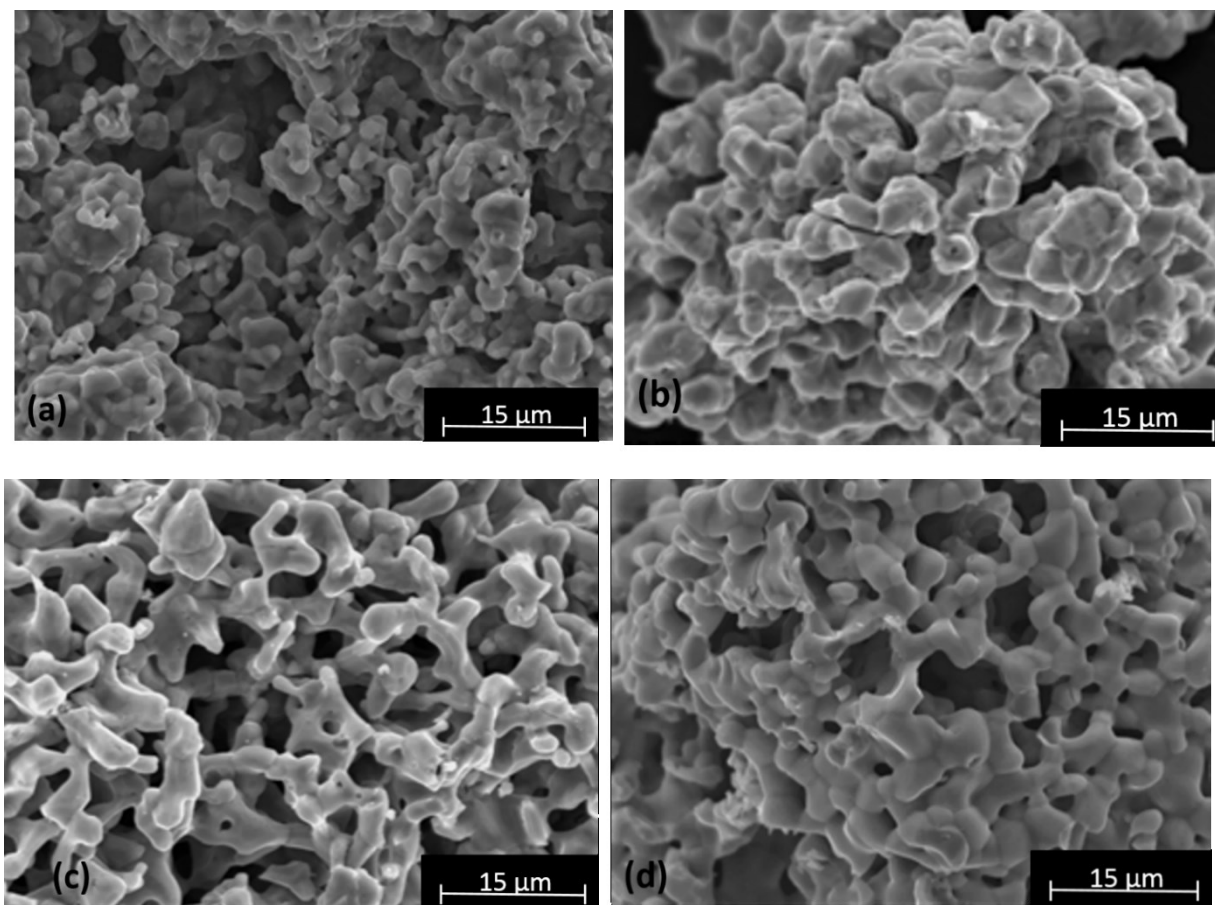


Figure 4.10. SEM images of CuO/AFC ratio of 30, reductions at a) 750, b) 790, c) 820 and d) 900 °C

Figure 4.10 (a-d) shows SEM images of residues of CuO/AFC ratio of 30 reduced at different temperatures including 750, 790, 820 and 900 °C. The sintering effect in solid residues at higher temperatures was observed in Figure 4.10 (c-d). As shown in Figure 4.10 (a-b), the sintering effect is not seen for lower temperatures of 750 and 790 °C. The structure of the particles remained unchanged and slightly changed after the reduction at 750 and 790 °C respectively. However, Figure 4.10 (c-d) shows that sintering started at 820 °C and continued to the high temperature of 900 °C. Due to the sintering effect the morphology of particles changed completely and the sintering of particles resulted in some of them as connected Y-shaped net structures, after being reduced at 820 °C.

4.3.6 Reaction mechanism of CuO as the oxygen carrier and AFC as the solid fuel

As it was shown in Figure 4.2, the final mass percentages of solid residues from AFC pyrolyzed at temperatures 450 and 900 °C most of all volatile matters (about 90%) in AFC were released at around 450 °C. This result implies that with sufficient contact and time between CuO and residual char, the combustion reaction of carbon can occur even at a lower temperature due to the induced gas-solid interactions. A similar observation was reported in the literature.²⁵ Figure 4.11 shows the TGA plots for the evaluation of the reaction mechanism of CuO/AFC ratio of 30 after reductions at 450, 750 and 800 °C. The thermal behavior of CuO/AFC ratio of 30 in terms of the mass loss was recorded. TGA curves of 450 and 750 °C show that there was about 1 % of mass loss difference between the final masses of these two curves. These results reveal that there were limited chemical reactions at this temperature range, because of the solid-solid interaction, whereas in the temperature range above 790 °C, auto-decomposition of CuO took place and significant mass loss occurred which is because of release of oxygen from CuO and combustion of char by the released oxygen.

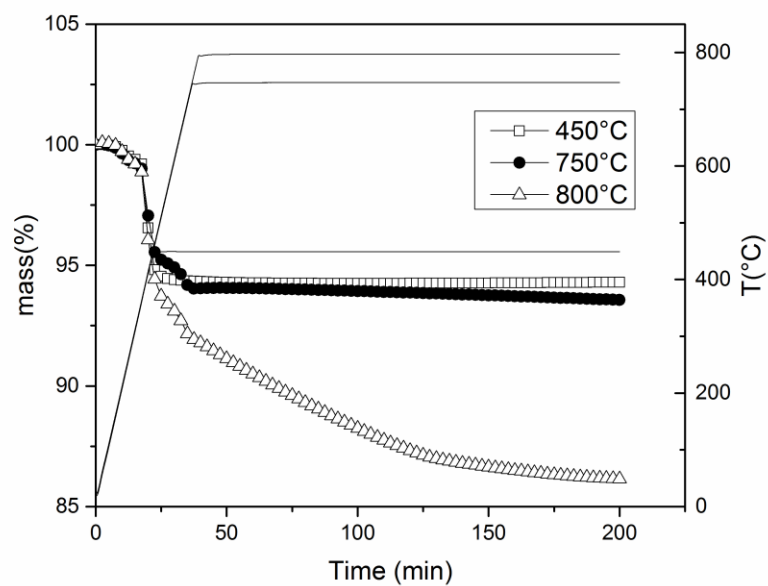


Figure 4.11. Thermal behavior of CuO/AFC ratio of 30, reduction at 450, 750 and 800 °C and evaluation of reaction mechanism

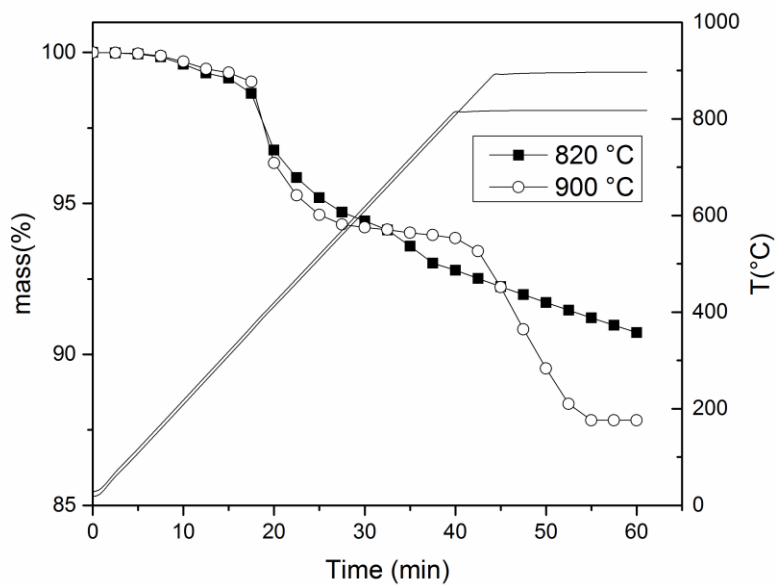


Figure 4.12. Auto-decomposition of CuO at 820 and 900 °C in CuO/AFC ratio of 40

Figure 4.12 shows the TGA plots of CuO/AFC ratio of 40 after reductions at 820 and 900 °C. For higher ratios of CuO and AFC mixture (for example CuO/AFC ratio of 40), there was some residual CuO in the pan. Auto-decomposition of CuO can occur at higher temperatures. Based on TGA results, this decomposition is initiating at 790 °C. From TGA graphs of CuO/AFC ratio of 40 after reductions at 820 and 900 °C it can be observed that decomposition occurs at 820 °C with a slower rate than decomposition at 900 °C (Figure 4.12). A TGA curve of 900 °C was reasonably stable after 55 minutes, and the final mass was 87.82%, which is due to faster reduction rate at 900 °C. However, mass loss behavior at 820 °C was not yet stable, and the final mass was 91.24% which shows that with enough time, there can be a complete auto-decomposition of CuO. Subsequently, the complete auto-decomposition of CuO occurred sooner at 900 than at 820 °C.

Table 4.2. Reaction pathways of CuO and AFC for different ratios (sub-stoichiometric, close to stoichiometric and above stoichiometric) below and above CuO auto-decomposition temperature ranges

Temperature	Sub-stoichiometric/ R10 and R20	Close to stoichiometric/ R30	Above stoichiometric/ R40 and R50
Below decomposition temperature ($<790\text{ }^{\circ}\text{C}$)	-Most of the volatile matters release from AFC	-Most of the volatile matters release from AFC	-Most of the volatile matters release from AFC
	-Most of Volatile matter reacts with CuO (induced gas-solid interactions)	- Most of Volatile matter reacts with CuO (induced gas-solid interactions)	- Most of Volatile matter reacts with CuO (induced gas-solid interactions)
	-Complete combustion cannot be achieved and carbon is leftover	-Solid char reacts with CuO (solid-solid interactions), therefore, complete combustion cannot be achieved and carbon is leftover	-Solid char reacts with CuO (solid-solid interactions), therefore, complete combustion cannot be achieved and carbon is leftover
	-Cu ₂ O converts to Cu to produce more oxygen (R10)	-A small amount of CuO is leftover	-Excess amount of CuO is leftover
	-Solid char reacts with CuO (solid-solid interactions) (R20)		
	-First three steps are same as decomposition $<790\text{ }^{\circ}\text{C}$, mentioned above	-First three steps are same as decomposition $<790\text{ }^{\circ}\text{C}$, mentioned above	-First three steps are same as decomposition $<790\text{ }^{\circ}\text{C}$, mentioned above
Above decomposition temperature ($>790\text{ }^{\circ}\text{C}$)	-Complete combustion cannot be achieved	-CuO decomposes to Cu ₂ O and oxygen released	-CuO decomposes to Cu ₂ O and oxygen, oxygen released from CuO is more than oxygen needed for combusting all volatile matters and all the char
	-All CuO decomposes to Cu ₂ O and oxygen released burns most of the VM	- Oxygen released from CuO is a little more than oxygen needed for combusting all volatile matters and all the char	
	-Cu ₂ O converts to Cu to produce more oxygen (R10)	-All CuO decomposes to Cu ₂ O	-All CuO decomposes to Cu ₂ O
	-Some AFC char is leftover		

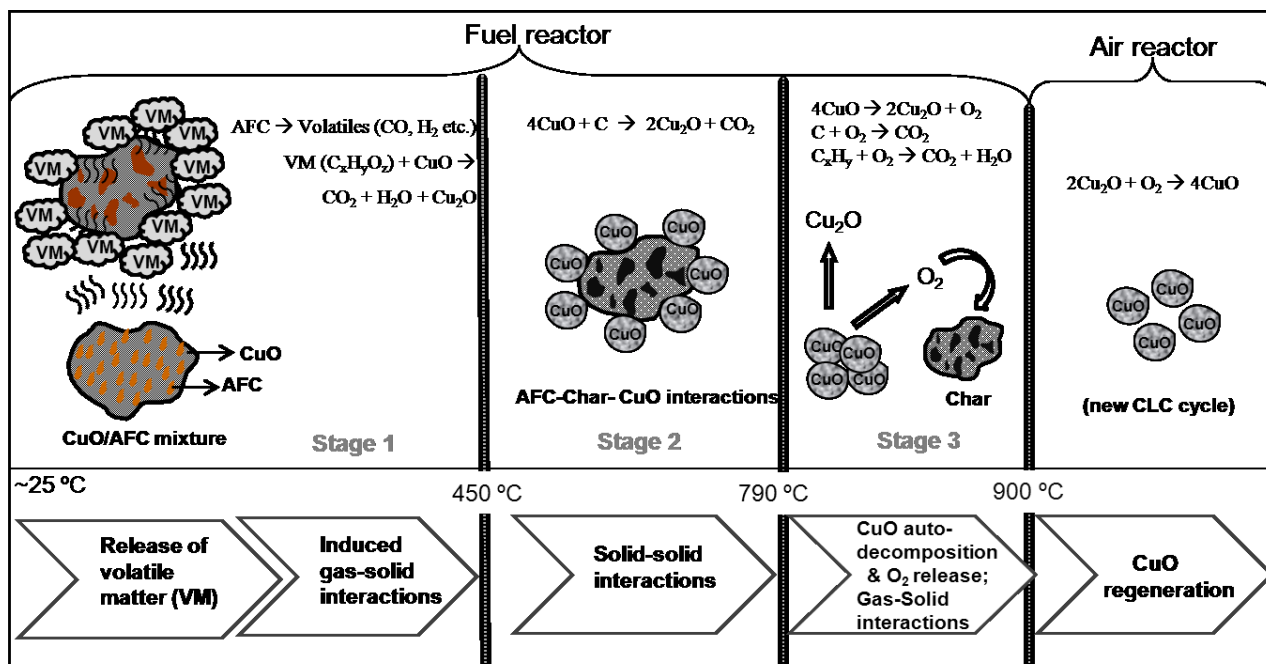


Figure 4.13. Schematic view of the reaction mechanism of CuO and AFC at different temperatures

From the experimental results, the reaction mechanism of CuO and AFC for different ratios of sub-stoichiometric, close to stoichiometric and above stoichiometric have been explained and classified into two temperature range, i.e. below (< 790 °C) and above (> 790 °C) auto-decomposition of CuO (Table 4.2). A schematic representation of the mechanism of CuO/AFC reactions during the CLC process has been proposed (Figure 4.13). From TGA curves at 450 °C, it was found that the mass loss (mainly release of volatile matter) from the CuO/AFC (R30) mixture was 5.7%. While moving from 450 to 800 °C, mass loss from the mixture reached 8.15% which is due to the interaction of CuO and AFC-char (solid-solid interactions plus auto-decomposition of CuO). To summarize, the mechanism steps in the fuel reactor occur in the following order: (i) release of volatiles from CuO/AFC mixture \rightarrow (ii) induced gas-solid interactions of volatile matter and CuO/AFC mixture \rightarrow (iii) solid-solid interactions between CuO and AFC-char \rightarrow (iv) auto-decomposition of CuO and release of O₂. In the air reactor, O₂ thus released reacts with Cu₂O and regenerates CuO (oxygen carrier regeneration step) and a new CLC cycle starts.

4.4. Reproducibility of data

Figure 4.14 shows three repeated TGA results for thermal behavior and reactivity of CuO/AFC ratio of 20 reduced at 900 °C. It is observed from Figure 4.14 that the obtained TGA graphs are almost the same for thermal behavior of CuO/AFC ratio of 20 at 900 °C with maximum 0.6 weight % error.

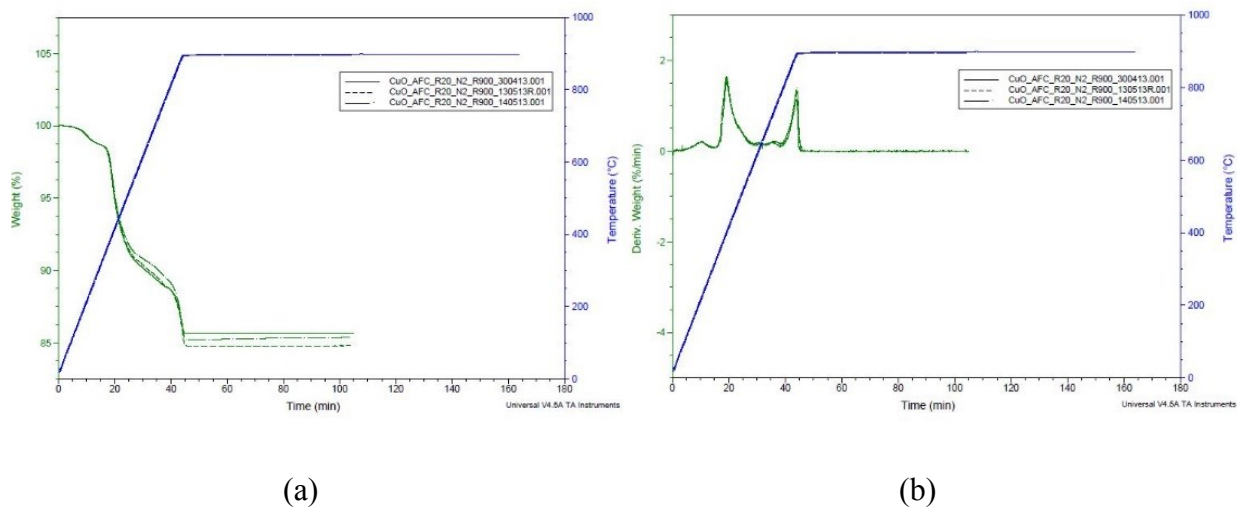


Figure 4.14. CuO/AFC ratio of 20 reduction at 900 °C a) thermal behavior b) reactivity

Figure 4.15 shows repeated TGA results of thermal behavior and reactivity of CuO/AFC ratio of 30 reduced at 820 °C. These results show the obtained data are highly reproducible.

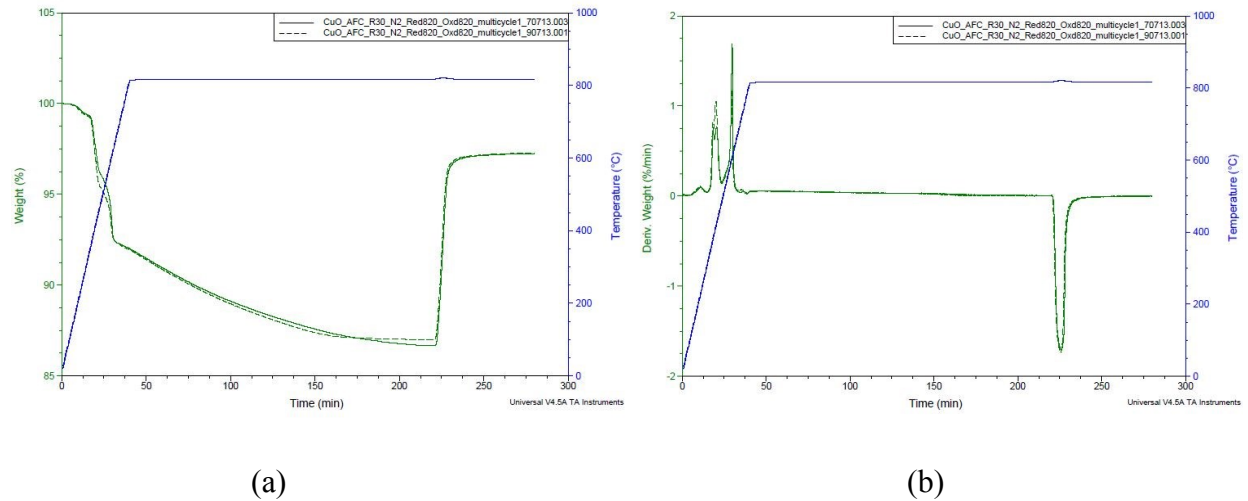


Figure 4.15 CuO/AFC ratio of 30 reduction at 820 °C a) thermal behavior b) reactivity

4.5. Conclusions

The CuO/AFC performance during the single cycle process in chemical looping combustion was assessed by TGA. CuO and AFC were physically mixed together with different ratios. TGA experiments were conducted at various temperatures and solid residues were collected from the TGA pan for analysis and characterization. Samples were analyzed by several analytical techniques including XRD, SEM and EDX. Thermodynamic predictions were also performed using FactSage software. Finally, the CLC reaction mechanisms were proposed and evaluated with the experimental results. Conclusions based on our experimental results are as follows:

1. In XRD analysis, Cu was detected in a residual mass of CuO/AFC ratio of 10. Based on FactSage calculations, apart from formation of elemental Cu, it was found that there was formation of CO and CO₂ in ratio of 10. Also FactSage was used for thermodynamic calculations to determine final equilibrium products for different ratios of CuO/AFC which supported the experimental results.
2. TGA analysis of CuO/AFC ratio of 30 samples was performed at different temperatures. It was found that the complete combustion of AFC is possible at temperatures greater than or equal to 790 °C. It was also found that there was sintering of CuO after reduction at higher temperatures (supported by SEM images). The best temperatures for CuO to react with AFC at ratio of 30 were between 790 and 820 °C based on TGA results and characterizations. With the increase in temperature, reactivity of the residual char increased. At lower temperatures, reactions were incomplete as the residual char did not completely react, and at higher temperatures the sintering of CuO was observed. The ultimate analysis of the residual samples from TGA shows that the combustion at above 790 °C was almost complete for R30. Whereas, at lower temperatures (less than the decomposition temperature of CuO) combustion was incomplete. For higher CuO/AFC ratios (R40 and R50) there was availability of excess amount of oxygen supply and CuO in the mixture.
3. XRD results show formation of Cu only in ratio of 10 and Cu₂O and CuO in higher ratios. SEM images show more sintering of reduced CuO at 900 °C and lesser sintering at lower temperatures. EDX analysis was carried out on the residual sample after TGA analysis in order to determine the actual composition of elements in residue; EDX analysis of the final residue at higher temperatures showed only Cu and oxygen as the major components.

4. The reaction mechanism for the CuO/AFC mixture was evaluated. The evaluation can be briefly summarized in three stages, as follows:

Stage 1: Most of the volatile matter was released from AFC at around 450 °C and combustion of these gases started at around 400 °C with CuO, which could be due to the induced gas-solid interactions.

Stage 2: From 450 to 790 °C, the solid-solid interaction of CuO and AFC-char occurred.

Stage 3: Auto-decomposition of CuO took place above 790 °C and oxygen was released at this stage, enhancing the solid-solid interaction between CuO and residual char at the threshold temperature.

CHAPTER 5

Thermogravimetric study: multicycle performance

5.1. Introduction

In chapter 4, it was shown that the CuO is a promising oxygen carrier for CLC of AFC in single cycle tests. It also has been found that ratio 30 of CuO/AFC is close to stoichiometric ratio and 790 to 820 °C is the appropriate range of operating temperature for CuO and AFC mixtures. It is essential to study the chemical stability and performance of CuO for multiple and longer operating conditions. So in this chapter, in order to investigate CuO and AFC performance in CLC process during longer operating time, multicycle TGA experiments were executed.

It is essential to study the chemical stability and performance of CuO for multiple and longer operating conditions. So in this chapter, in order to investigate CuO and AFC performance in CLC process during longer operating time, multicycle TGA experiments were executed. Close to stoichiometric ratio (R30) of CuO and AFC were prepared and tested at different operating temperatures for multiple cycles of reduction and oxidation processes. The thermal behavior and reactivity performances of CuO and AFC materials during multicycle experiments were assessed and compared. Moreover, to investigate their crystalline structure and surface morphological changes before and after the experiments samples were characterized by several advanced analytical techniques including XRD, SEM and BET.

5.2. Results and Discussion

Multicycle TGA experiments were performed for CLC of CuO/AFC with close to stoichiometric ratio (R30) during reduction and oxidation processes. Nitrogen was used as a carrier gas during combustion in TGA tests and oxidation carried with air. For both the cases, gas flow rate was 100 mLmin⁻¹ and ramping rate was 20 °C min⁻¹. Five consecutive cyclic tests were carried out during reduction and re-oxidation at 900 °C. Both fresh and used samples before and after

TGA experiments were characterized using XRD, SEM and BET to investigate their crystalline structure and surface morphological changes. Results for reduction and oxidation with different isothermal times are also compared.

5.2.1. Performance of CuO/AFC ratio of 30 during multicycle experiments

The multicycle TGA tests were performed for CuO/AFC ratio of 30 for evaluating the performance in longer operating condition. After investigating five cycles at 900 °C, it was found that there was higher reactivity for the first cycle compared to the second cycle which is because of significant sintering effect between the first and the second cycles. However, there is not much difference in reactivity of the second and the consecutive cycles which is because of not much sintering effect after the second cycle (supported by SEM images from Figure 5.2). Thus, there was no hindrance in the reaction between AFC and CuO and almost equal reactivity was achieved for each consecutive cycles which is one of the major advantages of using AFC as it does not reduce the performance of oxygen carrier. Even though, there was not much difference in reactivity in the consecutive cycles, the reactivity of the first cycle for reduction phase was found to be slightly higher and its reaction occurs at a lower temperature which was possibly because of sintering of CuO after the first cycle which hinders the rate of reaction of the consecutive cycles. The reactivity for re-oxidation was found to be nearly equal for each cycle. The CuO changes structure (decreased surface area due to sintering) only in the first cycle with negligible structural changes in the following cycles and therefore; there is no change in reactivity after the first cycle. Also there were two peaks of reactivity. The first peak was at around 400 °C, which is due to release of volatile matter and the combustion of the pyrolysis gases formed. The second peak was due to the oxidization of the residual char. This oxidization begins at a temperature of about 700 °C and reactivity was the maximum at the temperature of about 850 °C.

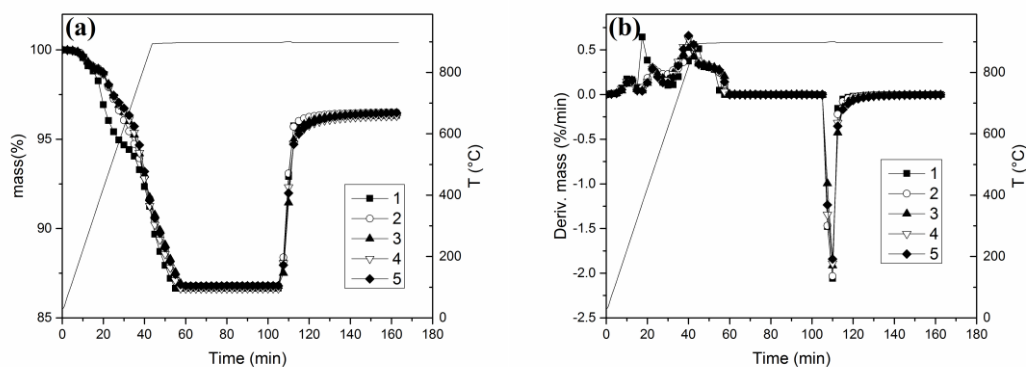
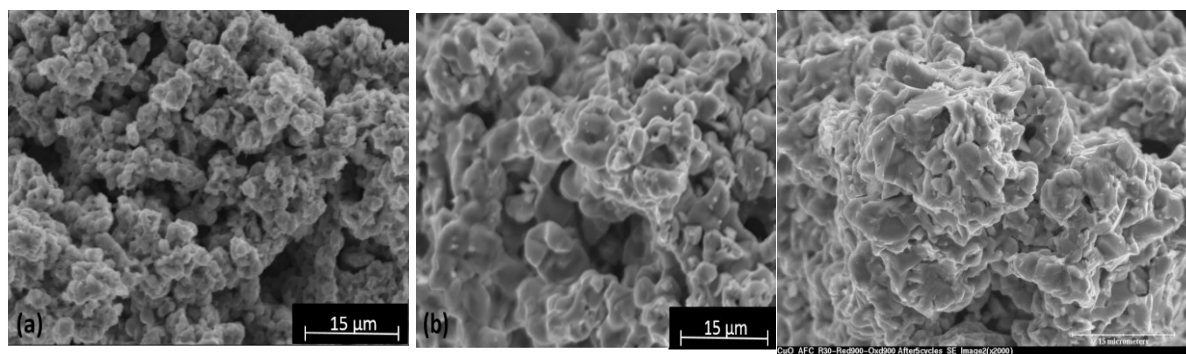


Figure 5.1. Performance of CuO/AFC ratio of 30 after reduction and oxidation for five cycles at 900 °C including a) thermal behavior and b) reactivity

Figure 5.1(a) shows thermal behavior of CuO/AFC ratio of 30 after reduction and oxidation for different cycles at 900 °C. Slightly different thermal behavior was observed during reduction for the first cycle and the rate of decrease in mass was higher for this cycle compared to consecutive cycles which is due to the availability of higher surface area for reaction in unused or fresh CuO. Hence, the volatile gases can instantaneously react with CuO, whereas there is hindrance in the reaction of following cycles due to the changes in the structure of CuO (supported by SEM images from Figure 5.2). Almost the similar behavior was observed for all the other cycles. Figure 5.1(b) shows TGA results of reactivity performance for CuO/AFC ratio of 30 during five cycles of reduction and oxidation at 900 °C. The reactivity during reduction was higher for the first cycle compared to the following cycles which is due to the sintering of CuO after reduction and oxidation at 900 °C during the first cycle.



(a) pure CuO

(b) first cycle

(c) fifth cycle

Figure 5.2. SEM images of a) pure CuO b) CuO/AFC ratio of 30 after first cycle of reduction and oxidation at 900 °C c) CuO/AFC ratio of 30 after five cycles of reduction and oxidation at 900 °C

Mass variation during multicycle experiments was investigated and shows that mass loss and mass gain curves during different cycles remain almost constant for CuO/AFC ratio of 30 which indicates that, there is no interference in the reaction for the next cycle and the reactions remain almost the same for all the cycles. These facts are also supported by Figure 5.3, which shows TGA results of mass variation during multicycle experiments for CuO/AFC ratio of 30 for reduction and oxidation at 900 °C. For comparison CLC multicycle experiments of CuO/BL raw coal (parent coal of AFC) ratio of 30 was performed. In contrast to the CLC of AFC, the final mass of the residue in case of raw coal was not the same in each consecutive cycle because of ash deposition (Figure 5.4). The results clearly showed the increasing trend in the amounts of residue after the reaction because of the ash accumulation after each cycle (0.4mg/cycle). However, in many consecutive cycles (industrial application) ash accumulation and its subsequent contamination effect might be significant which highlights the advantage of using AFC over raw coal in CLC process.

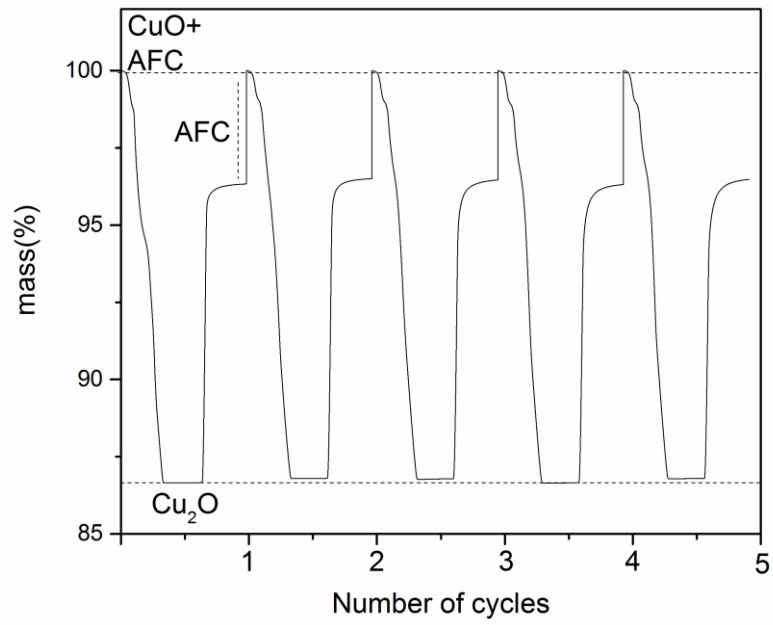


Figure 5.3. Mass variation during multicycle experiments for CuO/AFC ratio of 30 at 900 °C

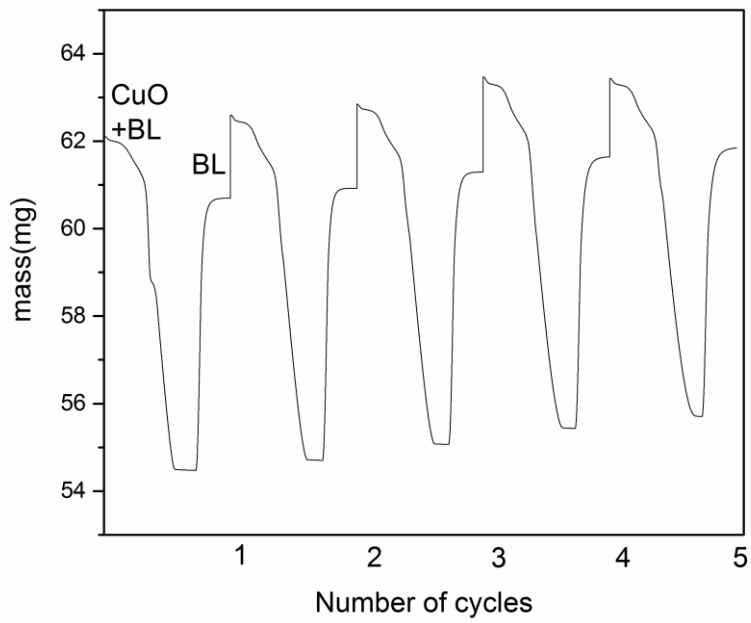


Figure 5.4. Mass variation during multicycle experiments for CuO/BL raw coal ratio of 30 at 900 °C

5.2.2. Isothermal time effect on performance of CuO/AFC ratio 30 with reduction and oxidation at 820 °C

Figure 5.5 shows TGA curves for two different isothermal times i.e. one and three hours during reduction of CuO/AFC ratio of 30 at 820 °C. In order to investigate the isothermal time effect, two experiments were performed with different isothermal times. It was observed that the combustion was incomplete at one hour of isothermal time and for three hours the combustion was relatively complete (final mass close to 88%). Almost the same type of curves were observed during oxidation for both the cases, with equal oxidized mass which showed that the final mass of reduced CuO did not have effect on the final oxidized weight during oxidation at 820 °C. Therefore, because of lower reactivity at lower temperature (820 °C) compared to 900 °C, performance of CuO/AFC ratio of 30 at 820 °C showed much longer time to reach steady state than 900 °C.

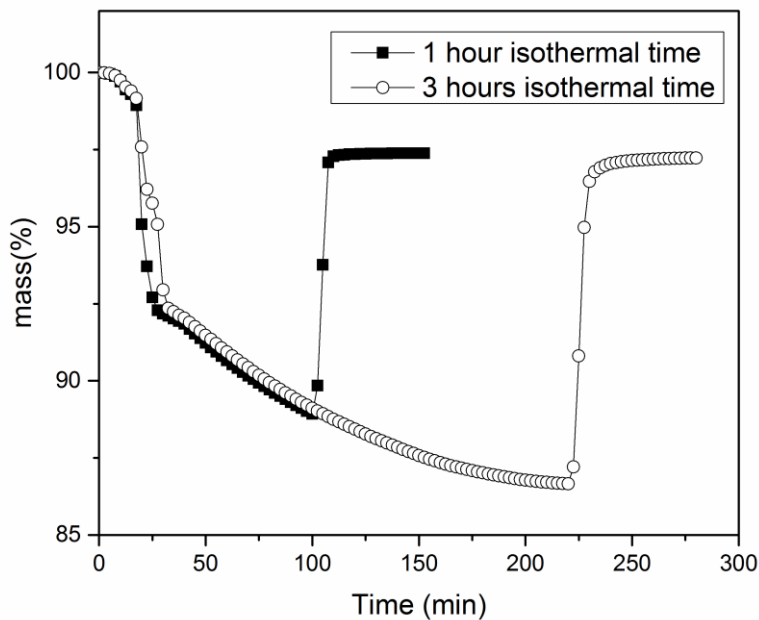


Figure 5.5. Comparison of different isothermal times for CuO/AFC ratio of 30 with reduction and oxidation at 820 °C

5.3. Characterizations of fresh CuO/AFC and solid residues after TGA experiments by analytical techniques

5.3.1. XRD and SEM characterizations

In order to assess crystalline structure changes, XRD was performed for CuO/AFC and CuO/BL raw coal ratio of 30 after five cycles with reduction and oxidation at 900 °C as shown in Figure 5.6 (a) and (b). CuO was detected in the solid residue in XRD analysis for CuO/AFC, which shows that all the reduced CuO is again oxidized back to CuO after oxidation during five cycles. However, for CuO/BL raw coal CuO and SiO₂ (ash) were detected.

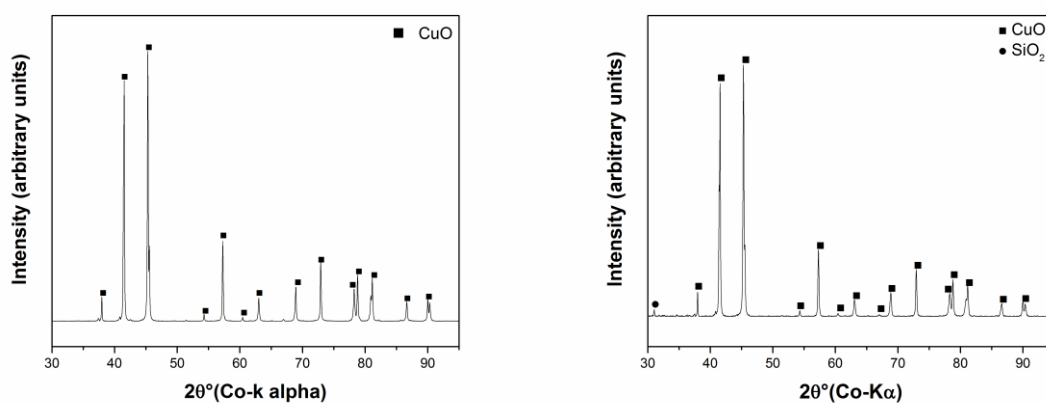


Figure 5.6. XRD patterns of a) CuO/AFC and b) CuO/BL raw coal ratio of 30 after five cycles with reduction and oxidation at 900 °C

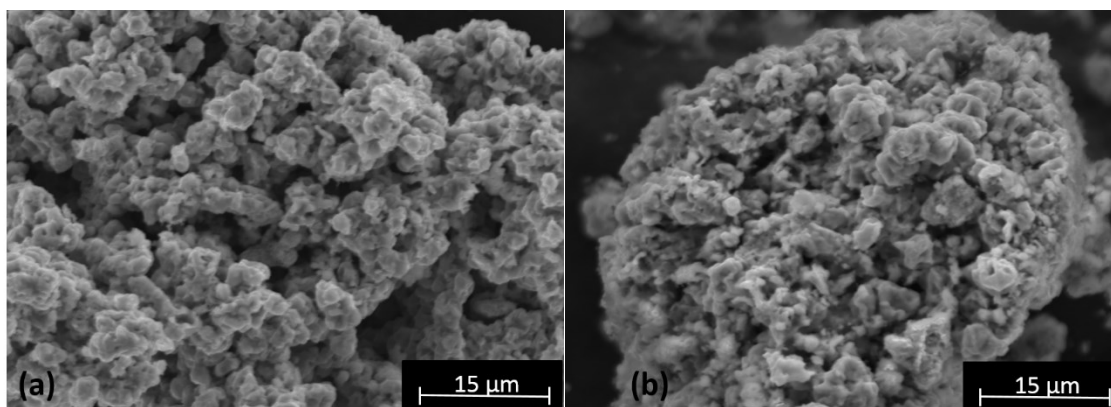


Figure 5.7. SEM images of (a) pure CuO and (b) CuO/AFC ratio of 30 before TGA test

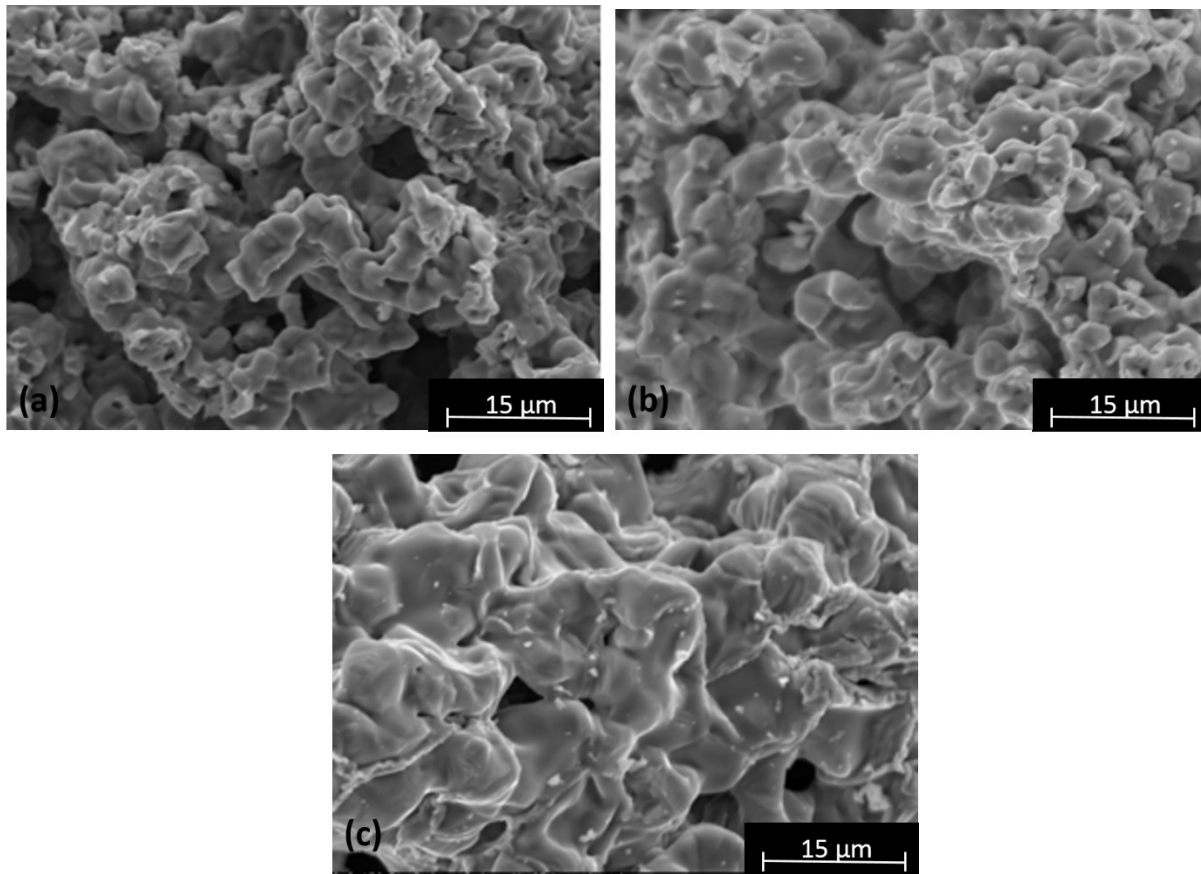


Figure 5.8. SEM images of residue of CuO/AFC ratio of 30 after first cycle with reduction and oxidation at a) 820, b) 900 and c) 1000 °C

In order to investigate surface morphological changes which occurred during multicycle experiments, SEM analysis were performed for both fresh and residual samples. Figure 5.8 (a) shows SEM image of CuO/AFC ratio of 30 after first cycle with reduction and oxidation at 820 °C. It can be observed from the images that sintering started and surfaces of particles become coarser after first cycle. Particles started to merge and there is an indication of sintering. Pores can be seen in the image, which allow air to pass through the material and react with particles during re-oxidation process. Thus, at 820 °C for CuO/AFC ratio of 30 sintering started unlike to the lower temperatures. Figure 5.8 (b) shows the trend for sintering in higher temperatures including 900 °C after the first reduction and oxidation. The effects of sintering are clearly visible, in comparing Figure 5.7 (b) and Figure 5.8 (b), the spherical shaped particles can be seen after the first cycle of reduction and oxidation at 900 °C. A high sintering effect can be seen at 900 °C even after first

reduction and oxidation. Sintering effect at higher temperatures can be seen after first cycle with reduction and oxidation at 1000 °C (Figure 5.8(c)). In all cases, the materials are merging together.

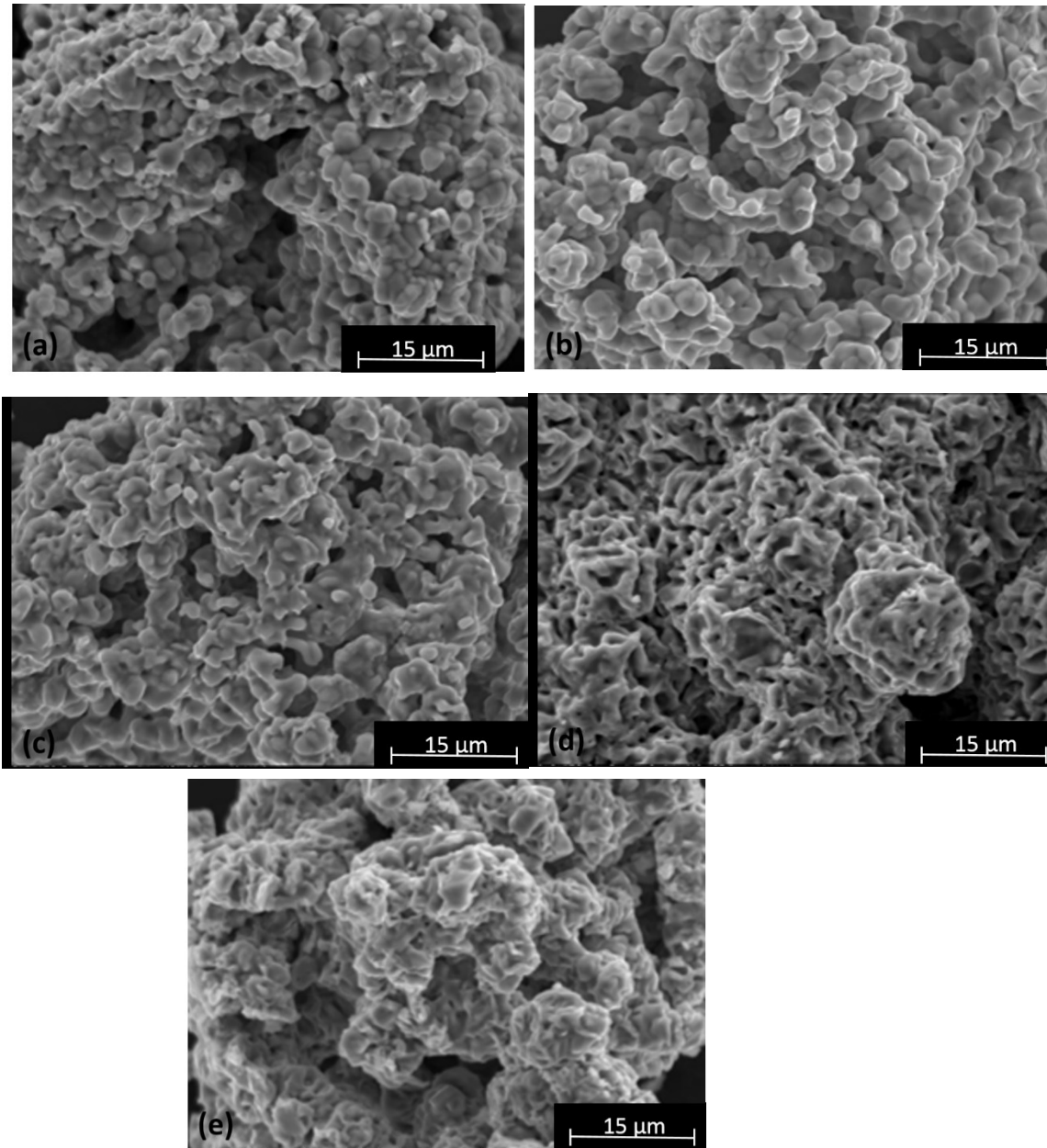


Figure 5.9. SEM images of residue of CuO/AFC ratio of 30 during five cycles after a) first, b) second, c) third, d) forth and e) fifth cycle with reduction and oxidation at 750 °C

Figure 5.9 shows SEM images of residue of CuO/AFC ratio 30 after first, second, third, fourth and fifth cycles with reduction and oxidation at 750 °C. It can be observed from these images that sintering effect starts more lately during multicycle tests at 750 °C compared to higher temperatures of reduction and oxidation including 820 and 900 °C. Comparison of images of the first reduction and oxidation cycle for 750, 820, 900 and 1000 °C (Figure 5.8 and 5.9) show that after the first cycle, particles at 820 °C densify due to sintering effect and this sintering effect is even higher for 900 and 1000 °C.

Comparing the images of five cycles after reduction and oxidation at 750 °C, the sintering effect can be seen in all these consecutive cycles (Figure 5.9). Start of sintering can be seen from the first up to the third cycle and no specific morphological changes were noticed. But for the fourth and the fifth cycle the morphological changes can be seen clearly. From SEM image of the fourth cycle, it can be observed that the shape of the sintered particles became as accumulated filaments merged together and in some areas they became as shape of spherical tissues. Sintering of particles became as a cocoon shape after five cycles. However, the degree of sintering is found to be lower at 750 °C compared to higher temperatures.

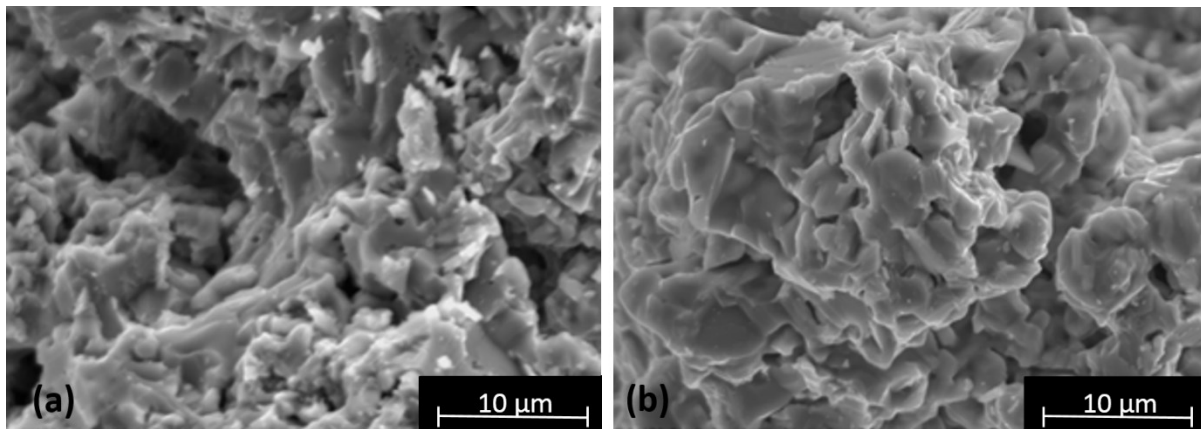


Figure 5.10. SEM images of residue of CuO/AFC ratio of 30 after five cycles with reduction and oxidation at a) 820 °C and b) 900 °C

Figure 5.10 shows SEM images of CuO/AFC ratio of 30 after five cycles with reduction and oxidation at (a) 820 °C and (b) 900 °C. Surfaces of particles look rough and there is a trend for particles to attach together at 820 °C (Figure 5.10 (a)). Furthermore, chunks of particles can be

seen in this image attaching to rough surfaces of the rest of the particles. However, the sintering effect at 820 °C is lower than that at 900 °C. As seen from Figure 5.10 (b), particles were sintered because of sintering effect at 900 °C. Sintered rough surfaces of particles joined together. However, some small areas have flat surfaces beside the cubic sugar type crystalline species attached to the rest of the accumulated particles.

5.3.2. BET surface area analysis

Table 5.1. BET results of porosity and surface area for two samples including pure CuO and CuO/AFC ratio of 30 after five cycles of reduction and oxidation at 820 °C

Materials	Total pore volume/ cm ³ g ⁻¹	Average pore radius/ BJH A°	Surface area/ BET m ² g ⁻¹
Pure CuO	3.91e-03	37.01	0.40
CuO after five cycles of reduction & oxidation of CuO/AFC ratio of 30 at 820 °C	6.16e-05	18.47	0.18

To assess the porosity and surface area changes after reduction and oxidation processes during multicycle experiments, BET analysis was performed for fresh CuO before experiment and CuO/AFC after the fifth cycle of TGA test with reduction and oxidation at 820 °C (Table 5.1). CuO/AFC residue after five cycles with reduction and oxidation at 820 °C was dense compared to pure CuO particles. The results also show decrease in surface area in multiple cycles after five cycles. The total pore volume, average pore radius of CuO/AFC after five cycles decreased compared to the pure CuO. After multicycle experiments, particles were sintered as a result the porosity of the particles being reduced. Because of the sintering these parameters decreased however this is not affecting the performance of CuO (at 900 °C). These results are also confirmed by SEM images as discussed earlier in section 5.3.1.

5.4. Conclusions

In this chapter, performance of CuO/AFC in CLC during multicycle experiments was investigated using TGA analyzer. Multicycle experiments were performed for slightly higher (10%) than stoichiometric ratio of CuO/AFC ratio of 30. Furthermore, the residual samples after experiments were characterized by XRD, SEM and BET in order to assess their changes after reduction and oxidation during multicycle tests. Conclusions based on this study are as follows:

1. The reactivity for the first cycle of CuO/AFC ratio of 30 was found to be slightly higher than the following cycles, which was due to the fresh CuO in the first cycle. The reactivity of further cycles was slightly lower from the first due to sintering, changes in the structure and decrease in pore sizes of the sample. Almost similar reactivity was observed for all the consecutive cycles. The similar trend for the consecutive cycles is because of no ash content in AFC and there is no ash accumulation and consequently no hindrance in the reaction could occur which is one of the main benefits of using AFC.
2. Mass variation during multicycle experiments showed constant masses of reduced and oxidized masses for CuO/AFC due to no ash content in AFC. The reaction reached to completion.
3. TGA experiments were performed to investigate the effect of CuO particle size on the CLC performance with AFC. The mass loss trend and the final mass values did not show any significant difference for different particle sizes.
4. XRD patterns of CuO/AFC ratio of 30 after oxidation during multicycle experiments showed the presence of CuO only which indicates that the reduced metal oxide is again oxidized back to CuO during oxidation and no other material was left. However, in case of CuO/BL raw coal CuO and SiO₂ (ash) were detected.
5. SEM images of multicycle experiments after reduction and oxidation at 750 °C showed an increase in sintering after each cycle. However, sintering was lower at 750 °C compared to higher temperatures. Sintering after each cycle at 820 °C was also noticed, similar in trend with 750 °C. Sintering at 820 °C was lower than that of 900 °C. Higher sintering occurred

after each reduction and oxidation at 900 °C. SEM images of reduction and oxidation at 1000 °C showed high sintering even after the first cycle.

6. BET results for pure CuO and CuO/AFC ratio of 30 after five cycles with reduction and oxidation at 820 °C, total pore volume and average pore radius after five reduction and oxidation cycles compared to the fresh CuO.

CHAPTER 6

Application of CLC in power generation

6.1. Introduction

In coal power plants, coal powders are burned to produce heat. The released heat is transferred to water to produce steam through heat exchanger tubes. The produced steam turns the blades of a steam turbine connected to a generator which produces electric power. Flue gas from coal combustion exits the power plant through a stack. In the coal power plants, flue gas cleaning and emission of CO₂ into the atmosphere are big challenges.

Unlike coal power plant, CLC power plant is used to capture CO₂ and to generate electricity. In this system the heat released from the air reactor and fuel reactor are transferred to the steam tubes around reactors to produce steam which produces electricity.

Based on the TGA results of AFC with CuO, obtained in this study, a special system is proposed for CLC of AFC for the application in power generation. Suitable temperatures for CuO-based oxygen carriers in air reactor were in the range of 850 to 900 °C and for the fuel reactor are in the range of 900 to 950 °C.¹⁵²⁻¹⁵⁵ Based on the TGA experiments among different operating temperatures (Figure 6.1), 900 and 950 °C showed good reactivity. However, SEM images showed sintering at the higher temperatures. Therefore, temperature of 900 °C was selected as desired temperatures of fuel reactor and air reactor. Based on TGA results (Figure 6.1), at these temperatures, oxidation time is about 5 minutes and reduction time is about 15 minutes as shown in Figure 6.1.

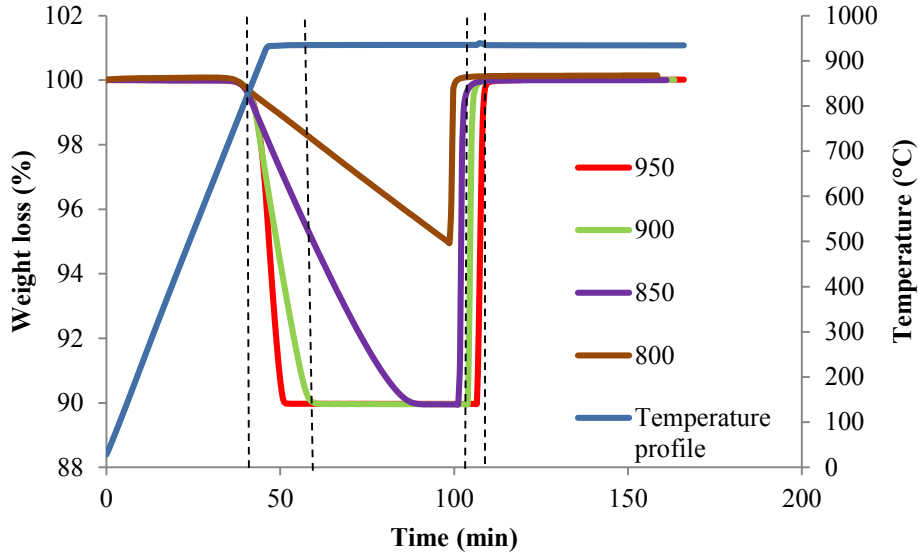


Figure 6.1. TGA results of reduction and oxidation of CuO at different temperatures of 800, 850, 900 and 950 °C (dash lines for 900 °C curve show about 15 minutes for reduction time and about 5 minutes for oxidation time)

6.2. Suggested CLC of AFC configuration

Two interconnected fluidized bed reactors are proposed for CLC of AFC as shown in Figure 6.2. In this system oxidation and reduction reactions take place during operation in air reactor and fuel reactor as indicated in Figure 6.2.

It is noteworthy to mention that the released heat from the reactors can be transferred to the steam tubes or water jackets around reactors to produce steam for steam turbine to generate electric power. The produced steam can also be used for heating purposes in industry.

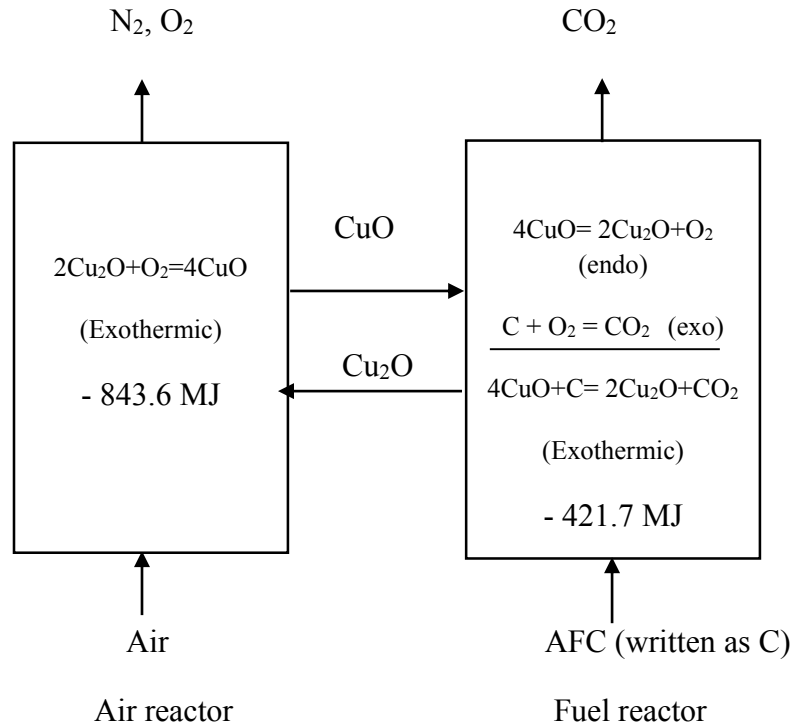


Figure 6.2. CuO and AFC reactions and overall heat releases in two interconnected fluidized bed reactors

6.3. Mass balance

To perform mass balance calculations for 500 MWe CLC unit, several assumptions are taken into consideration as follows: 1) efficiency of 40% for the system and total production of system based on MW_t which is equivalent to 1250 MW_t, 2) 100% conversion of AFC and 100% oxidation of oxygen carrier, 3) conversion of all CuO to Cu₂O, 4) about 10% of CuO material in the pipe lines and in the cyclones.

Moreover, it should be noted that 10% excess O₂ was considered for combustion based on CuO/AFC ratio of 30 at 900 °C from TGA experiments for these calculations. In this regard, 1250 MW_t is equivalent to 34.25 kg/s coal feed rate of AFC. Required flow rate of CuO in fuel reactor is equal to 1020 kg/s based on the stoichiometric ratio of CuO/AFC equal to 27.07 and 10% excess O₂ (Table 6.1).

Also, residence time of 15 minutes for reduction and 5 minutes for oxidation based on TGA results were considered. (Note: in industrial scale, in fluidized bed reactors the conversion are occurring faster and the residence time is much lower). Furthermore, HHV (High Heating Value)

of AFC is equal to 36.5 MJ/kg¹⁷⁰ and molecular weights of CuO and Cu₂O are equal to 79.545 g/mol and 143.09 g/mol respectively.

For 15 minutes residence time the amount of CuO hold up in the fuel reactor is equal to 918t. Similarly 917 kg/s of Cu₂O (equivalent of 1020 kg/s of CuO) is oxidized in the air reactor. According to residence time of 5 minutes for oxidation the hold up is equal to 275.1t of Cu₂O or 306t of CuO. Therefore, total required CuO is 1224t. Assuming about 10% of material in the pipe lines and in the cyclones, required CuO is 1346.4t (Table 6.2).

Table 6.1. Coal feed rate and required flow rate of CuO in fuel reactor for a 500 MW_e CLC unit with efficiency of 0.4 and (HHV of AFC = 36.5 MJ/Kg)¹⁷⁰

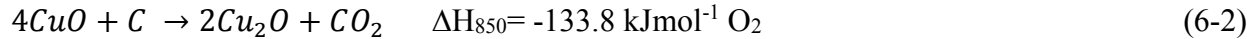
AFC (Kg/s)	CuO (Kg/s)
34.25	1020

Table 6.2. CuO material for a 500 MW CLC unit with efficiency of 0.4 and (HHV of AFC = 36.5 MJ/Kg)¹⁷⁰

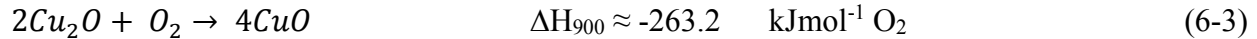
Material	15 minutes of reduction in fuel reactor	5 minutes of oxidation in air reactor	Total	In cyclone and pipelines
CuO (t)	918	306	1224	1346.4

6.4. Heat energy balance

Two main CuO reactions which take place during experiments in fuel reactor are as follows: the auto-decomposition of CuO produces Cu₂O and oxygen as shown in Eq. (6-1) and CuO reacts with AFC shown as (C) to produce cuprite Cu₂O and CO₂ as shown in Eq. (6-2).^{92,174}



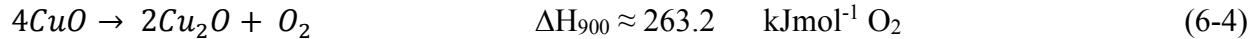
The released heat from air reactor at 900 °C is almost equal to the released heat at 850 °C. Therefore, the following reaction as shown in Eq. (6-3), occurs in air reactor at 900 °C based on Eq. 6.1.



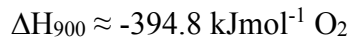
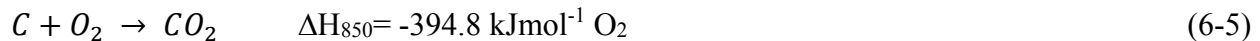
Moreover, for assessing the heat release from fuel reactor two reactions should be considered which are as follows:

- 1) $4CuO \rightarrow 2Cu_2O + O_2$ and 2) $C + O_2 \rightarrow CO_2$

For the first reaction, the released heat from fuel reactor at 900 °C is almost equal to the released heat at 850 °C. Therefore, the following reaction as shown in Eq. (6-4), occurs in fuel reactor at 900 °C based on Eq. 6.1.



For the second reaction, the released heat from fuel reactor at 900 °C is almost equal to the released heat at 850 °C. Therefore, the following reaction as shown in Eq. (6-5), occurs in fuel reactor at 900 °C.



To assess heat release rate in the reactor, CuO should be converted into equivalent O₂ moles. Flow rate of 1020 kg/s of CuO is equal to 12.82 kmol/s (MW of CuO is 79.545 g/mol) and is equivalent to 3.205 kmols of O₂/s. Calculation of the heat release rate of O₂ in the fuel reactor and the air reactor corresponds to this oxygen consumption or production in the two reactors.

Therefore, the released heat from air reactor is equal to 843.6 MJ/s. For the released heat from the fuel reactor, it should be noted that there are two reactions occurring in the fuel reactor as discussed earlier. The first reaction is an endothermic reaction which needs 843.6 MJ/s and the second reaction is an exothermic reaction which releases 1265.3 MJ/s heat energy. The total released heat energy from fuel reactor is equal to summation of the obtained heat for the first reaction and the released heat from the second reaction which is equal to 421.7 MJ/s. Table 6.3 presents the heat releases from air reactor and fuel reactor.

Table 6.3. Heat releases from the air reactor and the fuel reactor in two interconnected fluidized bed CLC system

Heat release from air reactor (MJ/s)	Heat release from fuel reactor (MJ/s)
843.6	421.7

There is difference between the released heat from the air reactor and the fuel reactor. Therefore, steam tubes with the larger surfaces and higher heat transfer area can be used for the heat release from the air reactor because of its higher heat release rate and steam tubes with lower surface area can be used for the heat release from the fuel reactor because of its lower heat release rate.

It is also noteworthy to mention that it is better to have minimum excess oxygen in the system for the higher purity of exiting CO₂ stream. When there is excess amount of oxygen in the fuel reactor, oxygen exits from fuel reactor with CO₂ which causes impurity for the exiting CO₂ stream.

6.5. Conclusions

The CLC system is used here for steam generation and the steam can be used in steam turbines to produce electricity. The released heat energy from the reactors can turn water to steam through the boiler water tubes. The generated steam can drive a steam turbine connected to an electricity generator followed by a transformer to generate electricity. The important aspect of CLC system is that the flue gas consists of concentrated CO₂.

The residence time in air and fuel reactors was based on TGA results obtained for CuO and AFC. Two interconnected fluidized bed reactors were suggested for CLC of AFC. For the CuO/AFC ratio of 30 which was found out to be the close to stoichiometric ratio, mass and energy balance of the system was carried out for a 500 MW_e CLC unit at 900 °C. Residence time of 15 minutes for reduction and 5 minutes for oxidation were considered based on TGA results. The required AFC as the solid fuel and CuO as an oxygen carrier were also calculated.

Moreover, the released heat energy from the fuel reactor and the air reactor were obtained. For the fuel reactor two reactions were considered separately including auto decomposition of CuO as the first reaction and coal combustion as the second reaction. It was determined that there is a difference between the released heat from the air reactor and the fuel reactor. Therefore, steam tubes with higher surface area can be used for the air reactor because of its higher heat release rate and steam tubes with the lower surface area can be used for the fuel reactor because of its lower heat release rate. As the beneficial result of using CuO as an oxygen carrier with AFC, overall reactions in the air reactor and the fuel reactor are exothermic.

CHAPTER 7

Conclusions and Future work

7.1 Conclusions

Fossil fuels, naturally abundant and inexpensive fuels, have been used in industry to produce heat and energy which is causing huge environmental impact and global warming due to the GHG emissions; CO₂ is one of the primary gases that is responsible. To overcome these issues, several CO₂ capture technologies are being developed; beside the conventional technologies a new approach for CO₂ capture is CLC. This technology is considered as one of the promising technologies for CO₂ capture due to its potential to reduce energy penalty and the cost associated with CO₂ capture from combustion off-gas. CLC is an energy and cost efficient technology because it does not require air separation unit to separate flue gases. CLC of solid fuel in which oxygen carrier releases oxygen is called CLOU. CLC and CLOU are the promising technologies which require proper metal oxides as oxygen carrier for CO₂ capture. To the best of our knowledge, AFC as solid fuel and CuO as oxygen carrier for CLOU process have not been reported earlier.

Methods and methodology of single cycle and multi cycle experiments for CuO/AFC samples were discussed. Also the background information, preparation process and properties of AFC were summarized. To investigate CLOU performance of CuO with AFC during reduction and oxidation processes, thermogravimetric analysis was carried out. Thermal reactivity behaviors of CuO and AFC by TGA with various ratios of CuO/AFC (10 to 50) at various temperatures (450-1000 °C) under nitrogen environment were studied. Initially favorable ratio of CuO/AFC was prepared by physically mixing the materials and then the mixture was heated in TGA from ambient temperature up to desired temperature in nitrogen environment. During reduction and oxidation, weight loss and weight gain performance of CuO/AFC were studied. The TGA results showed that at around 450 °C AFC induced CuO reduction initiated and at about 800 °C complete combustion occurred. Ratio 30 was figured out to be the close to stoichiometric ratio of CuO/AFC for complete combustion. Incomplete reactions took place at lower temperatures because residual char did not react completely and at higher temperatures sintering effect was detected during characterization. Theoretical calculations and thermodynamic assessments also confirmed the experimental results.

In addition, Factsage software was used to predict gas and solid compounds formed during CuO and AFC reaction for various ratios of CuO/AFC under equilibrium condition based on Gibbs energy minimization. CO was formed for CuO/AFC ratio of 10 but CO₂ was formed for higher ratios of CuO/AFC. The Factsage prediction showed the occurrence of auto decomposition of CuO to Cu₂O at above 719 °C, TGA results are in accordance to this.

Samples and residues of CuO/AFC were characterized with analytical techniques including XRD, SEM, EDX, CHNS analysis to investigate the interactions between oxygen carrier and volatile matter or coal. For residue of CuO/AFC ratio of 10, Cu and Cu₂O were detected by XRD but for higher ratios of CuO/AFC the results showed Cu₂O and CuO formation. Solid residues of CuO/AFC ratio of 30 after being reduced by TGA at several temperatures including 750, 790, 820 and 900 °C were studied by SEM. According to these results, sintering was shown at high temperatures. Sintering was not observed in SEM images at lower temperatures of 750 and 790 °C despite it was shown that from 820 °C effect of sintering starts and continues for higher temperatures including 900 °C. Morphology of materials was not changed widely at the lower temperatures but structure of particles are totally different (sintered and in some cases joint Y-shape structures) for CuO/AFC ratio of 30 after being reduced at 820 °C by TGA.

At various stages of CuO/AFC interactions, the evaluation of reaction mechanism of CuO/AFC was also carried out. Based on TGA result of only AFC the evaporation of most of volatile matters of AFC occurred at approximately 450 °C. Stages of CuO/AFC reaction mechanism in fuel reactor are as follows. Firstly, devolatilization of volatile matters from the mixture of CuO/AFC takes place. Then, an induced gas-solid interaction happens between gas and solid phases including volatile matters and CuO/AFC mixture. Afterwards, solid-solid interaction between CuO and AFC char occurs. Finally, auto decomposition of CuO occurs and oxygen is released from. The reaction between Cu₂O and oxygen occurs in air reactor and CuO is generated again.

Moreover, multicycle experiments were carried out in TGA to study the performance of CuO/AFC in CLC during longer operating conditions. Multicycle experiments were performed for close to stoichiometric ratio of CuO/AFC ratio of 30. The results showed that the reactivity for the first cycle of CuO/AFC ratio of 30 was slightly higher than the following cycles, which is due to the fresh CuO in the first cycle. Almost similar reactivity was observed for all the consecutive

cycles. This is because of no ash content in AFC and no ash accumulation in TGA pan which as a result no hindrance in the reaction could occur. This is one of the main advantages of using AFC over raw coal. Also TGA experiments were carried out to study the effect of CuO particle size on the CLC performance with AFC. The final mass values did not show any significant difference for various particle sizes.

The residual samples after experiments were characterized by XRD, SEM and BET in order to evaluate their changes after reduction and oxidation processes during multicycle experiments. Presence of CuO was only detected in XRD patterns of CuO/AFC ratio of 30 after oxidation during multicycle testes. However, the results showed CuO and SiO₂ for CuO/BL raw coal. Enhancement in sintering after each cycle was observed based on the SEM images of multicycle tests after reduction and oxidation processes at 750 °C. However, compared to higher temperatures, the extent of sintering was lower at 750 °C. In case of 820 °C, the sintering trend was the same as 750 °C after each cycle. After each reduction and oxidation at 900 °C, higher sintering was observed. Meanwhile, decrease in total pore volume, average pore radius and surface area after five reduction and oxidation cycles compared to the fresh CuO was shown by BET results for pure CuO and CuO/AFC ratio of 30 after five cycles with reduction and oxidation at 820 °C. Finally, application of CLC in power generation was assessed. For CLC of AFC, mass and heat energy balance of the system was carried out. It can be concluded that AFC as the solid fuel showed a promising oxidation/reduction performance which has a great potential to be used in the CLC process.

7.2. Future work and recommendations

The suggested recommendations for future work are as follows:

1. It is recommended to add inert support materials to CuO to enhance and improve its structural properties and taking the advantage of their positive effects on the performance of CuO as an oxygen carrier using AFC as the solid fuel in CLC process. These additions can be provided by different synthesis methods; thus, the effect of preparation method should also be studied.

2. In this study, TGA was used as the main equipment for investigating reduction and oxidation behavior of materials. To have a better understanding of performance of the oxygen carrier with AFC, packed bed or fluidized bed experiments are recommended.
3. Also to have a better understanding of changes during multicycle performances of materials TEM characterization is suggested for residual particle. More precise information about CuO changes during multicycle experiments would be obtained by TEM.
4. In this dissertation, CuO was used as the oxygen carrier with AFC in the experiments. However, other oxygen carriers such as NiO can also be tested to compare their behaviors with existing results using AFC as solid fuel. Other low cost materials such as biomass as solid fuel can also be tested for CLC performance.
5. Furthermore, an overall study in techno-economic evaluation of different oxygen carrier more in detail is needed.

References

1. García-Labiano, F., De Diego, L.F., Gayán, P., Adánez, J., Abad, A., & Dueso, C., “Effect of fuel gas composition in chemical-looping combustion with ni-based oxygen carriers. 1. Fate of sulfur.”, *Industrial and Engineering Chemistry Research*, 2009, 48, 5, 2499-2508
2. Solunke, R.D., Vesper, G., “Nanocomposite oxygen carriers for chemical-looping combustion of sulfur-contaminated synthesis gas”, *Energy and Fuels*, 2009, 23, 10, 4787-4796
3. Fang, H., Haibin, L., Zengli, Z., “Advancements in development of chemical-looping combustion: A review”, *International Journal of Chemical Engineering (1687806X)*, 2009, 2009, 1-16.
4. Adánez, J., Abad, A., García-Labiano, F., Gayán, P., De Diego, L.F., “Progress in chemical-looping combustion and reforming technologies”, *Progress in Energy and Combustion Science*, 2012, 38, 2, 215-282
5. Balaji, S., Ilic, J., Ydstie, B. E., Krogh, B. H., “Control-based modeling and simulation of the chemical-looping combustion process”, *Industrial and Engineering Chemistry Research*, 2010, 49, 10, 4566-4575
6. Ishida, M., Zheng, D., Akehata, T., “Evaluation of a chemical-looping-combustion power-generation system by graphic exergy analysis”, *Energy*, 1987, 12, 2, 147-154
7. Gilliland, E., “Production of industrial gas comprising carbon monoxide and hydrogen”, U.S.: 2,671,721, 1946
8. Hossain, M.M., De Lasa, H.I., “Chemical-looping combustion (CLC) for inherent separations-a review”, *Chemical Engineering Science*, 2008, 63, 18, 4433-4451
9. Eyring, E., Konya, G., “Chemical looping combustion kinetics”, (Utah Clean Coal Program Topical Report No. DE-FC26-06NT42808), University of Utah: Salt Lake City, 2009

10. Jin, H.G., Hong, H., Han, T., "Progress of energy system with chemical-looping combustion", *Chinese Science Bulletin*, 2009, 54, 6, 906-919
11. Moghtaderi, B., "Review of the recent chemical looping process developments for novel energy and fuel applications", *Energy and Fuels*, 2012, 26, 1, 15-40
12. Socolow, R.H., "Can we bury global warming?", *Scientific American*, 2005, 293, 1, 49-55
13. Mattisson, T., Lyngfelt, A., Leion, H., "Chemical-looping with oxygen uncoupling for combustion of solid fuels", *International Journal of Greenhouse Gas Control*, 2009, 3, 1, 11-19
14. Benson, S.M., Surles, T., "Carbon dioxide capture and storage: An overview with emphasis on capture and storage in deep geological formations", *Proceedings of the IEEE*, 2006, 94, 10, 1795-1804
15. Davison, J., Thambimuthu, K., *Proceedings of the 7th International Conference on Greenhouse Gas Control Technologies*, Vancouver, British Columbia, Canada, Sept 2-9, 2004
16. Steeneveldt, R., Berger, B., Torp, T.A., "CO₂ capture and storage: Closing the knowing-doing gap", *Chemical Engineering Research and Design*, 2006, 84, 9 A, 739-763
17. Ishida, M., Jin, H., "A novel combustor based on chemical-looping reactions and its reaction kinetics", *Journal of Chemical Engineering of Japan*, 1994, 27, 3, 296-301
18. Anheden, M., Na^osholm, A.-S., Svedberg, G., *In: Proceedings of the 30th Intersociety Energy Conversion Engineering Conference*, Orlando, FL, 1995, 75-81
19. Lyngfelt, A., Leckner, B., Mattisson, T., "A fluidized-bed combustion process with inherent CO₂ separation; Application of chemical-looping combustion", *Chemical Engineering Science*, 2001, 56, 10, 3101-3113

20. Brandvoll, O., Kolbeinsen, L., Olsen, N., Bolland, O., *In: Proceedings of ICheaP-6, The Sixth Italian Conference on Chemical and Process Engineering*, Pisa, Italy, Chemical Engineering Transactions, 2003, 3, 105-110
21. Adánez, J., De Diego, L.F., García-Labiano, F., Gayán, P., Abad, A., Palacios, J.M., “Selection of oxygen carriers for chemical-looping combustion”, *Energy and Fuels*, 2004, 18, 2, 371-377
22. Wolf, J., Anhedén, M., Yan, J., “Comparison of nickel- and iron-based oxygen carriers in chemical looping combustion for CO₂ capture in power generation”, *Fuel*, 2005, 84, 7-8, 993-1006
23. Kronberger, B., Johansson, E., Löffler, G., Mattisson, T., Lyngfelt, A., Hofbauer, H., “A two-compartment fluidized bed reactor for CO₂ capture by chemical-looping combustion”, *Chemical Engineering and Technology*, 2004, 27, 12, 1318–1326
24. Siriwardane, R., Tian, H., Richards, G., Simonyi, T., Poston, J., “Chemical-looping combustion of coal with metal oxide oxygen carriers”, *Energy and Fuels*, 2009, 23, 8, 3885-3892
25. Siriwardane, R., Tian, H., Miller, D., Richards, G., Simonyi, T., Poston, J., “Evaluation of reaction mechanism of coal-metal oxide interactions in chemical-looping combustion”, *Combustion and Flame*, 2010, 157, 11, 2198-2208
26. Luo, M., Wang, S., Wang, L., “Investigation of chemical-looping combustion of solid fuels”, *Applied Mechanics and Materials*, 2013, 316-317, 95-98
27. Lyngfelt, A., “Chemical-looping combustion of solid fuels - Status of development”, *Applied Energy*, 2014, 113, 1869-1873
28. Saha, C., Bhattacharya, S., “Comparison of CuO and NiO as oxygen carrier in chemical looping combustion of a Victorian brown coal”, *International Journal of Hydrogen Energy*, 2011, 36, 18, 12048-12057

29. Chuang, S.Y., Dennis, J.S., Hayhurst, A.N., Scott, S.A., “Development and performance of Cu-based oxygen carriers for chemical-looping combustion”, *Combustion and Flame*, 2008, 154, 1-2, 109-121
30. De Diego, L.F., García-Labiano, F., Adánez, J., Gayán, P., Abad, A., Corbella, B.M., Palacios J.M., “Development of Cu-based oxygen carriers for chemical-looping combustion”, *Fuel*, 2004, 83, 13, 1749-1757
31. Moghtaderi, B., Song, H., “Reduction properties of physically mixed metallic oxide oxygen carriers in chemical looping combustion”, *Energy and Fuels*, 2010, 24, 10, 5359-5368
32. Zhao, H.-, Liu, L.-, Xu, D., Zheng, C.-, Liu, G.-, Jiang, L.-, “NiO/NiAl₂O₄ oxygen carriers prepared by sol-gel for chemical-looping combustion fueled by gas”, *Journal of Fuel Chemistry and Technology*, 2008, 36, 3, 261-266
33. Saha, C., Zhang, S., Hein, K., Xiao, R., Bhattacharya, S., “Chemical looping combustion (CLC) of two Victorian brown coals - Part 1: Assessment of interaction between CuO and minerals inherent in coals during single cycle experiment”, *Fuel*, 2013, 104, 262-274
34. Rubel, A., Liu, K., Neathery, J., Taulbee, D., “Oxygen carriers for chemical looping combustion of solid fuels”, *Fuel*, 2009, 88, 5, 876-884
35. Cao, Y., Pan, W.P., “Investigation of chemical looping combustion by solid fuels. 1. Process analysis”, *Energy and Fuels*, 2006, 20, 5, 1836-1844
36. Cho, P., Mattisson, T., Lyngfelt, A., “Comparison of iron-, nickel-, copper- and manganese-based oxygen carriers for chemical-looping combustion”, *Fuel*, 2004, 83, 9, 1215-1225
37. Mattisson, T., Lyngfelt, A., Cho, P., “The use of iron oxide as an oxygen carrier in chemical-looping combustion of methane with inherent separation of CO₂”, *Fuel*, 2001, 80, 13, 1953-1962

38. Mattisson, T., Järnäs, A., Lyngfelt, A., “Reactivity of some metal oxides supported on alumina with alternating methane and oxygen - application for chemical-looping combustion”, *Energy and Fuels*, 2003, 17, 3, 643-651
39. Mattisson, T., Johansson, M., Lyngfelt, A., “Multicycle reduction and oxidation of different types of iron oxide particles – application to chemical-looping combustion”, *Energy and Fuels*, 2004, 18, 3, 628-637
40. Johansson, M., Mattisson, T., Lyngfelt, A., “Investigation of Fe₂O₃ with MgAl₂O₄ for chemical-looping combustion”, *Industrial and Engineering Chemistry Research*, 2004, 43, 22, 6978-6987
41. Cho, P., Mattisson, T., Lyngfelt, A., “Carbon formation on nickel and iron oxide-containing oxygen carriers for chemical-looping combustion”, *Industrial and Engineering Chemistry Research*, 2005, 44, 4, 668-676
42. Gayán, P., De Diego, L.F., García-Labiano, F., Adánez, J., Abad, A., Dueso, C., “Effect of support on reactivity and selectivity of ni-based oxygen carriers for chemical-looping combustion”, *Fuel*, 2008, 87, 12, 2641-2650
43. Ishida, M., Jin, H., Okamoto, T., “A fundamental study of a new kind of medium material for chemical-looping combustion”, *Energy and Fuels*, 1996, 10, 4, 958-963
44. Ishida, M., Jin, H., “A novel chemical-looping combustor without NO_x formation”, *Industrial and Engineering Chemistry Research*, 1996, 35, 7, 2469-2472
45. Jin, H., Okamoto, T., Ishida, M., “Development of a novel chemical-looping combustion: synthesis of a looping material with a double metal oxide of CoO-NiO”, *Energy and Fuels*, 1998, 12, 6, 1272-1277

46. Ishida, M., Jin, H., Okamoto, T., “Kinetic behavior of solid particle in chemical-looping combustion: suppressing carbon deposition in reduction”, *Energy and Fuels*, 1998, 12, 2, 223-229
47. Jin, H., Okamoto, T., Ishida, M., “Development of a novel chemical-looping combustion: synthesis of a solid looping material of NiO/NiAl₂O₄”, *Industrial and Engineering Chemistry Research*, 1999, 38, 1, 126-132
48. Jin, H., Ishida, M., “Reactivity study on natural-gas-fueled chemical-looping combustion by a fixed-bed reactor”, *Industrial and Engineering Chemistry Research*, 2002, 41, 16, 4004-4007
49. Ishida, M., Yamamoto, M., Ohba, T., “Experimental results of chemical-looping combustion with NiO/NiAl₂O₄ particle circulation at 1200 °C”, *Energy Conversion and Management*, 2002, 43, 9-12, 1469-1478
50. Mattisson, T., Zafar, Q., Johansson, M., Lyngfelt, A., “Chemical-looping combustion as a new CO₂ management technology”, *First Regional Symposium on Carbon Management*, Dhahran, Saudi-Arabia, 2006
51. Liang-Shih, F., “Chemical looping particles”, *Chemical looping systems for fossil energy conversions*, New Jersey: John Wiley & Sons, Inc., 2010, 82-86
52. Azis, M., Jerndal, E., Leion, H., Mattisson, T., Lyngfelt, A., “On the evaluation of synthetic and natural ilmenite using syngas as fuel in chemical-looping combustion (CLC)”, *Chemical Engineering Research and Design: Transactions of the Institution of Chemical Engineers Part A*, 2010, 88, 11, 1505-1514
53. Schwebel, G., Hein, D., Krumm, W., “Performance tests of ilmenite mineral as oxygen carrier in a laboratory fixed bed reactor-first step in developing a new technical approach of implementing chemical looping combustion”, *In: Proc. 4th Int Conf on Clean Coal Technologies (CCT2009)*, Dresden, Germany, 2009

54. Schwebel, G., Wiedenmann, F., Krumm, W., "Reduction performance of ilmenite and hematite oxygen carriers in the context of a new CLC reactor concept", *In: Proc. 1st Int Conf on Chemical Looping*, Lyon, France, 2010
55. Rydén, M., Cleverstam, E., Lyngfelt, A., Mattisson, T., "Waste products from the steel industry with NiO as additive as oxygen carrier for chemical-looping combustion", *International Journal of Greenhouse Gas Control*, 2009, 3, 6, 693-703
56. Ksepko, E., Siriwardane, R.V., Tian, H., Simonyi, T., Sciãzko, M., "Comparative investigation on chemical looping combustion of coal-derived synthesis gas containing H₂S over supported NiO oxygen carriers", *Energy and Fuels*, 2010, 24, 8, 4206-4214
57. Solunke, R.D., Vesper, G., "Integrating desulfurization with CO₂-capture in chemical-looping combustion", *Fuel*, 2011, 90, 2, 608-617
58. Jerndal, E., "Investigation of nickel- and iron-based oxygen carriers for chemical-looping combustion", (PhD thesis, Chalmers University of Technology), 2010
59. Arrhenius, S., "On the influence of carbonic acid in the air upon the temperature of the ground", *Philosophical Magazine*, (1798-1977), 1896, 41, 251, 237-276
60. Earth System Research Laboratory (ESRL), National Oceanic and Atmospheric Administration (NOAA). <http://www.esrl.noaa.gov/gmd/ccgg/trends/>
61. Luo, M., Wang, S., Wang, L., "Advances in chemical-looping combustion for solid fuels", *Applied Mechanics and Materials*, 2013, 316-317, 99-104
62. Herzog, H., Drake, E., Adams, E., A White Paper; U.S. Department of Energy: Washington, D.C., January, 1997, U.S.DOE/DEAF22-96PC01257
63. Herzog, H., Eliasson, B., Kaarstad, O., "Capturing greenhouse gases", *Scientific American*, 2000, 282, 2, 72-79

64. Yu, J., Corripio, A.B., Harrison, D.P., Copeland, R.J., “Analysis of the sorbent energy transfer system (SETS) for power generation and CO₂ capture”, *Advances in Environmental Research*, 2003, 7, 2, 335-345
65. Riemer, P., 1998, <http://www.ieagreen.org.uk/paper2.htm> (accessed Dec 2005)
66. Freund, P., Powergen 98 Conference. Milan, June, 1998, [http://www.ieagreen.org.uk/pge98.Htm](http://www.ieagreen.org.uk/pge98.htm) (accessed Dec 2005)
67. Lyngfelt, A., “Oxygen carriers for chemical looping combustion - 4000 h of operational experience”, *Oil and Gas Science and Technology*, 2011, 66, 2, 161-172
68. Lyngfelt, A., Mattisson, T., WILEY-VCH Verlag GmbH & Co. KGaA; Weinheim, 2011
69. Richter, H.J., Knoche, K.F., “Reversibility of combustion processes”, *ACS Symposium Series*, 1983, 235, 71-85
70. Zafar, Q., Mattisson, T., Gevert, B., “Integrated hydrogen and power production with CO₂ capture using chemical-looping reforming – redox reactivity of particles of CuO, Mn₂O₃, NiO, and Fe₂O₃ using SiO₂ as a support”, *Industrial and Engineering Chemistry Research*, 2005, 44, 10, 3485-3496
71. Lewis, W.K., Gilliland, E.R., Int. Pat. USA, 1954
72. Cao, Y., Riley, J. T., Pan, W.–P., *Preprint paper - American Chemical Society, Division of Fuel Chemistry*, 2004, 49, 2, 815-816
73. Pan, W., Cao, Y., Liu, K., Wu, W., Riley, J., *In: Abstracts of Papers, 228th ACS National Meeting, Philadelphia, PA, United States, Fuel*, 2004, 155

74. Dennis, J.S., Scott, S.A., Hayhurst, A.N., “In situ gasification of coal using steam with chemical looping: a technique for isolating CO₂ from burning a solid fuel”, *Journal of the Energy Institute*, 2006, 79, 3, 187-190
75. Scott, S.A., Dennis, J.S., Hayhurst, A.N., Brown, T., “In situ gasification of a solid fuel and CO₂ separation using chemical looping”, *AIChE Journal*, 2006, 52, 9, 3325-3328
76. Leion, H., Mattisson, T., Lyngfelt, A., “The use of petroleum coke as fuel in chemical-looping combustion”, *Fuel*, 2007, 86, 12-13, 1947-1958
77. Leion, H., Mattisson, T., Lyngfelt, A., “Solid fuels in chemical-looping combustion”, *International Journal of Greenhouse Gas Control*, 2008, 2, 2, 180-193
78. Berguerand, N., Lyngfelt, A., “Design and operation of a 10 kW_{th} chemical-looping combustor for solid fuels – Testing with South African coal”, *Fuel*, 2008, 87, 12, 2713-2726
79. U.S. DOE Project Fact Sheet, www.netl.doe.gov/coal (accessed Dec 2005)
80. Andrus, H. E., Jr., Chiu, J. H., Stromberg, P. T., Thibeault, P. R., Twenty-second Annual International Pittsburgh Coal Conference, Pittsburgh, PA, Sept 12-15, 2005
81. Bedick, R. C., Coal Utilization Technologies Workshop, National Research Center for Coal and Energy, Morgantown, WV, Sept 22, 2004
82. Cao, Y., Cheng, Z., Meng, L., Riley, J.T., Pan, W.-P., *Preprint Paper - American Chemical Society, Division of Fuel Chemistry*, 2005, 51, 99-100
83. Cao, Y., Pan, W.-P., *Preprint Paper - American Chemical Society, Division of Fuel Chemistry*, 2005, 51, 415-416

84. Johansson, E., Lyngfelt, A., Mattisson, T., Johnsson, F., “Gas leakage measurements in a cold model of an interconnected fluidized bed for chemical-looping combustion”, *Powder Technology*, 2003, 134, 3, 210-217
85. Berguerand, N., Lyngfelt, A., “The use of petroleum coke as fuel in a 10 kW_{th} chemical-looping combustor”, *International Journal of Greenhouse Gas Control*, 2008, 2, 2, 169-179
86. Abad, A., Mattisson, T., Lyngfelt, A., Ryde'n, M., “Chemical-looping combustion in a 300 W continuously operating reactor system using a manganese-based oxygen carrier”, *Fuel*, 2006, 85, 9, 1174-1185
87. Mattisson, T., Johansson, M., Lyngfelt, A., *In: The Clearwater Coal Conference, Clearwater, FL*, 2006
88. Abad, A., Mattisson, T., Lyngfelt, A., Johansson, M., “The use of iron oxide as oxygen carrier in a chemical-looping reactor”, *Fuel*, 2007, 86, 7-8, 1021-1035
89. Abad, A., García-Labiano, F., De Diego, L.F., Gayán, P., Adánez, J., “Reduction kinetics of Cu-, Ni-, and Fe-based oxygen carriers using syngas (CO + H₂) for chemical-looping combustion”, *Energy and Fuels*, 2007, 21, 4, 1843-1853
90. Mattisson, T., Leion, H., Lyngfelt, A., “Chemical-looping with oxygen uncoupling using CuO/ZrO₂ with petroleum coke”, *Fuel*, 2009, 88, 4, 683-690
91. Abad, A., Adánez-Rubio, I., Gayán, P., García-Labiano, F., De Diego, L.F., Adánez, J., “Demonstration of chemical-looping with oxygen uncoupling (CLOU) process in a 1.5 kW_{th} continuously operating unit using a Cu-based oxygen-carrier”, *International Journal of Greenhouse Gas Control*, 2012, 6, 189-200

92. Cao, Y., Casenas, B., Pan, W.-P., “Investigation of chemical looping combustion by solid fuels. 2. Redox reaction kinetics and product characterization with coal, biomass, and solid waste as solid fuels and CuO as an oxygen carrier”, *Energy and Fuels*, 2006, 20, 5, 1845-1854
93. Shen, L.H., Wu, J.H., Xiao, J., Song, Q.L., Xiao, R., “Chemical-looping combustion of biomass in a 10 kW_{th} reactor with iron oxide as an oxygen carrier”, *Energy and Fuels*, 2009, 23, 5, 2498-2505
94. Leion H., Jerndal, E., Steenari, B.M., Hermansson, S., Israelsson, M., Jansson, E., Johnsson, M., Thunberg, R., Vadenbo, A., Mattisson, T., Lyngfelt, A., “Solid fuels in chemical-looping combustion using oxide scale and unprocessed iron ore as oxygen carriers”, *Fuel*, 2009, 88, 10, 1945-1954
95. Xiao, R., Song, Q.L., Song, M., Lu, Z.J., Zhang, S., Shen, L.H., “Pressurized chemical-looping combustion of coal with an iron ore-based oxygen carrier”, *Combustion and Flame*, 2010, 157, 6, 1140-1153
96. Leion, H., Lyngfelt, A., Mattisson, T., “Solid fuels in chemical-looping combustion using a NiO-based oxygen carrier”, *Chemical Engineering Research and Design*, 2009, 87, 11, 1543-1550
97. Gao, Z.P., Shen, L.H., Xiao, J., Qing, C.J., Song, Q.L., “Use of coal as fuel for chemical-looping combustion with Ni-based oxygen carrier”, *Industrial and Engineering Chemistry Research*, 2008, 47, 23, 9279-9287
98. Shulman, A., Cleverstam, E., Mattisson, T., Lyngfelt, A., “Manganese/iron, manganese/nickel, and manganese/silicon oxides used in chemical-looping with oxygen uncoupling (CLOU) for combustion of methane”, *Energy and Fuels*, 2009, 23, 10, 5269-5275
99. Rydén M. et. al., *In: 2nd International conference on chemical looping*, Darmstadt, 2012

100. Shulman, A., Cleverstam, E., Mattisson, T., Lyngfelt, A., “Chemical-looping with oxygen uncoupling using Mn/Mg-based oxygen carriers – Oxygen release and reactivity with methane”, *Fuel*, 2011, 90, 3, 941-950
101. Azimi, G., Rydén, M., Leion, H., Mattisson, T., Lyngfelt, A., “ $(\text{Mn}_z\text{Fe}_{1-z})_y\text{O}_x$ combined oxides as oxygen carrier for chemical-looping with oxygen uncoupling”, *AIChE Journal*, 2013, 59, 2, 582-588
102. Rydén, M., Lyngfelt, A., Mattisson, T., “ $\text{CaMn}_{0.875}\text{Ti}_{0.125}\text{O}_3$ as oxygen carrier for chemical-looping combustion with oxygen uncoupling (CLOU) – Experiments in a continuously operating fluidized-bed reactor system”, *International Journal of Greenhouse Gas Control*, 2011, 5, 2, 356-366
103. Källén, M., Rydén, M., Dueso, C., Mattisson, T., Lyngfelt, A., “ $\text{CaMn}_{0.9}\text{Mg}_{0.1}\text{O}_{3-\delta}$ as oxygen carrier in a gas-fired 10 kW_{th} chemical-looping combustion unit”, *Industrial and Engineering Chemistry Research*, 2013, 52, 21, 6923-6932
104. Xiao, R., Song, Q., Zhang, Sh., Zheng, W., Yang, Y., “Pressurized chemical-looping combustion of Chinese bituminous coal: cyclic performance and characterization of iron ore-based oxygen carrier”, *Energy and Fuels*, 2010, 24, 2, 1449-1463
105. Gu, H., Shen, L., Xiao, J., Zhang, S., Song, T., ”Chemical looping combustion of biomass/coal with natural iron ore as oxygen carrier in a continuous reactor”, *Energy and Fuels*, 2011, 25, 1, 446-455
106. Linderholm, C., Lyngfelt, A., Cuadrat, A., Jerndal, E., “Chemical-looping combustion of solid fuels – operation in a 10 kW unit with two fuels, above-bed and in-bed fuel feed and two oxygen carriers, manganese ore and ilmenite”, *Fuel*, 2012, 102, 808-822
107. Ortiz, M., Gayán, P., De Diego, L.F., García-Labiano, F., Abad, A., Pans, M.A., Adánez, J., “Hydrogen production with CO₂ capture by coupling steam reforming of methane and chemical-

looping combustion: Use of an iron-based waste product as oxygen carrier burning a PSA tail gas”, *Journal of Power Sources*, 2011, 196, 9, 4370-4381

108. Jerndal, E., Leion, H., Axelsson, L., Ekvall, T., Hedberg, M., Johansson, K., Källén, M., Svensson, R., Mattisson, T., Lyngfelt, A., “Using low-cost iron-based materials as oxygen carriers for chemical looping combustion”, *Oil and Gas Science and Technology, Revue IFP Energies nouvelles*, 2011, 66, 2, 235-248

109. Cuadrat, A., Linderholm, C., Abad, A., Lyngfelt, A., Adánez, J., “Influence of limestone addition in a 10 kW_{th} chemical-looping combustion unit operated with petcoke”, *Energy and Fuels*, 2011, 25, 10, 4818-4828

110. Teysié, G., Leion, H., Schwebel, G.L., Lyngfelt, A., Mattisson, T., “Influence of lime addition to ilmenite in chemical-looping combustion (CLC) with solid fuels”, *Energy and Fuels*, 2011, 25, 8, 3843-3853

111. Zheng, W.G., Xiao, R., Song, Q.L., Deng, Z.Y., *In: Chinese Society of Engineering Thermophysics on Combustion*, Hefei, China, 2009

112. H, X.Y., C, H.Y., L, B.Q., *Coal Conversion*, 2000, 23, 72-75

113. Jerndal, E., Mattisson, T., Lyngfelt, A., “Thermal analysis of chemical-looping combustion”, *Chemical Engineering Research and Design*, 2006, 84, 9, 795-806

114. Song, Q.L., Xiao, R., Deng, Z.Y., Zheng, W.G., Shen, L.H., Xiao, J., “Multicycle study on chemical-looping combustion of simulated coal gas with a CaSO₄ oxygen carrier in a fluidized bed reactor”, *Energy and Fuels*, 2008, 22, 6, 3661-3672

115. Saha, C., Zhang, S., Xiao, R., Bhattacharya, S., “Chemical looping combustion (CLC) of two Victorian brown coals – Part 2: Assessment of interaction between CuO and minerals inherent in coals during multi cycle experiments”, *Fuel*, 2012, 96, 335-347

116. Shabani, A., Rahman, M., Pudasainee, D., Samanta, A., Sarkar, P., Gupta, R., *In: The 39th Int. Technical Conf. on Clean Coal and Fuel Systems, Clearwater, Florida, USA, 2014*
117. Berguerand, N., Lyngfelt, A., “Chemical-looping combustion of petroleum coke using ilmenite in a 10 kW_{th} unit-high-temperature operation”, *Energy and Fuels*, 2009, 23, 10, 5257-5268
118. Berguerand, N., Lyngfelt, A., “Operation in a 10 kW_{th} chemical-looping combustor for solid fuel - Testing with a Mexican petroleum coke”, *Energy Procedia*, 2009, 1, 1, 407-414
119. Shen, L., Wu, J., Xiao, J., “Experiments on chemical looping combustion of coal with a NiO based oxygen carrier”, *Combustion and Flame*, 2009, 156, 3, 721-728
120. Shen, L., Wu, J., Gao, Z., Xiao, J., “Reactivity deterioration of NiO/Al₂O₃ oxygen carrier for chemical looping combustion of coal in a 10 kW_{th} reactor”, *Combustion and Flame*, 2009, 156, 7, 1377-1385
121. Wu, J., Shen, L., Xiao, J., Wang, L., Hao, J., *Huagong Xuebao/CIESC Journal*, 2009, 60, 2080-2088
122. Wu, J., Shen, L., Hao, J., Gu, H., 1st International conference on chemical looping, Lyon, 2010
123. Song, T., Wu, J., Zhang, H., Shen, L., “Characterization of an Australia hematite oxygen carrier in chemical looping combustion with coal”, *International Journal of Greenhouse Gas Control*, 2012, 11, 326-336

124. Cuadrat, A., Abad, A., García-Labiano, F., Gayán, P., De Diego, L.F., Adánez, J., “Effect of operating conditions in chemical-looping combustion of coal in a 500 W_{th} unit”, *International Journal of Greenhouse Gas Control*, 2012, 6, 153-163
125. Cuadrat, A., Abad, A., García-Labiano, F., Gayán, P., De Diego, L.F., Adánez, J., “The use of ilmenite as oxygen-carrier in a 500 W_{th} chemical-looping coal combustion unit”, *International Journal of Greenhouse Gas Control*, 2011, 5, 6, 1630-1642
126. Cuadrat, A., Abad, A., García-Labiano, F., Gayán, P., De Diego, L.F., Adánez, J., “Ilmenite as oxygen carrier in a chemical looping combustion system with coal”, *Energy Procedia*, 2011, 4, 362-369
127. Cuadrat, A., Abad, A., García-Labiano, F., Gayán, P., De Diego, L.F., Adánez, J., “Relevance of the coal rank on the performance of the in situ gasification chemical-looping combustion”, *Chemical Engineering Journal*, 2012, 195-196, 91-102
128. Sozinho, T., Pelletant, W., Stainton, H., Guillou, F., Gauthier, T., 2nd International conference on chemical looping, Darmstadt, 2012
129. Thon, A., Kramp, M., Hartge, E., Heinrich, S., Werther, J., 2nd International conference on chemical looping, Darmstadt, 2012
130. Tong, A., Bayham, S., Kathe, M., Zeng, L., Luo, S., Fan, L-S., 2nd International conference on chemical looping, Darmstadt, 2012
131. Tong, A., Fan, L-S., NETL: CO₂ capture technology meeting, Pittsburgh, PA, 2012
132. Markström, P., Linderholm, C., Lyngfelt, A., 2nd International conference on chemical looping, Darmstadt, 2012

133. Markström, P., Linderholm, C., Lyngfelt, A., “Chemical-looping combustion of solid fuels – Design and operation of a 100 kW unit with bituminous coal”, *International Journal of Greenhouse Gas Control*, 2013, 15, 150-162
134. Markström, P., Linderholm, C., Lyngfelt, A., “Analytical model of gas conversion in a 100 kW chemical-looping combustor for solid fuels – Comparison with operational results”, *Chemical Engineering Science*, 2013, 96, 131-141
135. Orth, M., Ströhle, J., Epple, B., *In: 2nd International conference on chemical looping*, Darmstadt, 2012
136. Abdulally, I. et. al., *In: 37th International Technical Conference on Clean Coal and Fuel Systems*, Clearwater, Florida, 2012
137. Ströhle, J., Orth, M., Epple, B., *In: 1st International conference on chemical looping*, Lyon, 2010
138. Markström, P., Berguerand, N., Lyngfelt, A., “The application of a multistage-bed model for residence-time analysis in chemical-looping combustion of solid fuel”, *Chemical Engineering Science*, 2010, 65, 18, 5055-5066
139. Cuadrat, A., Abad, A., Gayán, P., De Diego, L.F., García-Labiano, F., Adánez, J., “Theoretical approach on the CLC performance with solid fuels: Optimizing the solids inventory”, *Fuel*, 2012, 97, 536-551
140. García-Labiano, F., De Diego, L.F., Gayán, P., Abad, A., Adánez, J., “Fuel reactor modelling in chemical-looping combustion of coal: 2-simulation and optimization”, *Chemical Engineering Science*, 2013, 87, 173-182

141. Berguerand, N., Lyngfelt, A., Mattisson, T., Markström, P., “Chemical looping combustion of solid fuels in a 10 kW_{th} unit”, *Oil and Gas Science and Technology, Revue IFP Energies nouvelles*, 2011, 66, 2, 181-191
142. Abad, A., Gayán, P., De Diego, L.F., García-Labiano, F., Adánez, J., “Fuel reactor modelling in chemical-looping combustion of coal: 1. model formulation”, *Chemical Engineering Science*, 2013, 87, 277-293
143. Mahalatkar, K., Kuhlman, J., Huckaby, E.D., O’Brien, Th., “Computational fluid dynamic simulations of chemical looping fuel reactors utilizing gaseous fuels”, *Chemical Engineering Science*, 2011, 66, 3, 469-479
144. Kronberger, B., Lyngfelt, A., Löffler, G., Hofbauer, H., “Design and fluid dynamic analysis of a bench-scale combustion system with CO₂ separation – chemical-looping combustion”, *Industrial and Engineering Chemistry Research*, 2005, 44, 3, 546-556
145. Pfaff, I., Kather, A., “Comparative thermodynamic analysis and integration issues of CCS steam power plants based on oxy-combustion with cryogenic or membrane based air separation”, *Energy Procedia*, 2009, 1, 1, 495-502
146. Kempkes, V., Kather, A., *In: Proc. 2nd International conference on chemical looping*, Darmstadt, Germany, 2012
147. Fillman, B., Anheden, M., Wolf, J., *In: 1st International conference on chemical looping*, Lyon, 2010
148. Ekström, C., Schwendig, F., Biede, O., Franco, F., Haupt, G., De Koeijer, G., Papapavlou, Ch., Røkke, P.E., “Techno-economic evaluations and benchmarking of pre-combustion CO₂ capture and oxy-fuel processes developed in the European ENCAP project”, *Energy Procedia*, 2009, 1, 1, 4233-4240

149. Perry, R.H., Green, D.W., *Perry's Chemical Engineers's Handbook*, 7th edition, The McGraw-Hill Companies, Inc.: New York, 1997
150. Lyngfelt, A., Kronberger, B., Adánez, J., Morin, J.-X., Hurst, P., “The GRACE project. Development of oxygen carrier particles for chemical-looping combustion. Design and operation of a 10 kW chemical-looping combustor”, to be presented at The Seventh International Conference on Greenhouse Gas Control Technologies (GHGT-7), Vancouver, Canada 5-9 September 2004
151. Cormos, A.-M., Cormos, C.-C., “Investigation of hydrogen and power co-generation based on direct coal chemical looping systems”, *International Journal of Hydrogen Energy*, 2014, 39, 5, 2067-2077
152. Peltola, P., Tynjälä, T., Ritvanen, J., Hyppänen, T., “Mass, energy, and exergy balance analysis of chemical looping with oxygen uncoupling (CLOU) process”, *Energy Conversion and Management*, 2014, 87, 483-494
153. Eyring, E.M., Konya, G., Lighty, J.S., Sahir, A.H., Sarofim, A.F., Whitty, K., “Chemical looping with copper oxide as carrier and coal as fuel”, *Oil and Gas Science and Technology – Rev IFP Energies Nouvelles*, 2011, 66, 2, 209-221
154. Gayán, P., Adánez-Rubio, I., Abad, A., De Diego, L.F., García-Labiano, F., Adánez, J., “Development of Cu-based oxygen carriers for chemical-looping with oxygen uncoupling (CLOU) process”, *Fuel*, 2012, 96, 226-238
155. Peterson, S.B., Konya, G., Clayton, C.K., Lewis, R.J., Wilde, B.R., Eyring, E.M., Whitty, K.J., “Characteristics and CLOU performance of a novel SiO₂-supported oxygen carrier prepared from CuO and β -SiC”, *Energy and Fuels*, 2013, 27, 10, 6040-6047

156. Mattison, T., “Materials for chemical-looping with oxygen uncoupling”, ISRN Chemical Engineering 2013, <http://dx.doi.org/10.1155/2013/526375>
157. Sahir, A.H., Sohn, H.Y., Leion, H., Lighty, J.S., “Rate analysis of chemical-looping with oxygen uncoupling (CLOU) for solid fuels”, *Energy and Fuels*, 2012, 26, 7, 4395-4404
158. Wen, Y., Li, Z., Xu, L., Cai, N., “Experimental study of natural Cu ore particles as oxygen carriers in chemical looping with oxygen uncoupling (CLOU)”, *Energy and Fuels*, 2012, 26, 6, 3919-3927
159. Whitty, K., Clayton, C., “Measurement and modeling of kinetics for copper-based chemical looping with oxygen uncoupling”, *In: 2nd international conference on chemical looping*, Germany, 2012
160. Gyftopoulos, E., Beretta, G., “Thermodynamics: foundations and applications”, New York: Dover Publications, 2005
161. Chase, M., NIST-JANAF thermochemical tables. New York: American Institute of Physics, 1998
162. Abad, A., Adánez, J., García-Labiano, F., De Diego, L.F., Gayán, P., Celaya, J., “Mapping of the range of operational conditions for Cu-, Fe-, and Ni-based oxygen carriers in chemical-looping combustion”, *Chemical Engineering Science*, 2007, 62, 1-2, 533-549
163. Arjmand, M., Keller, M., Leion, H., Mattisson, T., Lyngfelt, A., “Oxygen release and oxidation rates of MgAl₂O₄-supported CuO oxygen carrier for chemical-looping combustion with oxygen uncoupling (CLOU)”, *Energy and Fuels*, 2012, 26, 11, 6528-6539

164. Adánez-Rubio, I., Abad, A., Gayán, P., De Diego L.F., García-Labiano, F., Adánez, J., “Performance of CLOU process in the combustion of different types of coal with CO₂ capture”, *International Journal of Greenhouse Gas Control*, 2013, 12, 430-440
165. Peltola, P., Ritvanen, J., Tynjälä, T., Hyppänen, T., “Fuel reactor modelling in chemical looping with oxygen uncoupling process”, *Fuel*, 2015, 147, 184-194
166. Peltola, P., Ritvanen, J., Tynjälä, T., Pröll, T., Hyppänen, T., “One-dimensional modelling of chemical looping combustion in dual fluidized bed reactor system”, *International Journal of Greenhouse Gas Control*, 2013, 16, 72-82
167. Ylätaalo, J., Ritvanen, J., Arias, B., Tynjälä, T., Hyppänen, T., “1-Dimensional modelling and simulation of the calcium looping process”, *International Journal of Greenhouse Gas Control*, 2012, 9, 130-135
168. Gayán, P., Abad, A., De Diego, L.F., García-Labiano, F., Adánez, J., “Assessment of technological solutions for improving chemical looping combustion of solid fuels with CO₂ capture”, *Chemical Engineering Journal*, 2013, 233, 56-69
169. Clayton, C.K., Whitty, K.J., “Measurement and modeling of decomposition kinetics for copper oxide-based chemical looping with oxygen uncoupling”, *Applied Energy*, 2014, 116, 416-423
170. Rahman, M., Samanta, A., Gupta, R., “Production and characterization of ash-free coal from low-rank Canadian coal by solvent extraction”, *Fuel Processing Technology*, 2013, 115, 88-98
171. Adánez-Rubio, I., Gayán, P., García-Labiano, F., De Diego, L.F., Adánez, J., Abad, A., “Development of CuO-based oxygen-carrier materials suitable for chemical-looping with oxygen uncoupling (CLOU) process”, *Energy Procedia*, 2011, 4, 417-424

172. Zhao, H.-Y, Cao, Y., Orndorff, W., Pan, W.-P., “Study on modification of Cu-based oxygen carrier for chemical looping combustion”, *Journal of Thermal Analysis and Calorimetry*, 2013, 113, 3, 1123-1128

173. Zhao, H.-Y., Cao, Y., Kang, Z.-Z, Wang, Y.-B, Pan, W.-P, “Thermal characteristics of Cu-based oxygen carriers”, *Journal of Thermal Analysis and Calorimetry*, 2012, 109, 3, 1105-1109

174. Sahir, A. H., “Process modeling aspects of chemical-looping with oxygen uncoupling and chemical-looping combustion for solid fuels”, (PhD thesis, University of Utah), 2013

Appendix

Appendix.1 - Ash-free coal (AFC)

1. Background

In direct coal combustion, ash accumulation in the system is an important issue. In order to address this, coal de-mineralization has been carried out by means of physical and chemical cleaning. One approach of chemical de-mineralization of coal is solvent extraction of coaly matter– the product commonly called as ash-free coal (AFC).^{A1} AFC gets rid of all the operational problems related to ash forming minerals in utilizing coal in different advanced technologies such as catalytic gasification^{A2,A3} and direct carbon fuel cell.^{A4}

Since 1999, studies and researches have been performed to prepare AFC.^{A1} An Ultra-Clean Coal (UCC) preparation process was studied under hydrothermal conditions utilizing alkalis and strong acids to eliminate minerals of coal.^{A5-A8} The produced coal by this process contained between 1000 to 5000 ppm ash which is not favorable for researchers who were interested to utilize the produced coal directly into the gas turbines.^{A9} It is noteworthy to consider that deposition of coal ash in gas turbines causes big issues including fouling, corrosion and erosion of blades. AFC direct combustion in gas turbines can enhance thermal efficiency of the system and prevents problems caused by ash deposition on turbine blades.^{A9}

In order to have AFC production with significantly lower ash content compared to that produced from UCC, researchers from Kobe Steel, Ltd.^{A1} and Institute for Energy utilization, National Institute of Advanced Industrial Science and Technology^{A10} in Japan, suggested a solvent extraction method which is commonly called “hyper-coal”. This process is believed to be one of the most efficient and costly effective manufacturing methods for AFC production. Kobe Steel has built a bench scale plant to manufacture 0.1 t/day of Hyper-coal.^{A1,A4}

AFC evaluations by Okuyama and co-workers^{A1} show that the AFC calorie base price is competitive to the price of a general coal including the price of ash disposal in Japan. There has been a large scale demonstration research going on in this area to economize the production (i.e.

KOBE Steel in Japan has developed a demonstration pilot plant (capacity 0.1t/d).^{A1} Okuyama and co-workers^{A1} proposed and developed the costly effective approach which involved using the technology in which ash is removed from coal by a solvent to produce AFC. This hyper coal process utilizes solvent de-ashing which is a solid-liquid separating technology. The rate of coal extraction was nearly 70% wt [on the basis of dry and ash-free coal].^{A1} The extracted coal can be achieved at 360 °C utilizing 1-methylnaphthalene as the solvent for the hyper coal process and the ash content would be reduced to several hundreds of ppm values.^{A1} The organic matter was dissolved in the solvent. The mineral matter which was not soluble in the solvent was filtered. The organic matter in filtrate was precipitated as ash free coal by using hexane. The obtained residue was called AFC. Increasing the yield of hyper coal extraction and solvent recycling are two important parameters in the process of hyper coal.^{A1}

Yoshida and co-workers^{A10} utilized several organic solvents for different coals to produce hyper-coal with a high yield. Light cycle oil (LCO) was figured to be a good potential candidate to be utilized as a nonpolar solvent for the process.^{A10} For the seven of nine tested coals, they successfully produced treated coals with less than 0.1% ash content.^{A10} They also proposed the idea that higher extraction yields can be achieved for coals which do not have high softening points.^{A10.A11} Also it is suggested by Kim and co-workers^{A12} that for some kinds of coals there is no softening point and polar solvents should be utilized for the coal extraction in these cases. Moreover, it was shown that higher heating value (HHV) of AFC is much higher than that of raw coal.^{A11}

2. Preparation and properties

In Clean Coal Technology Lab in University of Alberta, Rahman and co-workers^{A11} prepared AFC from different low-rank Canadian coals utilizing industrial solvents. Combined polar and non-polar solvents and non-polar organic solvents were used to study the extraction yield of AFC from coals based on the type of used coals and solvents. The AFC maximum yield by solvent extraction was found out to be approximately 73% at temperature of 400 °C utilizing hydro treated solvents.^{A11} A non-polar solvent called 1-methylnaphthalene (1-MN) showed no considerable outcome for the extraction yields (about 30% based on dry ash-free basis), but a hydro treated aromatic hydrocarbon gives maximum yield of 73% (based on dry ash-free basis) for AFC yield at the temperature of 400 °C.^{A11} Table A.1 shows the extraction yield of AFC at temperature

of 400 °C from BL raw coal using different type of solvents including 1-MN, heavy aromatic hydrocarbons called SA (Solvent A) and hydro-treated heavy aromatic hydrocarbons called SB (Solvent B) which SA and SB are the vacuum residues from industry.

Table A.1. Extraction yield of AFC at temperature of 400 °C from BL raw coal^{A11}

(Reprinted from Rahman and co-workers^{A11}, 2013, with permission from Publisher (Elsevier))

Solvent	Yield % (daf) ^a
1-MN	29.5
SA	42.8
SB	67.0

^a Percentage yield based on residue (daf: dry ash free basis), Yield % = (wt. of feed coal(daf) wt. of residue(daf))/(wt. of feed coal(daf)) * 100

Furthermore, some of the experiments were carried out utilizing heavy aromatic hydrocarbons as a solvent which were hydro-treated. A 0.5 L autoclave as shown in Figure A.1 was used with the temperatures between 200 and 450 °C for performing the experiments for extraction.^{A11} The D-50 of AFC was 7 µm (50% mass below 7 µm). It was also figured out that the sulfur content of AFC was reduced and about 36-37MJ/kg was found out as the higher heating value (HHV) of AFC.^{A11}

In the study performed by Rahman and co-workers^{A11} low-rank Canadian coals were used as the coal samples. Canadian sub-bituminous coals including GEN and CV and various Canadian lignite coals including POP, BD and BL were utilized for performing the experiments.^{A11} AFC used in the present experiments was derived from Canadian lignite BL coal as heavy residue of solvent extraction process. The proximate and ultimate analysis of BL raw coal and BL-AFC coal are presented in Table A.2.

Table A.2. The proximate and ultimate analysis of BL raw coal and BL-AFC (mass %)^{A11}

Coal	M/%	V/%	A/%	FC/%	C/%	H/%	N/%	S/%	O ^a /%
BL raw	6.9	31.7	19.2	42.2	54.3	3.91	1.22	1.15	20.26
BL-AFC	1.40	62.93	0.07	35.60	86.50	5.73	3.00	0.45	4.31

^a Oxygen by difference

M-Moisture; V-Volatile Matter; A-Ash; FC-Fixed Carbon

3. AFC producing process

To prepare AFC, the coals were put in a ball-mill to obtain desired sizes of less than 150 μm . Then they were put in the vacuum for drying with time duration of 12 hours and temperature of 80 $^{\circ}\text{C}$.^{A11} It is noteworthy to mention that these coals were provided by industry. As the solvent purposes, industrial solvents including heavy aromatic hydrocarbons which were hydro-treated (SB) and heavy aromatic hydrocarbons (SA) were utilized in experiments.^{A11}

Initially, around 10 g of crushed coal with the size of less than 150 μm was put in the autoclave.^{A11} The coal sample was combined with solvent with the volume of 100 mL. It should be considered that the ratio of solvent to coal was about 1 to 10.^{A11} The prepared mixture of coal sample and the solvent were mixed continuously in the nitrogen environment and was heated up to reach the certain temperature. While the temperature was certain it was kept for approximately one hour time duration.^{A11} Afterwards, when the one hour time passed and solvent extraction occurred, papers for filtration with the size of 0.1 μm were used at the temperature of around 100 $^{\circ}\text{C}$ for the separation of liquid and solid phase of the mixture.^{A11} Then, THF or toluene was used for washing the remained solid residue for couple of times and at 80 $^{\circ}\text{C}$ drying took place in vacuum condition.^{A11} The filtrate material gradually was mixed with hexane continuously and its ratio to hexane was about 1 to 40.^{A11} Then the material which could not dissolve in hexane precipitate and was treated, filtered and dried. The obtained material after these treatments is called AFC. It is noteworthy to mention that a rotavapor was utilized for the recovery of solvent which was more than 95 %.^{A11} Figure A.1 shows the system of solvent extraction which was used for the experimental procedures of manufacturing of AFC.

Hydrotreated coal tar distillate or in other word hydrotreated industrial solvent was used to prepare AFC used in CLC experiments. AFC derived by solvent extraction of BL-coal using hydrotreated heavy aromatic hydrocarbons (SB) at 400 $^{\circ}\text{C}$ ^{A11} has been used as the solid fuel in CLC process to perform single cycle and multi cycle experiments in TGA.

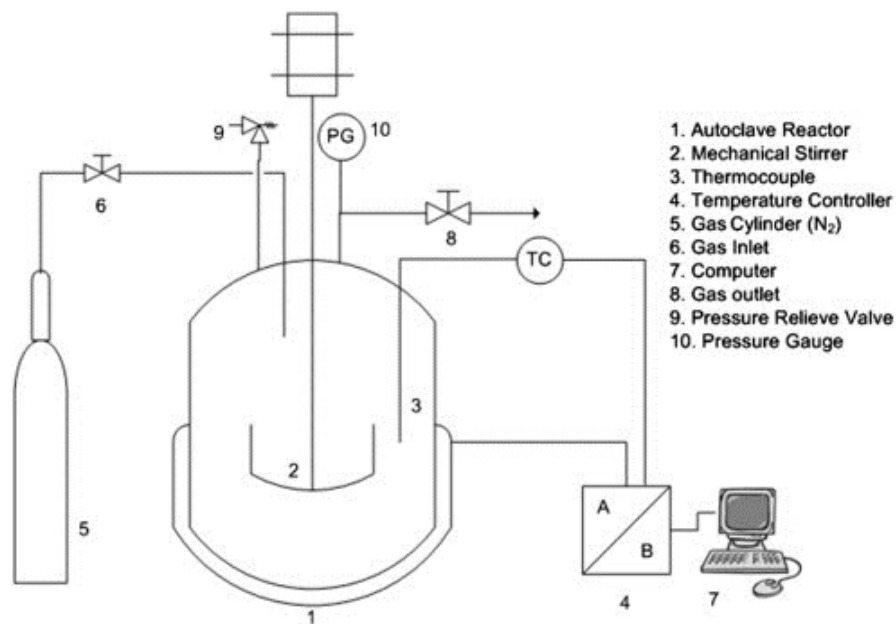


Figure A.1. Experimental procedures of solvent extraction^{A11}

(Reprinted from Rahman and co-workers^{A11}, 2013, with permission from Publisher (Elsevier))

4. Advantages of AFC

The main advantage of using AFC is that ash content is removed from coal in advance and the produced coal does no mineral content. Therefore, no mineral compound formation/deposition or ash contamination would occur in the system while utilizing AFC. As a result, AFC eliminates the issue of separation of ash from oxygen carrier and operational problems caused by ash forming minerals in coal in the system.

AFC can be used in various technologies such as catalytic gasification^{A2,A3} and direct carbon fuel cell.^{A4} It also should be noted that in gas turbines, corrosion, fouling and erosion of blades are caused by ash deposition in the system. Using AFC in gas turbines and its direct combustion in these systems avoid the operational problems and formation of ash on the blades and increases the system's thermal efficiency.^{A9}

Moreover, AFC prevents using additional CO₂ separation units in CLC technology and reduces the associated cost and energy penalty for the system which lead to decrease CO₂ emission significantly.

5. Summary

The preparation process and properties of AFC were also discussed. In University of Alberta, Rahman and co-workers^{A11} produced AFC from low-rank Canadian coals by solvent extraction using industrial solvents. Maximum yield of produced AFC was figured out to be nearly 73% utilizing hydro treated solvents at 400 °C.^{A11} To perform the experiments, a 0.5 L autoclave was used with the operating temperatures between 200 and 450 °C. AFC has a particle size distribution with D-50 of 7 µm.^{A11}

The main advantage of using AFC is that there is no ash content in the coal. Therefore, there is no ash formation in the system which can cause operational problems. One of the technologies that AFC can be used in is CLC. The benefit of using AFC as the solid fuel in CLC is that AFC contains no mineral matter that can react with the oxygen carrier. It also prevents using additional separation units in the system and additional cost which cause significant CO₂ emission. However, mass production of AFC in a cost effective manner would be beneficial in order to establish some kind of CLC process with AFC.

In order to address the issues caused by ash formation, AFC prepared by the solvent extraction of BL-coal using hydrotreated heavy aromatic hydrocarbons (SB) - hydrotreated coal tar distillate or in other word hydrotreated industrial solvent - at 400 °C^{A11} has been used as the solid fuel in CLC process to perform single cycle and multi cycle experiments in TGA.

References

- A1. Okuyama, N., Komatsu, N., Shigehisa, T., Kaneko, T., Tsuruya, S., “Hyper-coal process to produce the ash-free coal”, *Fuel Processing Technology*, 2004, 85, 8-10, 947-967
- A2. Sharma, A., Takanohashi, T., Morishita, K., Takarada, T., Saito, I., “Low temperature catalytic steam gasification of HyperCoal to produce H₂ and synthesis gas”, *Fuel*, 2008, 87, 4-5, 491-497
- A3. Kopyscinski, J., Rahman, M., Gupta, R., Mims, C.A., Hill, J.M., “K₂CO₃ catalyzed CO₂ gasification of ash-free coal. Interactions of the catalyst with carbon in N₂ and CO₂ atmosphere”, *Fuel*, 2014, 117, 1181-1189
- A4. Dudek, M., Tomczyk, P., Socha, R., Hamaguchi, M., “Use of ash-free “Hyper-coal” as a fuel for a direct carbon fuel cell with solid oxide electrolyte.” *International Journal of Hydrogen Energy*, 2014, 39, 12386-12394
- A5. Steel, K.M., Besida, J., O’Donnell, T.A., Wood, D.G., “Production of ultra clean coal Part I Dissolution behaviour of mineral matter in black coal toward hydrochloric and hydrofluoric acids”, *Fuel Processing Technology*, 2001, 70, 3, 171-192
- A6. Steel, K.M., Besida, J., O’Donnell, T.A., Wood, D.G., “Production of ultra clean coal Part II - Ionic equilibria in solution when mineral matter from black coal is treated with aqueous hydrofluoric acid”, *Fuel Processing Technology*, 2001, 70, 3, 193-219
- A7. Steel, K.M., Patrick, J.W., “The production of ultra clean coal by chemical demineralization”, *Fuel*, 2001, 80, 14, 2019-2023
- A8. Steel, K.M., Besida, J., O’Donnell, T.A., Wood, D.G., “Production of ultra clean coal Part III. Effect of coal’s carbonaceous matrix on the dissolution of mineral matter using hydrofluoric acid”, *Fuel Processing Technology*, 2002, 76, 1, 51-59

A9. Takanohashi, T., Shishido, T., Kawashima, H., Saito, I., “Characterisation of HyperCoals from coals of various ranks”, *Fuel*, 2008, 87, 592-598

A10. Yoshida, T., Takanohashi, T., Sakanishi, K., Saito, I., Fujita, M., Mashimo, K., “The effect of extraction condition on “HyperCoal” production (1) - under room-temperature filtration”, *Fuel*, 2002, 81, 1463-1469

A11. Rahman, M., Samanta, A., Gupta, R., “Production and characterization of ash-free coal from low-rank Canadian coal by solvent extraction”, *Fuel Processing Technology*, 2013, 115, 88-98

A12. Kim, S.D., Woo, K.J., Jeong, S.K., Rhim, Y.J., Lee, S.H., “Production of low ash coal by thermal extraction with N-methyl-2-pyrrolidinone”, *Korean Journal of Chemical Engineering*, 2008, 25, 758-763

Appendix.2 - Stoichiometric calculations

a) Calculations of stoichiometric ratio of CuO/AFC:

Basis: AFC= 3.057 mg

(AFC amount equal to 3.057 mg as one of the tested TGA samples)

$$\text{C: } 3.057 \times (0.865) = 2.6443 \text{ mg} / 12 = 0.2204 \text{ mmol}$$

$$\text{H}_2: 3.057 \times (0.0573) = 0.1752 \text{ mg} / 2 = 0.0876 \text{ mmol}$$

$$\text{O}_2: 3.057 \times (0.0431) = 0.1318 \text{ mg} / 32 = 0.0041 \text{ mmol}$$

$$\text{H}_2\text{O} = 0.0876 \text{ mmol}$$

$$\text{CO}_2 = 0.2204 \text{ mmol}$$

$$\text{O}_2 \text{ needed from CuO for combustion of all AFC: } (0.2204 + 0.0876/2 - 0.0041) = 0.2601 \text{ mmol}$$

$$\text{Mmol of CuO needed} = 0.2601 \times 4 = 1.0404 \text{ mmol}$$

$$\text{Molecular weight of CuO} = 79.545 \text{ g/mol}$$

$$\text{CuO reqd: } 1.0404 \times 79.545 = 82.7586 \text{ mg}$$

$$\text{Stoich Ratio} = 82.7586 / 3.057 = 27.0718$$



b) Empirical formula for AFC:



Basis: 100 g of AFC

$$\text{C} : 100*(0.865) = 86.5\text{g} / 12 = 7.21 \text{ mol}$$

$$\text{H}_2 : 100*(0.0573) = 5.73 \text{ g} / 2 = 2.865 \text{ mol}$$

$$\text{O}_2 : 100*(0.0431) = 4.31\text{g} / 32 = 0.1347 \text{ mol}$$

$$\text{N}_2 : 100*(0.03) = 3\text{g} / 28 = 0.1071 \text{ mol}$$

$$\text{S}_2 : 100*(0.0045) = 0.45\text{g}/64.2 = 0.0070 \text{ mol}$$

$$\text{H}_2\text{O formed: } 2*0.1347 = 0.2694 \text{ mol}$$

$$\text{H}_2 \text{ left: } 2.865 - 0.2694 = 2.5956 \text{ mol}$$

Moles of Carbon and Hydrogen in 100 grams of AFC coal:

(Remaining Hydrogen and carbon on dry basis)

$$\text{H}_2 = 2.6 \text{ mol}$$

$$\text{C} = 7.21 \text{ mol}$$

$$\text{AFC} = \text{C}_{7.21} \text{H}_{5.2}$$

$$\text{AFC} = \text{CH}_{0.72}$$

(Considering all the elements of AFC based on the ultimate analysis)

$$C = 7.21 \text{ mol}$$

$$H_2 = 2.865 \text{ mol}$$

$$O_2 = 0.1347 \text{ mol}$$

$$N_2 = 0.1071 \text{ mol}$$

$$S_2 = 0.0070 \text{ mol}$$

$$AFC = C_{7.21} H_{5.73} O_{0.27} N_{0.21} S_{0.014}$$